DOI: 10.31891/2079-1372

THE INTERNATIONAL SCIENTIFIC JOURNAL

PROBLEMS OF TRIBOLOGY

Volume 29 ***No 3/113-2024***

МІЖНАРОДНИЙ НАУКОВИЙ ЖУРНАЛ

ПРОБЛЕМИ ТРИБОЛОГІЇ

PROBLEMS OF TRIBOLOGY

INTERNATIONAL SCIENTIFIC JOURNAL

Published since 1996, four time a year

Volume 29 No 3/113-2024

Establishers:
Khmelnytskyi National University (Ukraine)
Lublin University of Technology (Poland)

Associated establisher:
Vytautas Magnus University (Lithuania)

Editorial board address:
International scientific journal "Problems of Tribology",
Khmelnytskyi National University,
Instytutska str. 11, Khmelnytskyi, 29016, Ukraine
phone +380975546925

Indexed: CrossRef, DOAJ, Ulrichsweb, ASCI, Google Scholar, Index Copernicus

E-mail: tribology@khmnu.edu.ua

Internet: http://tribology.khnu.km.ua

ПРОБЛЕМИ ТРИБОЛОГІЇ

МІЖНАРОДНИЙ НАУКОВИЙ ЖУРНАЛ

Видається з 1996 р. ***Виходить 4 рази на рік***

Том 29 **№ 3/113-2024**

Адреса редакції:
Україна, 29016, м. Хмельницький, вул. Інститутська 11, к. 4-401
Хмельницький національний університет, редакція журналу "Проблеми трибології"
тел. +380975546925, **E-mail**: tribology@khmnu.edu.ua

Internet: http://tribology.khnu.km.ua

Зареєстровано Міністерством юстиції України
Свідоцтво про держреєстрацію друкованого ЗМІ: Серія КВ № 1917 від 14.03. 1996 р.
(перереєстрація № 24271-14111ПР від 22.10.2019 року)

Входить до переліку наукових фахових видань України
(Наказ Міністерства освіти і науки України № 612/07.05.19. Категорія Б.)

Індексується в МНБ: CrossRef, DOAJ, Ulrichsweb, ASCI, Google Scholar, Index Copernicus

Рекомендовано до друку рішенням вченої ради ХНУ, протокол № 2 від 26.09.2024 р.

Problems of Tribology, *V. 29, No 3/113-2024*

Problems of Tribology

Website: http://tribology.khnu.km.ua/index.php/ProbTrib
E-mail: tribosenator@gmail.com

CONTENTS

***Problems of Tribology**, V. 29, No 3/113-2024*

Problems of Tribology
Website: http://tribology.khnu.km.ua/index.php/ProbTrib
E-mail: tribosenator@gmail.com

ЗМІСТ

***Problems of Tribology**, V. 29, No 3/113-2024, 6-14*

Problems of Tribology
Website: http://tribology.khnu.km.ua/index.php/ProbTrib
E-mail: tribosenator@gmail.com

DOI: https://doi.org/10.31891/2079-1372-2024-113-3-6-14

Analysis of the directions of improving regular micro reliefs

V.O. Dzyura, R.O. Bytsa

Ternopil Ivan Puluy National Technical University, Ukraine
E-mail: volodymyrdzyura@gmail.com

Received: 05 June 2024: Revised: 25 June 2024: Accept: 05 July 2024

Abstract

The article analyzes the features of planar regular microreliefs with the shape of grooves, the axis of which lies in a plane that is parallel or coincident with the surface on which the microrelief is formed and can be described by a periodic function. It was established that the main parameter that determines the operational properties of a surface with regular microreliefs is the relative area of the microrelief. The hypothesis is put forward that the geometric shape of the grooves of the microrelief practically does not affect the operational properties of the surface. Microreliefs of groove axes that a periodic function can describe are technologically imperfect because when forming the tops of microrelief grooves, the tool must make stops to change the trajectory of movement. The complex geometry of microrelief grooves reduces the productivity of their formation, and the complexity of ensuring regularity ensures the surface's heterogeneous physical and mechanical properties. Directions for improving the forms of microreliefs are proposed, which will ensure an increase in the productivity of their formation and provide an opportunity to control the operational properties of the surface.

Key words: regular micro reliefs, operational properties, geometric parameters, surface engineering, periodic functions, friction pair

Introduction

Ensuring the operational properties of machine parts is an important task of modern engineering. For this purpose, technologies for processing responsible surfaces and methods for ensuring their geometric and physico-mechanical quality parameters are constantly being improved. The direction of engineering science aimed at ensuring the necessary operational properties of the working surfaces of machine parts is called surface engineering. In this direction, an important place is occupied by the technology of creating periodically repeating organized surface structures, which are called regular microreliefs. In the scientific literature, these organized structures are called "Surface Texture", "Surface topography " or " Regular Micro Relief (RMR)". The creation of new micro reliefs that would provide better operational properties is an important task for modern mechanical engineering.

Literature review

The work [1] gives the results of studies of the influence of different forms of grooves of regular microrelief, which was formed on the surfaces of the test sample, on the coefficient of friction, the temperature in the friction zone, and the ability of the surface to remove wear products. Reducing the coefficient of friction leads to a reduction in the consumption of energy resources that are spent to set mechanisms in motion, which can be very relevant both in the aviation industry and in any other field of transport.

In works [2, 3], the results of the research are presented, which indicate that the formation of a microstructure in the form of an ordered microrelief on the inner cylindrical surface of the cylinder liner contributes to the ability of this surface to retain an oil film. This property of the working surface of the hydraulic cylinder sleeve improves the operational properties of the surface and increases the resources of the unit as a whole.

A large number of studies have confirmed that the formation of an ordered microstructure on the working surface reduces the roughness of the treated surface and increases the surface microhardness [4, 5, 6].

To ensure the specified operational properties of the working surfaces, microreliefs with grooves of various shapes and sizes are formed.

For example, in [7], the authors conducted a comparative study of the operational properties of flat rotating surfaces of discs. Regular microreliefs were formed on these surfaces, the elements of which in the first case were periodically repeated spherical holes, and in the other, traces of segments of different lengths (chevrons) intersecting at acute angles in the range of 60° - 90°. The result of the study was the determination of the coefficient of friction of surfaces with formed microreliefs and the search for the optimal shape, sizes and mutual location of the elements of such a microrelief.

Studies similar in object were conducted in work [8]. The authors investigated surface structures with a depth of 8 nm, the traces of which in the vertical plane will be in the form of a circle, an ellipse, and a triangle. The influence of the shape of the texture on the coefficient of friction was studied. It was also established that, given the same area, the same area ratio, and the same depth, elliptical and triangular pits have a lower load-bearing capacity compared to a round pit.

Surface structures in the form of square holes and grooves were studied in [9]. The surface area covered by microrelief elements was 25%. After forming on the surface of the test samples a texture in the form of grooves and square holes with a depth of 20 nm, they were subjected to the action of friction with a similar surface, simulating the process of wear. Each sample carried out relative movements in the amount of 20 thousand cycles. After simulating the wear process, the samples were compared with a control sample with a flat surface without formed microrelief. The result of the research is the conclusion that surfaces with formed surface structures have better operational properties. Surface operational defects during the period of research were observed only on the surface without formed microreliefs.

In the work [10], the authors proposed an approach in which regular microrelief is considered from the standpoint of factors that determine its characteristics, in particular: size and shape and mutual placement of microrelief elements; orientation of microrelief elements relative to the surface on which it is formed; the relationship between microrelief parameters; hierarchical ranking. Examples of regular microreliefs in the form of ordered microstructures in the environment are given, the sizes of their constituent elements are given, and their orientation is shown. Factors affecting the functional properties of surfaces with regular surface structures are considered.

Article [11] is interesting from the point of view of carrying out classifications. The classification of directions of scientific research of textured surfaces is presented, in particular: technologies for creating regular microreliefs; input/output characteristics of such surfaces; modelling of their interaction and further research in this direction. This work also provides a classification of the main methods of creating textured surfaces, such as methods of thermal, mechanical, electrochemical interaction, micro- and nano-finishing and micro-casting. The article provides technological diagrams of the processes of formation of surface microstructures with justification of the main technological parameters. The result of the authors' research is a table describing the various tool materials, work materials and cutting parameters used in machining with a micro-textured tool and a table of texture generation methods along with the dimensions and geometry of the grooves.

The microstructure of the surface in the form of rectilinear grooves was studied in [12]. These microstructures with a depth of 80-120 nm at the angle of the grooves 0°, 45°, 90° were created by a laser beam. The authors studied the frictional properties of these surfaces. The research was carried out by applying a load that presses the ball to the test sample with a force of 20 to 100 N and performs relative cyclic movements in the amount of 10 thousand cycles, simulating wear. The obtained results of the change in the coefficient of friction were compared with a control sample with a surface without creating surface microstructures. The work also established a mechanism for filling the grooves with the products of surface interaction and searched for the optimal location of the grooves to remove them from the contact zone of the conjugated surfaces.

The technology of creating a regular microrelief is proposed in [13, 14]. The use of a special tool with an indenter in the form of a ball with the ability to adjust the interaction force on the surface creates a regular micro relief with sinusoidal grooves on the surface. In this way, a completely regular microrelief with hexagonal cells is formed on the surface. The article presents the results of the study of the influence of the main technological parameters on the geometric parameters of the created microrelief.

Studies confirming the ability of textured surfaces to hold liquids better are given in [15]. The authors conducted a study of the rolling speed of liquid drops from surfaces with different microreliefs. Test samples with nine types of regular microreliefs of different shapes were produced. It was established that surfaces with formed microreliefs, in particular longitudinal grooves, retain drops longer than flat surfaces and surfaces with other types of microreliefs.

Scientific articles [16, 17] are devoted to the classification and mathematical modelling of partially regular micro reliefs, the regularity of which is ensured only for certain geometric parameters formed on the end surfaces of the bodies of rotation. Such micro reliefs are created on the end surfaces of the bodies of rotation. At the same time, the axial step of the grooves gradually decreases as they approach the center of rotation. To ensure the regularity of this parameter, the concept of the angular step of the groove is introduced, which is the same for grooves placed at different distances from the center of rotation of the end surface.

One of the main characteristics of the regular microrelief formed on the surface is its relative area F_n - expressed as a percentage of the ratio of the area of the grooves of the microrelief to the total area of the surface on which it is formed. It is this parameter that several researchers consider to be the one that determines the operational properties of a surface with a regular micro relief [18, 20].

In [20] it is indicated that the relative surface area F_n is a parameter of a partially regular microrelief that most fully characterizes almost all operational properties of the surface and, first of all, the actual contact area of the conjugated surfaces.

Summing up, it can be concluded that in all cases, regardless of the schemes and modes of application of the "pattern", the optimal value of the area of the grooves of the micro relief F_n was within 25-45%. At lower F_n values, the oil capacity of the mating surfaces is insufficient, and at higher values, their bearing capacity is significantly reduced.

Purpose

The problem of finding new types of regular and partially regular microreliefs is an important task for modern mechanical engineering.

Results

Regular micro reliefs [18] are periodically repeated grooves of the same depth, certain sizes and shape, the axial line of a continuous regular irregularity which is described by a periodic function. They are formed on the working surfaces of the parts and are characterized by the following constant parameters: amplitude A_k; step S_k which corresponds to the period of the periodic function; groove width b_k; the shape of the grooves - sinusoidal, triangular and other; by the type of microrelief, which determines the placement of rows of grooves between each other (I, II, III), which is determined by the interaxial step of the grooves of the micro relief S_o. The general appearance of the elements of the grooves of the regular microrelief is shown in Fig. 1.

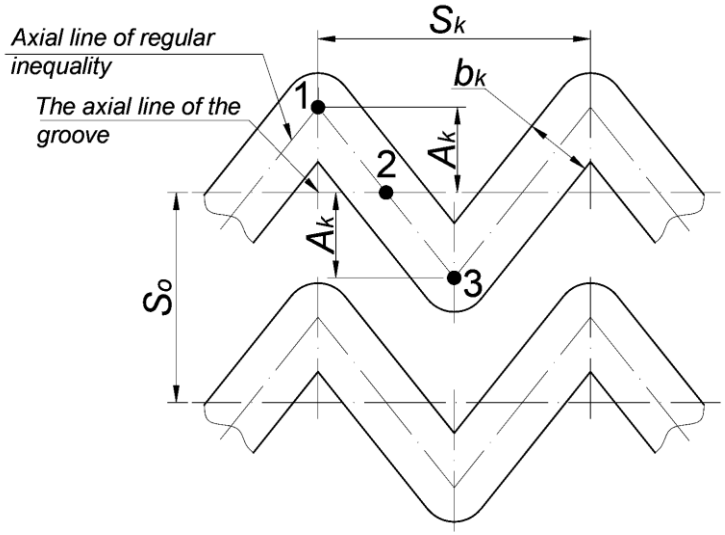

Fig. 1. Image of groove elements of regular type I microrelief (with grooves that do not touch) [18]

Since the depth of the grooves of such a microrelief is a constant value, and the change in the direction of the axial line of the grooves of the microrelief occurs in a plane parallel or coincident with the surface on which the microrelief is formed, it can be stated that such microreliefs are planar.

The creation of regular microreliefs on the working surfaces of machine parts ensures certain operational properties of these surfaces, in particular:

– reduction of the force of relative movement of conjugated surfaces;
– increase in the surface setting temperature under difficult operating conditions;
– increase in corrosion resistance of the surface;
- increase in oil capacity of the surface;
– increase in microhardness of the surface;
- increasing the fatigue strength limit of the surface and others.

Modern scientific research in the field of surface engineering is aimed at overcoming technical contradictions that arise when using regular microreliefs to ensure better operational properties of the working surfaces of machine parts.

The contradictions consist in finding a balance between the bearing capacity of the surface, which is greater with a larger contact area of the surfaces of the mating parts, and the area of the grooves of the microrelief, the growth of which provides the above advantages.

The classification of current areas of scientific research, in particular, forming technologies, tools, forming properties, process modelling, and others is given in the work [19].

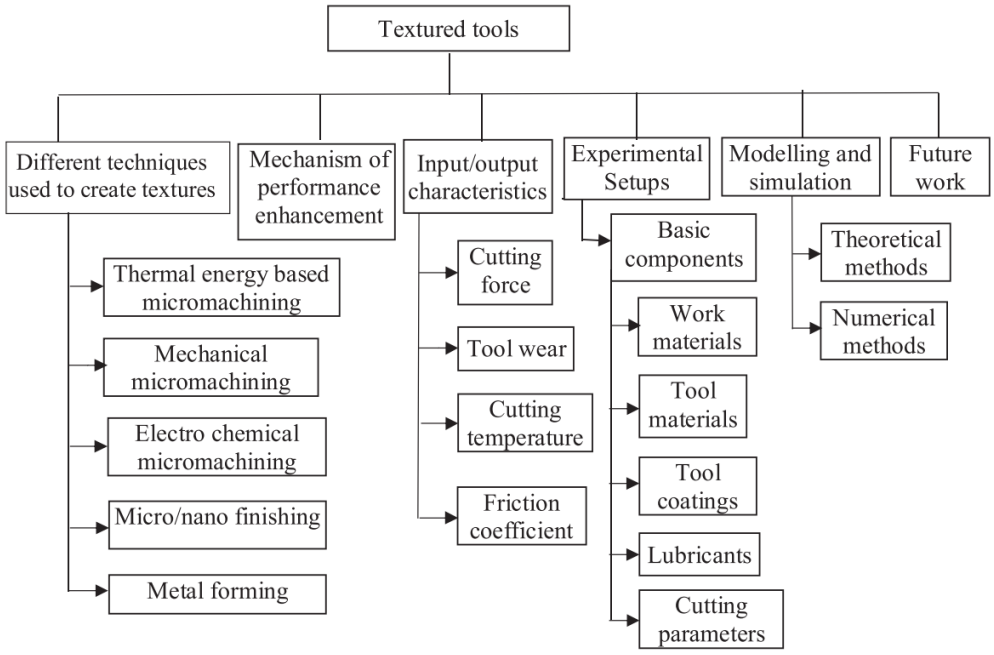

Fig. 2. Classification of areas of scientific research in the field of formation of regular micro reliefs [19]

To ensure the specified operational properties of the working surfaces, microreliefs with grooves of various shapes and sizes are formed. For example, in [19], the authors conducted a comparative study of the operational properties of flat rotating surfaces.

The analysis of scientific publications in the direction of the geometry of regular microreliefs allows us to identify the following directions for improving the geometry of regular microreliefs.

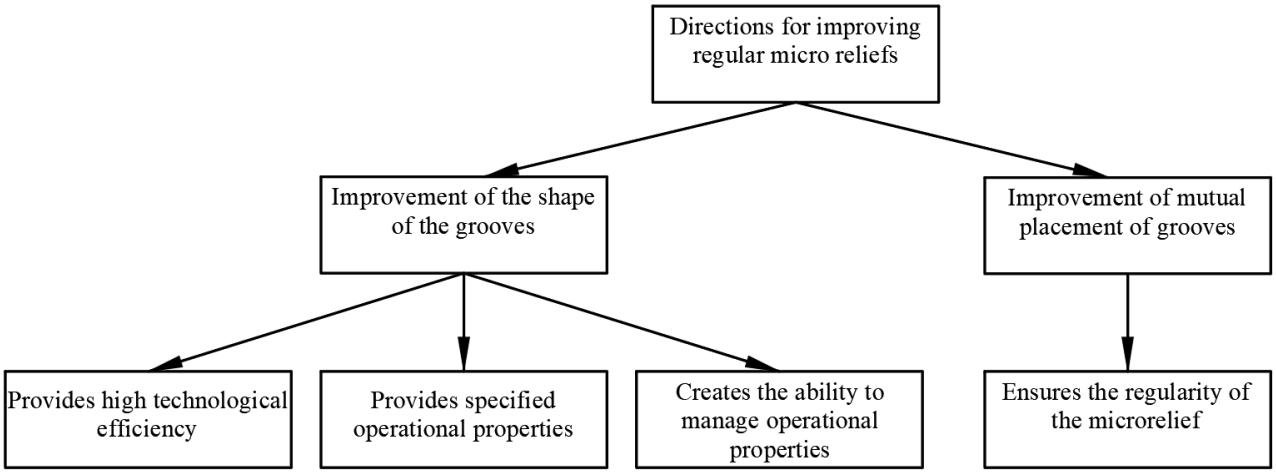

Fig. 3. Directions for improving the geometry of regular microreliefs

Most of the scientific research in this field is currently focused on ensuring the specified operational properties of surfaces with regular microreliefs and the regularity of microrelief grooves. The classic approach to this problem involves further gradual deterioration of the operational properties of the surface during operation.

In our opinion, the perspective lies in finding such a geometry of microrelief grooves, which would provide an opportunity to control the operational properties of the surface during its operation.

The reduction of the relative movement force is ensured by the reduction of the actual contact area of the conjugated surfaces with regular microreliefs, which is confirmed by numerous studies in this field [21] The relative area of the micro relief parameter shows a decreased in the share of the contact area of the conjugated surfaces of the friction pair.

The parameter related to the relative area of the microrelief is the relative reference area of the profile element – the ratio of the reference area of the profile elements to the base area of the surface elements, which is determined as a percentage [18]. As the relative area of the microrelief increases, the relative support area will decrease. An increase in the relative area of the microrelief increases the ability of the surface to hold an oil film, which improves its oil capacity. So finding a balance between the relative area of the microrelief and the relative support area is an important task. The relative bearing area can be increased by treating the surface of the friction pair with PPD methods. Therefore, an approach that provides full surface treatment by PPD methods with subsequent formation of microrelief grooves is promising. This idea is based on the fact that in the process of operation, the contact of the friction pair is carried out precisely by plane surfaces, and the formed microrelief only provides certain properties. Such properties include a reduction in the force of the relative movement of the coupled surfaces of the friction pair, an increase in the oil capacity of the surfaces, and others. We also put forward the hypothesis that the shape of the groove of the microrelief does not have a significant effect on the operational properties of the surface. One of the main parameters that determines the operational properties of a surface with regular microreliefs is the numerical value of the relative area of the microrelief.

We substantiate our proposed direction of improvement of regular microreliefs, which concerns the simplification of the shape of the grooves to a rectilinear one, that is, the improvement of their manufacturability. To form a profile of a microrelief with the shape of grooves, the axis of which lies in a plane that is parallel or coincident with the surface on which the microrelief is formed and can be described by a periodic function, the vibration method is used (usually on general-purpose machines) with special devices that ensure the oscillatory movement of the deformable element (usually a ball) of the tool, during which it performs reciprocating movements by the amplitude A_k with simultaneous longitudinal movement along the longitudinal axis of the microrelief groove. Also, for the formation of PMR, machines with CNC are often used, which perform the formation of the groove profile by the calculated coordinates of the control program.

The rate of deformation of the surface material by the deforming element during the formation of the micro relief is important since it determines the amount of plastic deformation, the surface structure of the formed groove, and its physical and mechanical properties. Experimental studies [22, 23] established that the optimum from the point of view of ensuring the overall roughness of the surface with a regular microrelief is the deformation speed of 1000 mm/min.

The technological imperfection of these microreliefs is that the real rate of deformation of the groove material will be reached only in the central part of the groove at point 2 (Fig. 1), and at points 1 and 3 (Fig. 1) the deforming element of the tool will change the direction of movement, respectively its speed will be zero. Accordingly, the planned physical and mechanical properties of the surface will also be obtained only in the central part of the groove of the microrelief, i.e. in the vicinity of point 2. Near the tops of the groove - points 1 and 3, the surface properties will be different, and the overall structure of the surface will be heterogeneous.

Therefore, to ensure the calculated rates of formation of microrelief groove surfaces and deformation of the surface material, the shape of the groove elements mustn't have tool stop points. This form can be grooves in the form of straight lines (Fig. 4) or grooves in the form of trochoids, cycloids and elements of circles.

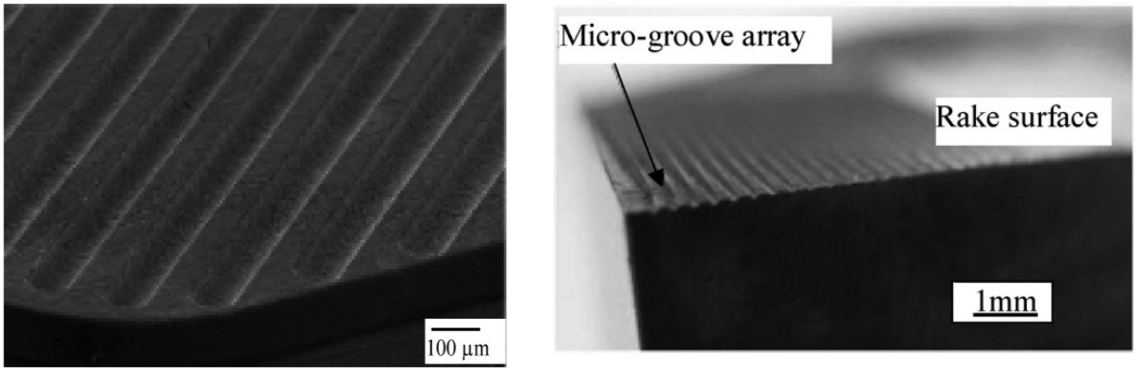

a **b**

Fig. 4. Regular microrelief with rectilinear grooves
Shape of linear texture created using Micro EDM [24] (a) **Diagonal texture created on the rake surface of the carbide tool [25] (b)**

Another technological difficulty in the formation of planar microreliefs, the axial line of a continuous regular unevenness described by a periodic function, is ensuring the regularity of the grooves of the microrelief. Violation of the regularity of the grooves of the microrelief is manifested in the change in the mutual arrangement of the elements of the grooves in a row and the rows of grooves of the microrelief between each other. The reason for this phenomenon on machines with mechanical gearboxes is the probabilistic nature of tool feed. This causes an increase in the value of the accumulated error and, accordingly, the pitch of the groove of the microrelief S_o (Fig. 5).

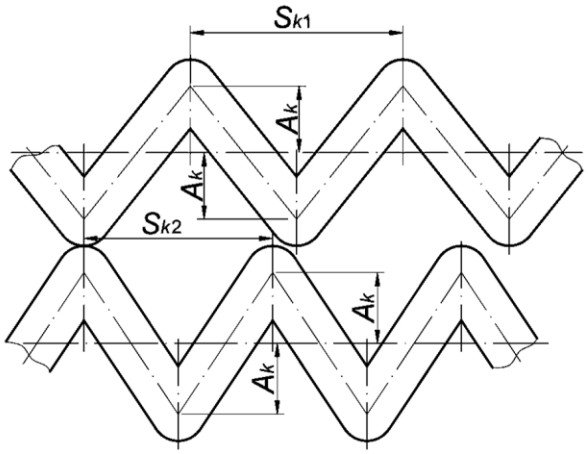

Fig. 5. Irregularity of microrelief grooves formed due to the difference in steps S_{k1} and S_{k2}

From the point of view of providing the necessary numerical value of the relative area of the microrelief, the violation of regularity is not a significant problem, since the regularity does not affect the value of the relative area of the microrelief. However, the violation of the regularity of the grooves of the microrelief creates heterogeneity of the physical and mechanical properties of the surface and its operational properties. It should be noted that when using CNC machines to form regular microreliefs, the problem of irregularity of the grooves is not observed.

Researchers are conducting other properties of textured surfaces. Studies confirming the ability of textured surfaces to hold liquids better are given in [26]. The authors conducted a study of the rolling speed of liquid drops from surfaces with different microreliefs. Test samples with nine types of regular microreliefs of different shapes were produced.

The results of these studies indicate that surfaces with formed microreliefs, in particular longitudinal grooves, can retain drops longer than flat surfaces and surfaces with other types of microreliefs.

Research studies in the direction of determining the optimal geometry of microrelief grooves that provide the minimum friction coefficient are given in [28].

The authors conducted a very important experiment to find the optimal geometry of the microrelief to ensure the minimum coefficient of friction. For comparison, 6 test samples with microrelief grooves of different geometric shapes were made.

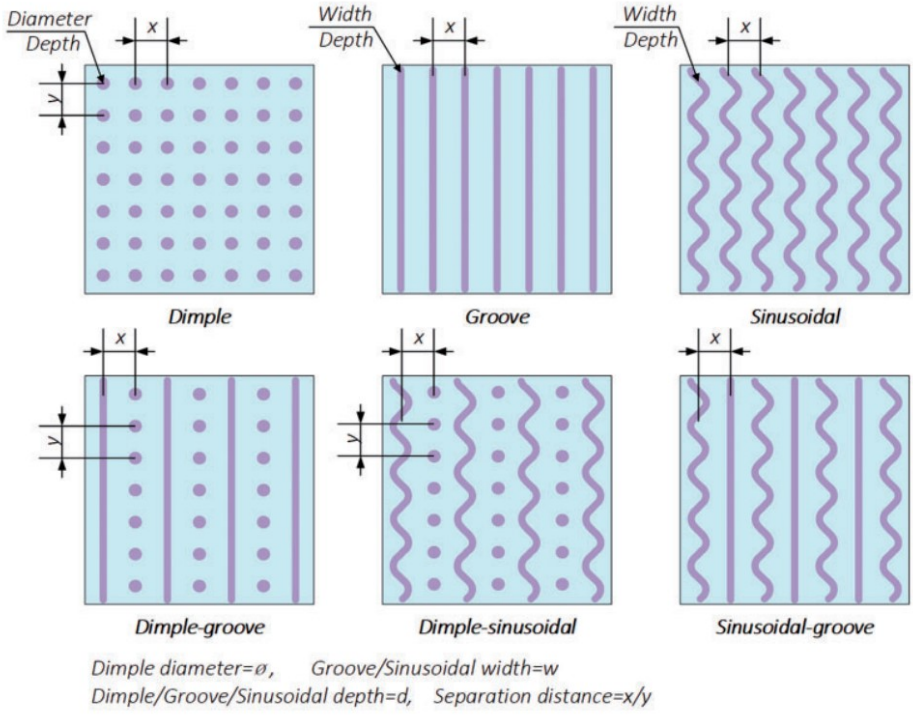

Fig. 6. Test samples with different geometries of grooves for determining the coefficient of sliding friction [28]

The results of research on the effect of the shape of the microrelief grooves on the friction coefficient are shown in Fig. 8 and indicate that the minimum friction coefficient is provided by the sample with the sinusoidal

shape of the microrelief grooves. However, the authors of this study made a false conclusion regarding the optimal shape of the microrelief, since the test samples, although they had the same dimensions, had different contact areas due to the different relative areas of the grooves of the microrelief.

We determined the relative area of the microrelief grooves of each of the grooves shown in Fig. 7 test samples and it was established that the test sample with sinusoidal grooves (ST) has the largest value of the relative area of the microrelief (Fig. 8). This explains the minimum value of the coefficient of friction since the contact area of the mating surfaces was minimal due to the maximum area of the grooves of the micro relief.

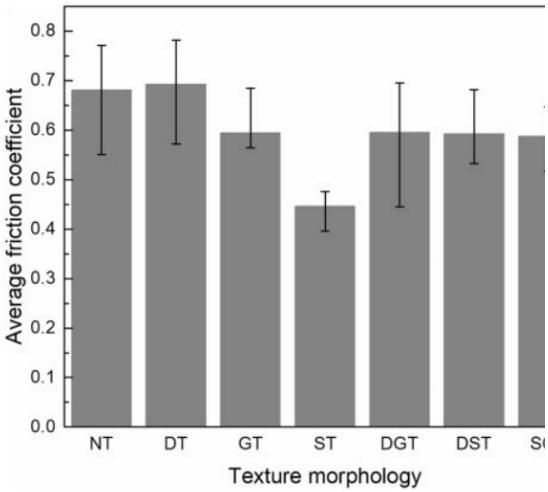

Fig. 7. Average friction coefficient of non-textured and textured surfaces [28]

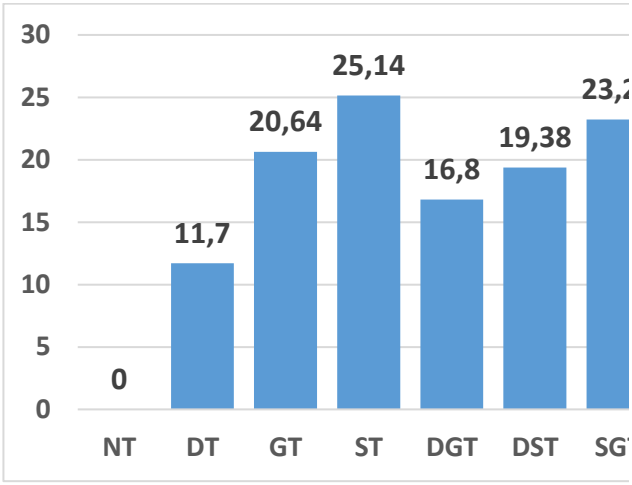

NT: non-textured ; DT: dimple-textured ; GT: groove-textured ; ST: sinusoidal-textured ; DGT: dimple – groove-textured ; DST: dimple – sinusoidal-textured ; SGT: sinusoidal – groove-textured

Fig. 8. Value of the relative area of microrelief grooves on the surface of the test samples

This study confirms our hypothesis that the numerical value of the relative area of microrelief is decisive in the formation of operational properties of a surface with regular microrelief. The pattern of microrelief grooves does not have a significant effect on the friction coefficient of the mating surfaces. Taking this into account, it is advisable to apply such a form of a groove, which is more technologically simpler and will provide higher labour productivity when forming a surface with regular microrelief and the possibility of controlling the operational properties of the surface.

Conclusions

1. To ensure the improvement of the operational properties of the working surfaces of parts of machines and mechanisms, it is advisable to use surface regularization methods, and the geometric characteristics of the created microrelief should be determined depending on the specific operating conditions.

2. Analysis of planar regular microreliefs with the shape of grooves, the axis of which lies in a plane that is parallel or coincident with the surface on which the microrelief is formed and can be described by a periodic function, allows us to state that they are technologically imperfect. This is manifested in the fact that the formation of periodically repeated vertices of elements in their geometry requires periodic stops of the tool, which leads to a decrease in productivity.

3. The analysis of the operational properties of surfaces with regular microreliefs established that these properties are provided mainly by the optimal value of the relative area of the microrelief and the uniform placement of the grooves of the microrelief on the surface. The shape of the grooves of the microrelief does not significantly affect the operational properties of the surface.

4. More optimal forms of grooves of microreliefs are proposed, which are technologically easier to manufacture (straight-line, cycloid, trochoid) and provide the possibility of controlling the operational properties of the surface by changing the geometry of the groove in the plane perpendicular to the surface on which they are formed. Pre-treatment of the surface by PPD methods followed by the formation of PMR will allow to increase in the relative support area of the friction pair.

References

1. Wu W, Chen G, Fan B, Liu J (2016) Effect of Groove Surface Texture on Tribological Characteristics and Energy Consumption under High Temperature Friction. PLoS ONE 11(4): e0152100. https://doi.org/10.1371/journal.pone.0152100

2. Zhang, Y., Zeng, L., Wu, Z., Ding, X. and Chen, K. (2019), Synergy of surface textures on a hydraulic cylinder piston. Micro Nano Lett., 14: 424-429. https://doi.org/10.1049/mnl.2018.5535

3. Koszela W, Pawlus P, Reizer R, Liskiewicz T, The combined effect of surface texturing and DLC coating on the functional properties of internal combustion engines, Tribology International (2018), doi: 10.1016/j.triboint.2018.06.034.

4. John, M.R. & Wilson, A. & Bhardwaj, A. & Abraham, Avinav & Vinayagam, B.. (2016). An investigation of ball burnishing process on CNC lathe using finite element analysis. Simulation Modelling Practice and Theory. 62. 88-101. https://doi.org/10.1016/j.simpat.2016.01.004

5. Sagbas, Aysun. (2011). Analysis and optimization of surface roughness in the ball burnishing process using response surface methodology and desirabilty function. Advances in Engineering Software. 42. 992-998. https://doi.org/10.1016/j.advengsoft.2011.05.021

6. Bataineh, Omar. (2019). Effect of Roller Burnishing on the Surface Roughness and Hardness of 6061-T6 Aluminum Alloy Using ANOVA. 8. 565-569. 10.18178/ijmerr.8.4.565-569

7. Wos, S., Koszela, W., & Pawlus, P. (2020). Comparing tribological effects of various chevron-based surface textures under lubricated unidirectional sliding. Tribology International, 146, 106205. https://doi.org/10.1016/j.triboint.2020.106205

8. Yu, H., Wang, X. & Zhou, F. Geometric Shape Effects of Surface Texture on the Generation of Hydrodynamic Pressure Between Conformal Contacting Surfaces. *Tribol Lett* **37**, 123–130 (2010). https://doi.org/10.1007/s11249-009-9497-4

9. Petterson, U.; Jacobson, S. Influence of surface texture on boundary lubricated sliding contacts. Tribol. Int. 2003, 36, 857–864. https://doi.org/10.1016/S0301-679X(03)00104-X

10. Ajay P. Malshe, Salil Bapat, Kamlakar P. Rajurkar, Han Haitjema. Bio-inspired textures for functional applications. CIRP Annals - Manufacturing Technology (2018), Volume 67, Issue 2, 2018, Pages 627-650 https://doi.org/10.1016/j.cirp.2018.05.001

11. Priya Ranjan, Somashekhar S. Hiremath. Role of textured tool in improving machining performance: A review. Journal of Manufacturing Processes. Volume 43, Part A, 2019. – pages 47-73. https://doi.org/10.1016/j.jmapro.2019.04.011

12. Jianfei Wang, Weihai Xue, Siyang Gao, Shu Li, Deli Duan. Effect of groove surface texture on the fretting wear of Ti–6Al–4V alloy. Wear. Vol. 486–487, 2021, 204079, https://doi.org/10.1016/j.wear.2021.204079

13. Slavov, Stoyan & Dimitrov, Diyan. (2018). A study for determining the most significant parameters of the ball-burnishing process over some roughness parameters of planar surfaces carried out on CNC milling machine. MATEC Web of Conferences. 178. 02005. https://doi.org/10.1051/matecconf/201817802005

14. Slavov, S.; Van, L.S.B.; Dimitrov, D.; Nikolov, B. An Approach for 3D Modeling of the Regular Relief Surface Topography Formed by a Ball Burnishing Process Using 2D Images and Measured Profilograms. Sensors 2023, 23, 5801. https://doi.org/10.3390/s23135801

15. Zhao, M.; Li, W.; Wu, Y.; Zhao, X.; Tan, M.; Xing, J. Performance Investigation on Different Designs of Superhydrophobic Surface Texture for Composite Insulator. *Materials* 2019, *12*, 1164. https://doi.org/10.3390/ma12071164

16. Dzyura, V. Classification of Partially Regular Microreliefs Formed on the End Surfaces of Rotary Bodies. Central Ukrainian scientific bulletin. Technical scientist. № 3(34), 2020. – p.129-135. https://doi.org/10.32515/2664-262X.2020.3(34).129-135

17. V. Dzyura, "Modeling of partially regular microreliefs formed on the end faces of rotation bodies by a vibration method", Ukrainian Journal of Mechanical Engineering and Materials Science, vol. 6, no. 1, pp. 30-38, 2020. https://doi.org/10.23939/ujmems2020.01.030

18. ГОСТ 24773-81 Поверхности с регулярным микрорельефом. Классификация, параметры и характеристики. Введ. 1982–07–01. – М. : Изд.-во стандартов, 1988. – 14 с.

19. Wos, S., Koszela, W., & Pawlus, P. (2020). Comparing tribological effects of various chevron-based surface textures under lubricated unidirectional sliding. Tribology International, 146, 106205. https://doi.org/10.1016/j.triboint.2020.106205

20. Sheider Yu.G. Service properties of parts with regular microrelief, 2nd ed., revised and augmented, Leningrad, Mashinostroenie, 1982, 248 p. (in Russian).

21. Pawlus, P.; Reizer, R.; Wieczorowski, M. Functional importance of surface texture parameters. Materials 2021, 14, 5326. https://doi.org/ 10.3390/ma14185326

22. Dzyura, V.; Maruschak, P.; Slavov, S.; Dimitrov, D.; Semehen, V.; Markov, O. Evaluating Some Functional Properties of Surfaces with Partially Regular Microreliefs Formed by Ball-Burnishing. Machines 2023, 11, 633. https://doi.org/ 10.3390/machines11060633

23. Dzyura, V., Maruschak, P., Slavov, S., & Dimitrov, D. (2023). Applying regular relief onto conical surfaces of continuously variable transmission to enhance its wear resistance. Transport, 38(3), 178–189. https://doi.org/10.3846/transport.2023.20628

24. L, Hiremath SS. A state-of-the-art review on micro electro-discharge machining. Procedia Technol 2016;25:1281–8. https://doi.org/10.1016/j.protcy. 2016.08.222

25. Xie J, Luo MJ, He JL, Liu XR, Tan TW. Micro-grinding of the micro-groove array on tool rake surface for dry cutting of titanium alloy. Int J Precis Eng Manuf 2012;13:1845–52. https://doi.org/10.1007/s12541-012-0242-9

26. Zhao, M.; Li, W.; Wu, Y.; Zhao, X.; Tan, M.; Xing, J. Performance Investigation on Different Designs of Superhydrophobic Surface Texture for Composite Insulator. Materials 2019, 12, 1164. https://doi.org/10.3390/ma12071164

27. Jianfei Wang, Weihai Xue, Siyang Gao, Shu Li, Deli Duan. Effect of groove surface texture on the fretting wear of Ti–6Al–4V alloy. Wear. Vol. 486–487, 2021, 204079, https://doi.org/10.1016/j.wear.2021.204079.

28. Zhan X, Yi P, Liu Y, Xiao P, Zhu X, Ma J. Effects of single- and multi-shape laser-textured surfaces on tribological properties under dry friction. Proceedings of the Institution of Mechanical Engineers, Part C: Journal of Mechanical Engineering Science. 2020;234(7):1382-1392. doi:10.1177/0954406219892294.

В.О. Дзюра Р.О. Бица. Аналіз напрямків вдосконалення регулярних мікрорельєфів.

В статті проведено аналіз особливостей площинних регулярних мікрорельєфів із формою канавок, вісь яких лежить в площині, що паралельна чи співпадає із поверхнею на якій формують мікрорельєф і її можна описати періодичною функцією. Встановлено, що основним параметром, який визначає експлуатаційні властивості поверхні з регулярними мікрорельєфами є відносна площа мікрорельєфу. Висунута гіпотеза про те, що геометрична форма канавок мікрорельєфу практично не впливає на експлуатаційні властивості поверхні. Мікрорельєфи вісь канавок яких можна описати періодичною функцією є технологічно недосконалими, оскільки при формуванні вершин канавок мікрорельєфу інструмент повинен здійснювати зупинки для зміни траєкторії руху. Складна геометрія канавок мікрорельєфу зменшує продуктивність їх формування, а складність забезпечення регулярності забезпечує неоднорідні фізико-механічні властивості поверхні. Запропоновано напрями вдосконалення форм мікрорельєфів, які забезпечать підвищення продуктивності їх формування та нададуть можливість керувати експлуатаційними властивостями поверхні.

Ключові слова: регулярні мікрорельєфи, експлуатаційні властивості, геометричні параметри, інженерія поверхні, періодичні функції, пара тертя

***Problems of Tribology**, V. 29, No 3/113-2024, 15-23*

Problems of Tribology
Website: http://tribology.khnu.km.ua/index.php/ProbTrib
E-mail: tribosenator@gmail.com

DOI: https://doi.org/10.31891/2079-1372-2024-113-3-15-23

Self-organization of the tribosystem under non-stationary conditions of friction from the standpoint of deformation-wave representations

Yu. O. Malinovskiy[1], O.A. Ilina[2], D. P. Vlasenkov[1], S. Yu. Oliinyk[3], O.O. Mikosianchyk[2]*

[1]Krivyi Rih professional college of National Aviation University, Ukraine
[2]National Aviation University, Ukraine
[3]Krivyi Rih National University, Ukraine
**E-mail: oksana.mikos@ukr.net*

Received: 10 June 2024: Revised: 28 June 2024: Accept: 15 July 2024

Abstract

Mechanisms of structural adaptation of contact surfaces and lubricating materials during friction with the dominance of deformation processes in tribocontact have been analyzed. The purpose of the work was to model the elastic-plastic properties of dissipative structures taking into account the anisotropic properties of the surface layers of the friction pairs and the boundary layers of the lubricating material. The modeling took into account the structural state of the latter formed due to heating and saturation with wear products, along with the physical and mechanical interaction of this layer with the outer surface of the part. An algorithm for determining the distributed tangent force along the length of the boundary layer of the lubricating material adjacent to the part has been developed based on the hypothesis of the wave-like state of the surface layer of the lubricating material on an absolutely flat (non-deformed) rough surface. Herein, under the action of tangent forces, the strip of lubricant is subject to horizontal compression and transverse movement. The distributed tangent stress along the length of the adjacency of the layer of densified lubricant to the part causes micro-slipping of the layer. Amplitude horizontal displacements of the boundary of the lubricant layer are determined when the beam-film is loaded with longitudinal stresses, which leads to partial disorientation of the film and loss of its originally rectilinear structured form, the transition of the lubricant layer to the state of the wave surface of a sinusoid shape. Also, a procedure for calculation of tangent forces causing the loss of elastic stability of the lubricant boundary layers resulting in the direct mechanical destruction of the lubricant boundary layer in the slipping zone of the contact surface is proposed based on the elastic-frictional interaction of this layer with the near-surface layer of the metal.

Key words: wear, self-organization, lubrication, deformation, boundary layers, tangent forces, rough surface.

Introduction

In terms of energy, contact interaction during friction can be represented as a set of processes of surface interaction with the flow of mechanical energy, whose law of distribution on the friction plane is adequate to the diagrams of tangent stresses and relative sliding speeds.The action of such source provokes changes in the internal structural and energy states of the contact layers of materials and the microgeometry of the contact, while most of the flow of mechanical energy is transformed into heat. The non-dissipative component of the mechanical energy is spent on the formation of secondary structures and wear [1].

The resistance of the lubricating film to mechanical destruction due to an increase in the shear rate gradient is a determining factor that ensures the normal performance of friction pairs under critical conditions. The destruction of the lubricating film during friction is one of the leading factors causing the intensification of energy processes occurring in the contact zone. First of all, this manifests itself in the violation of the structural adaptation of the contact surfaces and lubricant under critical friction conditions and the destruction of previously formed metastable structures [2].

Under the conditions of loading of flat surfaces by tangent forces with significant overloads (over the level of critical forces), flat surfaces are loaded by sliding forces and lose their original shape taking the shape of wavy surfaces, i.e. they acquire, in addition to longitudinal, noticeable transverse deformation.

Many effects under friction and wear of interacting surfaces in the presence of lubricant in the contact zone can be explained in terms of a deformation-wave approach, according to which, wave-like deformations appear in the zone located in front of the moving part. Tangent forces applied through a moving part (stamp) cause deformation-wave processes, in both stationary and moving parts. The deformation waves appear on the front surfaces of the interacting half-spaces of the contact surfaces and attenuate in the surface layer of the material at a length of 2-3 deformation half-waves. During the movement of the stamp, the deformation wave precedes the moving part by 2-3 half-waves.

In such a case, questions about the deflection arrow of the wave-like surface, the length of the deformation section of the beam-strip of the densified lubricating material, and the deformation half-wave length remain open. To determine these parameters, additional information is needed, which can be obtained on the basis of data from the energy indicators of interacting parts in the contact zone and data on the attenuation of the tribosystem's total energy along the deformation wave length.

Literature review

The service life, reliability in operation, structural strength, technical and economic indicators of the operation of parts of machines and mechanisms are largely determined by the mechanical properties of the steels and alloys of which they are made. Improving the quality of the surface of parts of machines and mechanisms increases the service life, especially when determined by the mechanical and tribotechnical properties of the surfaces [3].

The main changes in the material during friction are localized in a thin (up to several micrometers) surface layer. Localization of stresses and their impulsive character during friction lead to the generation of deformation defects such as point defects, dislocations, slip bands, etc. [4]. In [5], the peculiarities of the microdeformation of the surface layers and the mechanisms of titanium wear have been investigated. As shown, a decrease in the workaction of elastic-plastic deformation leads to a decrease in the resistance to the destruction of titanium during friction by 2-3 times, compared to the initial state. Wear occurs due to the formation of cracks and brittle destruction of surface layers. After the abrasion of the flooded layer, the plastic deformation of microprotrusions predominates.

Paper [6] considers thermodynamic systems where only deformation processes or tribochemical reactions dominate. Herein, irreversible damage to the metal is associated with the accumulation and interaction of structural defects, chemical or electrochemical interaction between the metal and the environment, and the formation of new surfaces during dislocation discharge. The thermodynamic system is homogeneous and isotropic, and fatigue processes occur under isobaric-isothermal conditions.

Initially, a sign-changing contact load plastically deforms the near-surface layers, causing their strengthening to a state that is akin to active static strengthening. The following reversible loads are associated with elastic re-deformation of the surface layers. The transition to the regime of elastic cyclic deformation is caused, on the one hand, by the strengthening of the metal and, on the other hand, by a decrease in the effective amplitude of the sign-alternating load due to the easing friction conditions when wear products appear. Further, the processes develop by the usual fatigue laws [7]: previously weakened layers are first disordered to a certain level, and after that (under pre-deformation conditions), their re-strengthening takes place, and these processes are periodically repeated [8]. Fatigue processes are accompanied by intensive formation of vacancies, the coalescence of which leads to the appearance of pores and microcracks [9].

The surface levels of the half-spaces in the tribocontact zone cannot move freely along the joint surface of the parts and meet on their way horizontal connections in the form of strong tangent forces which prevent a free shift of the elements of deformation layers. That is why, when tangent forces reach certain critical values, such layers become capable of bending, which gives them the ability to implement longitudinal stresses [10]. Under such a mechanism of interaction of parts, their surface layers either lose the longitudinal stability, or fall under the influence of cycic elastic deformations which disappear after the load is removed. Note that during the interaction of contacting parts, their surface layers (dissipative structures) are initially prone to plastic deformations due to the action of the dissipating component of the kinetic energy of the part movement and converting it into thermal energy. With further movement of the parts, surface strengthening of the outer layer occurs with a softer (pliable) base of the lower material layers of the contacting surfaces. It should be noted that the operation of friction pairs in the elastohydrodynamic and boundary lubrication mode leads to the densification of the lubricating layer on the contact surfaces activated by friction and the formation of boundary films of the lubricant in the zones adjacent to the surface layers of the parts as a result of structural adaptation. The loaded layers of the parts become covered with a densified and viscous boundary layer of the lubricant, whose consistency thickens due to the acquisition of non-Newtonian properties by the anisotropic layers, the appearance of small products of parts' wear and chemical interaction of metal surfaces and components of the lubricant. As a result of such interaction, the formation of a metal layer (beam-strip) and an elastoplastic coating of lubricant material takes place on the densified surface.

If we adhere to the idea of the formation of dissipative structures on metal parts under friction, then the parts under consideration represent an anisotropic medium that bears the load in the boundary layers (a densified beam-strip with an upper elastic-plastic layer of lubricant) from the tangent forces in the surface layer. These two outer layers lie on the inner layers of the parts ("elastic" base) through longitudinal and transverse connections.

Thus, the evaluation of the elastic-plastic properties of lubricating anisotropic layers under the conditions of tangent stresses is an important task in modeling the processes of physical-mechanical interaction of the base metal, oxides, and boundary layers of the lubricating material.

Purpose

To model the elastic-plastic properties of dissipative structures taking into account the anisotropic properties of the surface layers of friction pairs and the boundary layers of lubricants.

Modeling of elastic wave-like deformation processes under loading of contact surfaces by tangent forces during friction

Considering an anisotropic (three-layer) zone for interacting parts, we assume that the acting tangent force does not exceed certain critical force for the beam-strip $T_1 < T_{cr1}$. This means that the part that has a densified oil layer is located on an absolutely flat (non-deformed) rough surface. In this case, the beam-strip is under the action of limiters of transverse movements caused by the transverse connections of the elastic base. We also assume that there is a reactive tangent force between the densified layer of lubricant and the beam-strip

$$T = \Delta T + ql + cu(x), \tag{1}$$

where $q = f_{ad}Pb$ is the limit force of friction per unit length of the strip on the densified lubricant (l – is a number corresponding to the length of the beam-strip); P – is tht vertical load on the part; b – is the width of beam-strip; $u = u(x)$ is the longitudinal replacement of the densified lubricant; f_{ad} – is the coefficient of contact friction (adhesion) between the densified layer of lubricant (with wear particles of parts) and the beam-strip (surface layer of the part); c – is the longitudinal stiffness of the densified layer.

Using the values of dimensionless parameters according to [12] and assuming that $T_1 < T_{1cr}$ where T_{1cr} is the critical force for the beam-strip, we can obtain the dependence of the critical force on the length of the beam-strip. So, if

$$\bar{l} = \frac{l}{\pi}\sqrt[4]{\frac{k}{E_c I}} \tag{2}$$

and

$$\bar{T} = \frac{T}{\sqrt{kE_c I}}, \tag{3}$$

then by [12]

$$T_{cr} \approx 2\sqrt{kE_c I}. \tag{4}$$

In expressions (1) – (4), ΔT – is the excessive tangent force (the degree of overload T compared to T_{cr}); k – is the coefficient of stiffness of the elastic base by Winkler; E_c – is the modulus of elasticity of the surface layer of the part.

Considering the anisotropic three-layer problem (densified lubricant, densified surface layer of metal, and elastic base), we assume that there is an elastic-frictional connection between the metal layer and the densified layer of lubricant (Fig. 1). For such a task, the critical Euler force is determined by the coefficient of friction for liquid (or boundary) lubrication and does not depend on the length of the beam-strip (at least when the number of half-waves n on the outer side of the beam-film is $n \geq 3$ [1]). Therefore, significant inaccuracies in the formulation and solution of sthe problem are not allowed: the length of the beam-film l can be determined as the limit length under the conditions of relative mutual slippage for the beam-film with the three-layer anisotropic surface.

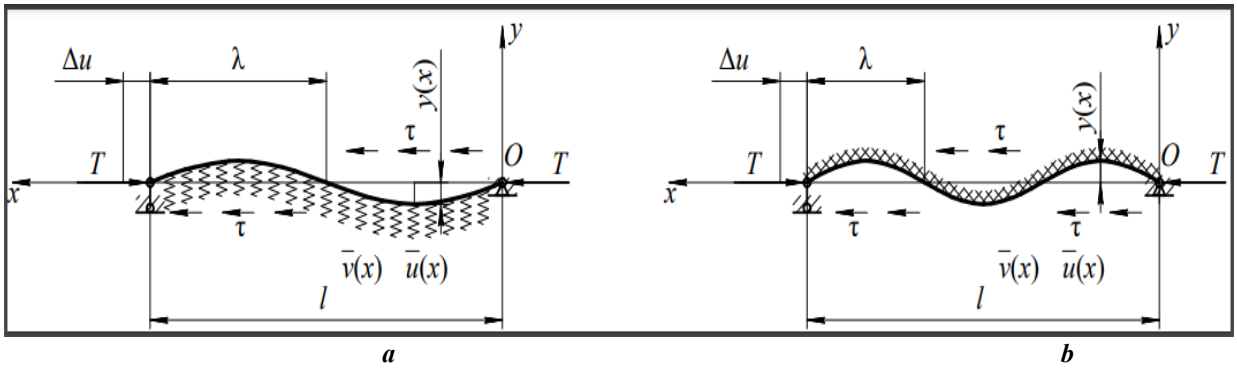

Fig. 1. Longitudinal bending of a beam-film: a – shape with two half-waves; b – shape with three half-waves

Let us consider a densified layer of lubricant on the surface of the part, assuming that this layer undergoes a mechanical-thermal destruction, densifies, becomes saturated with wear products, and interacts with the outer flat film strip of the part. This layer can be called the outer layer of the part that takes on itself the external normal and tangent loads on the friction pair.

The normal load is applied to the place where the parts join, whereas the tangent load acts in front of the moving part (stamp). Thus, the densified layer of lubricant, which is attached to the outer layer of metal, can be considered a thin elastic-plastic plate subjected to tangent forces in front of the stamp (Fig. 1).

Then the differential equation that describes the longitudinal bending of such a beam-strip (plate) under the action of tangent forces, has the form:

$$E_c I y^{IV} + T y'' + k y = 0, \tag{5}$$

where E_c – is the reduced modulus of elasticity of the densified layer of lubricant; $T = \Delta T + ql + cu(x)$ is the tangent force applied to the plate from the surface layers of the lubricant, which is spent on the loss of longitudinal stability of these layers and their accumulation of irreversible deformations; ΔT – is an excess tangent force, which is spent on the accumulation of final wave-like deformations in the surface layers; T_{cr} – is Euler's critical force for a beam-strip, at which the beam-strip loses its longitudinal stability; k – is the coefficient of stiffness of the elastic base of the part for the densified lubricant (herein, the reactive forces in the bases between the layers vary sinusoidally*); I* – is the moment of inertia of the cross-section of the hardened lubricant layer.

In expressions (5) and (15), the force T is such a longitudinal force that corresponds to the case when anisotropic layers of beam-films of parts and the elastic base do not meet the hypothesis of flat sections (that is, they undergo deplanation of flat sections).

The boundary conditions of the beam-film have the form:

$$\begin{matrix} y(0)=0;\, y''(0)=0; \\ y(l)=0;\, y''(l)=0, \end{matrix} \tag{6}$$

Considering the support of the rod as hinged, let us consider the set of functions*:*

$$y_n(x) = A_n sin\frac{\pi n x}{l}, \quad \text{where } n = 1, 2, 3, \ldots \tag{7}$$

Let us denote $\alpha_n = \frac{\pi n x}{l}$ where n is the number of half-waves on a curved beam of length l.

The set of functions (7) represents a system of the eigenfunctions of problem (5). For a beam-strip lubricant on a part of length l, two cases of lubrication can be calculated: 1 –- the lubricant strip lies on an elastic base ($k \neq 0$); 2 – the lubricant strip hinges on a part without an elastic base ($k=0$).

Turning to equation (7) and using the notion of deflection functions as the eigenfunctions of the problem

$$y(x) = A_n sin\alpha_n x, \tag{8}$$

then substituting (8) into equation (5), we obtain:

$$T_c = E_c I \alpha_n^2 + \frac{E}{2\alpha_n}. \tag{9}$$

The minimum (9) is found from the equation

$$\frac{\partial T_c}{\partial \alpha_n} = 0. \tag{10}$$

which yields

$$\alpha_n = \sqrt[3]{\frac{E}{4E_c I}}. \tag{11}$$

As follows from [13], the stiffness coefficient of the elastic base

$$k = \frac{E\alpha_n}{2} \tag{12}$$

or

$$k = \frac{E}{2} \cdot \sqrt[3]{\frac{E}{4E_c I}} \tag{13}$$

Based on (12), α_n can be interpreted as an unknown number of half-waves per film section of length π. In this case, we present $\lambda_n = \pi\sqrt[3]{\frac{4E_c I}{E}}$ as the half-wave length of the section of hardened lubricant that lost its stability.

The length of the film section that lost stability is equal to

$$l = n\lambda_n. \tag{14}$$

The critical load for a beam-film (an analogue of the Euler force) is determined based on (4) and (13).

Therefore, the initial growth rate of A_n (increase in corrugations) becomes less intense as they are filled, their longitudinal wave-like deformation is preserved, the hypothesis of a wave-like surface layer is realized, and the Winkler-Fuss hypothesis of a beam on an elastic base remains valid.

Turning to the function *y(x)*, we will treat A_n as the arrow of the beam-film deflection under the action of the tangent force (friction force). Initially, the deformed beam-film has a corrugated surface. In the process of further exfoliation of metal particles, their chemical interaction with oxide particles, and partial mechanical destruction of the boundary layers of the lubricant, the adjacent depressions between the corrugations will be filled with solid, heated to significant temperatures, metal wear elements, coked lubricant, and dust. At the same time, this process is reduced to the filling of the open elements of the corrugations with the mentioned sludge and the growth of an insignificant layer of a spot-strip, which under the influence of tangent force of liquid or semi-liquid friction also acquires a wave-like shape from the outside of the open corrugations. The height of these corrugations will be $\overline{A}_n < A_n$, and each subsequent layer of the oil film will fill the open corrugations of the deformed surface. Therefore, the initial rate of growth of A_n, that is the growth of corrugations, becomes less intense as they are filled,

their longitudinal wave-like deformation is preserved, the hypothesis of a wave-like surface layer is realized, and the Winkler-Fuss hypothesis of a beam on an elastic base remains valid.

Let us complicate the problem by taking into account that under the action of horizontal forces, the lubricant strip is subject to horizontal compression *u(x)* and transverse displacement *y(x)*. During longitudinal displacements of the lubricant strip, a compressive force acts on it, which consists of the overload force ΔT (as a result of applying a force to the strip from another moving part with a dynamic coefficient); ql is the adhesion force of the rigid lubricant to the surface layer of the metal; *cu(x)* is the elastic force under horizontal loading of the lubricant (in the middle of the strip thickness). Taking into account such loading of the beam-strip, the horizontal tangent force that acts on the lubricant layer is determined as follows:

$$T = \Delta T + ql + cu(x), \tag{15}$$

where $q=f_{ad}\ Pb$ – is the boundary limit value of the friction force (adhesion) between the metal and the solid lubricant layer; P – is the vertical load on the lubricant layer and the part; b – is the width of the lubricant layer; $u=u(x)$ – is the longitudinal displacement of the lubricant layer along the part during their mutual slipping; l – is the length of the lubricant layer during its slipping (in other words, the boundary length of the lubricant layer in front of the moving part); c – is the stiffness (horizontal) of the lubricant layer during its slipping; $u=u(x)$ – is the longitudinal (elastic) slippage of the lubricant layer during its deformation.

Note that the longitudinal stiffness $c = E_cF$ is equal to the product of the elasticity modulus of the elastic lubricant layer and its cross section $F = bh$ (where h is the lubricant layer thickness).

Then $\Delta T' = cu(x)$ is the distributed tangent force along the length of the lubricant layer adjoining the part. $\Delta T'$ is the reactive force preventing the loss of stability of the lubricant layer due to the action of the horizontal connection (in the zone under the stamp). Based on these considerations (and neglecting half the thickness of the lubricant film to exclude film compression processes), we can write a modified equation for the longitudinal stability of the lubricant film (instead of (5)) in the following form:

$$E_cIy^{IV} + Ty'' + ky - E_cFu = 0. \tag{16}$$

This equation includes the transverse displacement of the beam-film *y(x)* and the longitudinal displacement of the film beam *u(x).* Both of them arise under the action of the longitudinal force T and the bending deformation of the film beam. When the longitudinal force acts in the film beam, its movable end longitudinally shifts by the value $l - u$. Herein, the other end of the beam remains stationary. Then a nonlinear relationship is established between the longitudinal displacement of the beam-film and the transverse deflection. We find the longitudinal displacement of the movable end as the difference between the initial length of the film beam and the projection of the curved axis of the beam [14]:

$$u = l - \int_0^l cos\varphi\, ds = l - \int_0^l \sqrt{1 - \left(\frac{\partial y}{\partial s}\right)^2}\, ds, \tag{17}$$

where φ is the angle between the tangent to the arc of the curved beam-film and the longitudinal axis *Ox*.

Let us expand the integrand in a series using the Newton binomial formula:

$$\sqrt{1 - \left(\frac{\partial y}{\partial s}\right)^2} = 1 + \frac{1}{2}\left(\frac{\partial y}{\partial s}\right)^2 + \frac{1}{8}\left(\frac{\partial y}{\partial s}\right)^4 + \cdots. \tag{18}$$

If we substitute into expression (18) instead of *y(x){y(s)}* its value (8), then having performed needed transformations, we obtain:

$$u = \frac{\pi^2 A_n^2}{4l} + \frac{3}{64}\frac{\pi^4 A_n^4}{l^3} + \cdots. \tag{19}$$

With longitudinal displacements of the beam-film, an increment of the longitudinal force $\Delta T'$ occurs, which can be expressed through the deflection arrow A_n:

$$\Delta T' = E_cFu = E_cFu(A_n) \tag{20}$$

Substituting the expression for $u(A_n)$ in the differential equation (16) taking into account $\Delta T'$ and performing simple mathematical transformations, we arrive at an expression containing the deflection arrow of the film beam (for transverse deformations):

$$E_cI\frac{\pi^4}{l^4}A_n + T\frac{\pi^2}{l^2}A_n + kA_n - \left(\frac{\pi^2 A_n^2}{4l} + \frac{3}{64}\frac{\pi^4 A_n^4}{l^3}\right)E_cI = 0. \tag{21}$$

In evaluating the contribution of each term to the result when calculating A_n, we assume that the influence of the term containing A_n^4 is less significant than the others', so we write the result for A_n as follows:

$$A_n = E_cI\frac{4\pi^2}{l^3} + \frac{T}{l} + k\frac{4l}{\pi^2}. \tag{22}$$

Thus, we have obtained an expression for the deflection arrow of the beam-film on the elastic base of the part.

Since the film beam has bending, its transverse deflection is expressed by formula (22) through the modulus of elasticity of the first kind E_c, the moment of inertia of the beam cross section I, the compressive force that can reach its critical value T_{cr}, and the stiffness coefficient of the elastic base k. When $n = 1$, A_n takes the greatest value.

Since the transverse deflections of the beam-film (and in some cases -- of a flat membrane*) y(x)* are presented in the form:

$$y(x) = \sum_{n=1}^{\infty} A_n sin \frac{n\pi x}{l}, \tag{23}$$

where $sin \frac{n\pi x}{l}$ are the eigenfunctions of the film beam, then the curved surface (axis) of the film beam in front of the moving part (stamp) can consist of one, two, three or more half-waves (n=1,2,3,…).

The amplitude horizontal displacements $u(A_n)$ are determined in the first approximation from formula (19), retaining only the first term in the expansion.

When the beam-film is loaded with longitudinal forces, it loses its original rectilinear shape and acquires the shape of a wave surface. In this case, the vertices-sinusoids of the film break away from the still flat base. Herein, one end of the beam film remains movable, and when the surface layer of the part is shortened, micro-sli of the densified lubricant layer relative to the part occurs due to longitudinal deformation of the film-strip. In this case, the adhesion forces of the densified lubricant layer keep the beam-film from shifting relative to the part, as a whole. This indicates that the complete displacement of the lubricant layer of length l will occur when

$$T \geq ql, \tag{24}$$

that is, when

$$l \leq \frac{T}{q}. \tag{25}$$

In this problem, we determine the largest value of the amplitude of bending (transverse) waves

The eigenmodes can have the form of sinusoids, as shown in Fig. 1. The amplitude horizontal displacements $u\ (A_n)$ are determined in the first approximation from formula (19), taking only the first term in the expansion.

Based on these considerations, the length of the film-strip can be determined by formula (25).

Note that the tangent forces acting in anisotropic lubricant layers manifest themselves differently. In particular, in a densified lubricant layer adjacent to the metal, due to the physical and mechanical interaction of the base metal and oxides that fall into the boundary lubricant layer, the friction (adhesion) coefficient will be very high and exceed the dry friction coefficient in the outer layers of metal parts.

The coefficient of liquid friction between interacting parts is characteristic for the medium of oil films that have not been subjected to thickening and the ingress of solid particles, therefore it can be determined according to the theory of G.E. Svirsky [14] or other similar theories. Calculations by the Svirsky formulas are carried out taking into account the change in the kinetic energy of the material body under the assumption that the dissipation of the kinetic energy of a moving body occurs in the contact layer of small thickness h. The author [14] proceeded from the fact that the space between the rubbing bodies is filled with a mixture of gases, liquid vapors, and wear particles which are set in motion by the moving surfaces and provide additional viscous resistance expressed by the second term in (26). Then, for liquid lubrication, we obtain the following expression for the friction coefficient:

$$f = f_0(1 + \alpha_0^2 v^2)e^{-\alpha^2 v^2} + \frac{\xi}{hq_{sp}} v, \tag{26}$$

where f_0 – is the coefficient of static friction; α_0 – is a function of the densities of bodies 1 and 2; α – is a statistical coefficient associated with the probability law of the displacement of moving bodies; v – is the relative speed of moving bodies; ξ – is the viscosity coefficient of the liquid medium between the rubbing bodies; and q_{sp} – is the specific load.

Further, we will assume that the contact layer of thickness h consists of densified wear particles and chemically reacted lubricant particles.

Modeling of elastic-frictional connections between the surface film-strip and the base material of the part

Let us consider a qualitatively different approach to supporting the outer lubricant layers on an elastic base in terms of the action of elastic-frictional connections on the outer flat and rough surface of the interacting half-spaces. Therefore, we will take into consideration such connections that also protect the beam-strip (film) from losing elastic stability and direct layer displacement.

First, consider an analogy between the metal outer layer of the part and part's main mass, and the densified layer (film) of lubricant and the main mass of the part. It can be argued that in both cases, there is an elastic-frictional connection between the surface film and the base.

Therefore, we will proceed from the elastic-frictional interaction of the film-strip of lubricant with the boundary layer of metal, which lies on the metal massif supported by an elastic base (from vertical connections). On the other hand, the layer of oil film is connected to the base metal by horizontal connections. This means that

we introduce in the consideration the elastic-frictional interaction of the film-strip and the non-deformed layer from the linear displacement and deformation of the densified layer of lubricant (along the horizontal axis *Ox)*. That is, the displacements of the left end of the beam occur under the action of the tangent force T (Fig. 2), which can be applied smoothly with the coefficient of application intensity in the range $0 \le \alpha \le 1$.

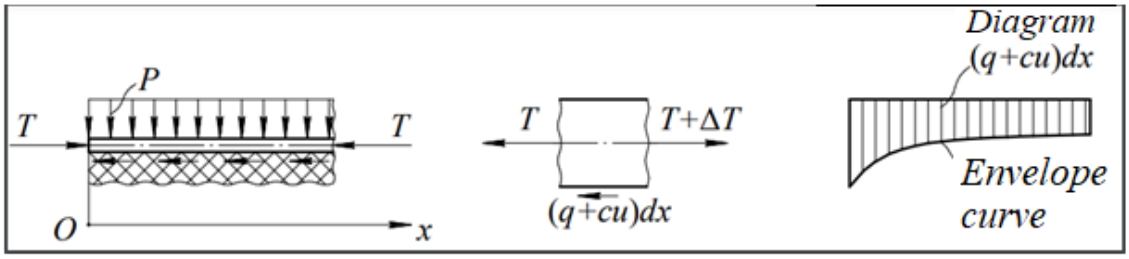

Fig. 2. Diagram of a beam-strip with horizontal connections

The dissipative structure of the lubricant densified layer (the beam-strip on an elastic base) is in equilibrium under the action of a system of horizontal forces. The equilibrium equation of an element is:

$$\frac{dT}{dx} - cu - q = 0, \tag{27}$$

where $cu(x) = s$ (per length unit) – is the intensity of tangent connections; c is the stiffness coefficient of elastic connections; q – is the limit friction force per strip length unit.

Longitudial force T can be expressed through deformation of the strip:

$$T = EF\frac{du}{dx}. \tag{28}$$

Then (22) may be written as:

$$\frac{d^2u}{dx^2} - \beta^2 u = \frac{q}{EF}, \tag{29}$$

where $\beta = \sqrt{\frac{c}{EF}}$ is a parameter characterizing the relative stiffness of elastic connections.

Equation (29) can have a solution in the form

$$u(x) = C_1 sh\beta x + D_1 ch\beta x - \frac{q}{c}. \tag{30}$$

Arbitrary constants C_1, D_1, as well as unknown length of the slipping zone a_1, are determined from three initial conditions

$$u(a_1, \alpha) = 0; u'(a, \alpha) = 0; u'(0, \alpha) = -\frac{\alpha T}{EF}. \tag{31}$$

The first two conditions relate to the right boundary of the zone, whereas the third one – to the initial strip cross section.

Then equation (29) acquires the form:

$$u(x, \alpha) = \frac{q}{c}\left[\sqrt{1 + \left(\alpha\beta\frac{T}{q}\right)^2}\, ch\beta x - \alpha\beta\frac{T}{q} sh\beta x - 1\right]. \tag{32}$$

In particular, at $x = 0$, that is at the beginning of the strip,

$$u(0, \alpha) = \frac{q}{c}\left[\sqrt{1 + \left(\alpha\beta\frac{T}{q}\right)^2} - 1\right]. \tag{33}$$

In equation (32), the force T can be considered applied suddenly (α=1), then (32) determines the initial displacement of the strip at x=*0*.

The equation is valid when the tangent force T is significantly less than the critical force for the strip, $T \ll T_{cr}$. That is, in this case, the hypothesis of flat sections is satisfied for the strip and longitudinal bending of the strip is not realized due to the action of tangent elastic connections.

Conclusions

1. An algorithm for determining the distributed tangent force along the length of the boundary layer of the lubricating material adjacent to the part was developed taking into account the anisotropic properties of dissipative structures and the hypothesis about the wave-like state of the surface layer of the densified lubricating material on an absolutely flat (non-deformed) rough surface on an elastic base.

2. A procedure for calculation of the tangent forces leading to the loss of elastic stability of the boundary layers of the lubricating material, which causes the direct mechanical destruction of the boundary layer in the zone of slipping of the contact surfaces, is proposed taking into account the elastic-frictional interaction of the boundary layer of the lubricating material and the surface layer of the metal.

References

1. Yakubov F.Ya. Synergetics and self-organization processes during friction and wear. *Printed scientific works: Modern technologies of engineering*, Kharkiv: NTU «KhPI», 2010, 5, P.122-133. http://library.kpi.kharkov.ua/files/JUR/sutech5_2010.pdf

2. Mnatsakanov R. G., Mikosianchyk O. A., Yakobchuk O. Ye., Tokaruk V. V. Forecasting of the maximum linear wear of contact surfaces in extreme friction conditions. *Problems of friction and wear*, 2018, 4 (81), C. 4 - 12. https://doi.org/10.18372/0370-2197.4(81).13321

3. Meng D., Lv Z., Yang S. et all. A time-varying mechanical structure reliability analysis method based on performance degradation. *Structures*. 2021. Volume 34. P. 3247-3256. https://doi.org/10.1016/j.istruc.2021.09.085

4. He X., Gu F., Ball A. A review of numerical analysis of friction stir welding. *Progress in Materials Science*. 2014. Vol. 65. P. 1-66. https://doi.org/10.1016/j.pmatsci.2014.03.003

5. Pokhmursky V.V., Vynar V.A., Vasyliv Kh. B. et al. Peculiarities microstrain of surface layers and mechanisms wear α-titanium under the influence of hydrogen. *Problems of Tribology,* 2013, № 2, P. 21-26.

6. Kadin Y., Sherif M. Y. Energy dissipation at rubbing crack faces in rolling contact fatigue as the mechanism of white etching area formation. *International Journal of Fatigue,* 2017, Vol. 96, P. 114-126. https://doi.org/10.1016/j.ijfatigue.2016.11.006

7. Mughrabi H. Cyclic Slip Irreversibilities and the Evolution of Fatigue Damage. *Metallurgical and Materials Transactions A*, 2009, Vol. 40. P. 1257–1279. https://doi.org/10.1007/s11661-009-9839-8

8. Mikosyanchyk, O.O., Mnatsakanov, R.H., Lopata, L.A. et al. Wear Resistance of 30KhGSA Steel Under the Conditions of Rolling with Sliding. *Materials Science*. 2019. Vol. 55, P. 402–408. https://doi.org/10.1007/s11003-019-00317-9

9. Wang X-S. Fatigue Cracking Behaviors and Influence Factors of Cast Magnesium Alloys. *Special Issues on Magnesium Alloys*. InTech. 2011. Available at: http://dx.doi.org/10.5772/19075.

10. Mi Ch. Surface mechanics induced stress disturbances in an elastic half-space subjected to tangential surface loads. *European Journal of Mechanics - A/Solids*, 2017, Vol. 65, P. 59-69 https://doi.org/10.1016/j.euromechsol.2017.03.006

11. Chawla N., Chawla K. K. Metal Matrix Composites. Springer Science+Business Media New York, 2013. 370 p. https://doi.org/10.1007/978-1-4614-9548-2

12. Luongo A., Ferretti M., Simona Di N. Stability and Bifurcation of Structures: Statical and Dynamical Systems. Springer Cham, 2023, 706p. https://doi.org/10.1007/978-3-031-27572-2

13. Wang X. Z., Yi J. T., Sun M. J. et al. Determination of elastic stiffness coefficients for spudcan foundations in a spatially varying clayey seabed. *Applied Ocean Research,* 2022, Vol. 128, P. 103336. https://doi.org/10.1016/j.apor.2022.103336Get rights and content

14. Uchitel A. D., Malinovsky Yu. A.,. Danilina G. V et al. Influence of parametric resonance on the mechanism of destruction of contacting surfaces during training and wearing. *Metal Journal,* 2018, №4. C. 65-73. https://www.metaljournal.com.ua/assets/Journal/Uchitel.pdf

Маліновський Ю. О., Ільїна О. А., Власенков Д. П., Олійник С. Ю, Мікосянчик О. О. Самоорганізація трибосистеми в нестаціонарних умовах тертя з позицій деформаційно-хвильових уявлень.

Проаналізовано механізми структурної пристосованості контактних поверхонь та мастильного матеріалу при терті при домінуванні деформаційних процесів в трибоконтакті. Мета роботи полягала в моделюванні пружньо-пластичних властивостей дисипативних структур з урахуванням анізотропних властивостей поверхневих шарів пар тертя та граничних шарів змащувального матеріалу. При моделюванні враховувався структурний стан граничного мастильного шару, набутий в результаті його нагрівання та насичення продуктами зносу, а також враховувалася фізико-механічна взаємодія цього шару із зовнішньою поверхнею деталі. Розроблено алгоритм визначення розподіленого дотичного зусилля по довжині примикання граничного шару мастильного матеріалу до деталі з урахуванням гіпотези про хвилеподібний стан поверхневого шару мастильного ущільненого матеріалу на абсолютно плоскій (недеформованій) шорсткій поверхні з пружною основою. Враховано, що під дією дотичних сил смужка мастильного матеріалу піддається дії горизонтального стиснення та поперечного переміщення. Розподілене дотичне зусилля по довжині примикання шару мастильного матеріалу до деталі обумовлює мікроковзання шару ущільненого мастильного матеріалу. Амплітудні горизонтальні зміщення граничного шару мастильного матеріалу визначаються при навантаженні балки-плівки поздовжніми зусиллями, що призводять до часткової дезорієнтації плівки і втрати своєї первісно прямолінійної структурованої форми, що сприяє переходу шару мастильного матеріалу в стан хвильової поверхні у формі синусоїда. Також запропоновано розрахунок визначення дотичних зусиль, спрямованих на втрату пружної стійкості граничних шарів мастильного матеріалу, що призводить до безпосередньої механодеструкції граничного шару в зоні проковзування контактних поверхонь, з урахуванням пружно-фрикційної взаємодії граничного шару мастильного матеріалу з приповерхневим шаром металу.

Ключові слова: wear, самоорганизація, змащування, деформація, граничні шари, дотичні зусилля, шорстка поверхня.

***Problems of Tribology**, V. 29, No 3/113-2024, 24-30*

Problems of Tribology
Website: http://tribology.khnu.km.ua/index.php/ProbTrib
E-mail: tribosenator@gmail.com

DOI: https://doi.org/10.31891/2079-1372-2024-113-3-24-30

Dependence of wear of friction pairs of the mechanism for loading solid household waste into a garbage truck on the characteristics of antifriction materials

O.V. Bereziuk[1], V.I. Savulyak[1], V.O. Kharzhevskyi[2], O.V. Serdiuk[1], V.Ye. Yavorskyi[1]

[1]Vinnytsia National Technical University, Ukraine
[2]Khmelnytskyi National University, Ukraine
E-mail: berezyukoleg@i.ua

Received: 15 June 2024: Revised:10 July 2024: Accept: 30 July 2024

Abstract

The article is dedicated to the establishment a regression dependence of wear of friction units of the mechanism of loading a garbage truck on the properties of antifriction materials. By using a first-order planning of experiment with first-order interaction effects using the Box-Wilson method, an appropriate regularity of wear of friction units of the garbage truck loading mechanism on the properties of antifriction materials has been determined. It is established that, according to the Student's criterion, among the studied factors of influence, the wear of friction units of the garbage truck loading mechanism is most influenced by the pressure in the friction zone, and the least – by the Brinell hardness of the antifriction material. The response surfaces of the objective function – wear of friction units of the garbage truck loading mechanism and their two-dimensional cross-sections in the planes of the influence parameters are shown, which allow to clearly illustrate the specified dependence of this objective function on individual influence parameters. It has been established that an increase in the pressure in the friction zone and sliding speed by 60% leads to an increase in the wear of friction units of the garbage truck loading mechanism during reverse motion by 6.3...34%, depending on the properties of antifriction materials. The expediency of conducting further research to determine ways to further improve the wear resistance of friction units of the mechanism for loading solid household waste into a garbage truck has been shown.

Keywords: wear, friction units, loading mechanism, garbage truck, solid household waste, dependence, experiment planning.

Introduction

Among the actual tasks of the municipal engineering industry of Ukraine, in particular for mobile equipment of the manipulator type, which include garbage trucks, the problems of increasing the wear resistance, reliability and durability of machine parts have a prominent place [1, 2]. In Ukraine, collection and transportation of municipal solid waste (MSW) is carried out mainly by body garbage trucks with manipulators as loading bodies. There are almost 3,700 garbage trucks in use in Ukraine that are capable of compacting solid waste, reducing transportation costs and the required landfill space. At the time of the technological operation of loading MSW into a garbage truck, the friction units in the form of hinge joints of its manipulator are subject to intensive wear. This is due to the considerable weight of the container with solid waste (up to 500 kg) that is lifted, operation in reverse mode (reverse rotation), a significant number of work cycles per route, as well as operation in a wide range of relative humidity, temperature, and environmental dust. Deterioration of material quality or insufficient lubrication leads to increased friction forces in hinge joints and increased vibrations in the system, which in turn can affect the dynamic stability of the manipulator and its ability to withstand high loads in reverse friction conditions. Wear and tear on friction components can affect the efficiency and safety of a refuse garbage truck's manipulator, which can have negative consequences for both operators and the environment. According to statistics, the wear and tear of the fleet of garbage trucks owned by municipal enterprises in Khmelnytskyi region

over the 2015-2020 years, despite the measures taken, has decreased only from 63 % to 59 % [3]. According to the Resolution of the Cabinet of Ministers of Ukraine No. 265 [4], the problem of ensuring of the usage of modern, highly efficient garbage trucks in the domestic municipal sector as the main link in the structure of machines for the collection, transportation and primary processing of solid waste is a key task. This allows to solve a number of environmental problems and improve the overall reliability of the country's utilities. Planning for the renewal, maintenance and repair of garbage trucks is facilitated by determining the regression dependence of wear of the friction units of the garbage truck loading mechanism on the properties of antifriction materials.

Analysis of the recent research and publications

In the work [5] a method for optimizing a robotic cell by changing the placement of the robot manipulator in the cell in applications with a fixed endpoint trajectory is described. The aim of the study was to reduce the overall wear of the robot's joints and prevent uneven wear of the joints when one or more joints are under more load than others. Joint wear was approximated by calculating the integral of the mechanical work of each joint along the entire trajectory, which depends on angular velocity and torque. The method is based on the usage of dynamic modelling to estimate the torques and velocities in the robot's joints for its certain positions. It is established that, provided the robot base is correctly positioned, the total wear of the joints of the robotic arm of the robot manipulator can be reduced by 22...53%, depending on the trajectory.

The scientific article [6] investigates the performance of reversible friction joints in the control systems of transport machines under various operating conditions. It is noted that hinge assemblies and joints are among the most critical and highly loaded connections of industrial transport machines, and are also the most metal-intensive and heavily loaded machine elements that connect the main structural elements and functional units. As a result of the analysis of the wear of parts of reversible joints of transport machines in a corrosive and abrasive environment, their increased wear and unreliability in operation were observed. The study of the operating loads of the hinge parts of coupling devices has made it possible to establish that plastic contact occurs in the friction pair, which leads to increased wear of the friction surfaces. Improvements to the design of the joints are proposed, which provide auto-compensation for wear of the friction surfaces of mating parts and improve their operation by constantly supplying lubricant to the friction zone.

The authors of the paper [7] determine a dependence of maximum impact dynamic stresses in the most loaded section of the garbage truck boom depending on the wear of the manipulator joint and the level of its load, according to the Fisher criterion. It is established that, according to the Student's criterion, among the considered factors of influence, the wear of the manipulator joint has the greatest impact on the maximum impact dynamic stresses in the most loaded section of the manipulator boom, and the level of its load has the least impact. The response surface of the target function – the maximum impact dynamic stresses in the most loaded section of the manipulator boom and their two-dimensional sections in the planes of the impact parameters are shown, which allow to clearly illustrate the specified dependence of this target function on individual impact parameters. It is established that the wear of the joint by 1000 μm leads to an increase in the maximum impact dynamic stresses in the most loaded section of the garbage truck manipulator boom by 2.6...4 times, depending on the level of its load. The expediency of further studies of the influence of antifriction materials on the wear of friction units of the mechanism for loading solid household waste into a garbage truck has been shown.

Article [8] analyses the types of wear of hinge joints of forestry manipulators, which made it possible to identify possible ways to increase their wear resistance, which will help design engineers to increase the working life of hinge joints depending on the requirements for them in the process of work. It is noted that manipulator-type machines often operate in conditions of ambient temperature differences, which negatively affects the properties of lubricants and joint materials. At low temperatures, the materials of friction pairs become more brittle, the yield strength decreases and the stiffness of working surfaces increases. This complicates the processes of dislocation movement and annihilation, the occurrence of exoelectronic emission and, in turn, intensifies the wear process. At low ambient temperatures, the lubricant hardens or its viscosity increases, significantly reducing its lubricating properties. In the summer time, at high temperatures, the lubricant heats up and can leak out of the friction zone, which negatively affects the lubrication and cooling of working surfaces. To prevent this, it is proposed to protect the hinge joints of manipulators from the polluting and corrosive effects of the environment, as well as from leakage of lubricant, with special sealing devices. The expediency of introducing contact and labyrinth sealing into the design of hinges has been established.

In the work [9], a mathematical model is proposed to determine the geometric parameters of the manipulator's structural elements depending on the maximum outreach, load capacity, and other kinematic parameters of the machine. Given the frequency of operation of the manipulator's hinge joints, it is noted that there is no hydrodynamic friction process there, since the process proceeds under conditions of semi-dry and boundary friction. In contrast to the established hydrodynamic friction process, the operation of sliding bearings under semi-dry and boundary friction increases the wear of friction surfaces. This, in turn, causes a violation of kinematic accuracy, additional dynamic loads, impacts, vibrations, which lead to fretting corrosion and destruction. It is proposed to reduce the friction force by applying lead, phosphate, indium coatings to the mating parts of manipulator joints. It is established that contact wear can be reduced by introducing oil and fat-based lubricants or

grease lubricants, which at a temperature of 25 °C take on a thick ointment-like consistency. The expediency of using phosphate and anodic metal coatings for better lubricant retention on the surface has been determined.

The work [10] describes a method for synthesizing the trajectory of a manipulation robot by degrees of mobility. It was found that the bending of the rod causes support reactions in the contact zone, as in a beam on two supports. After determining the contact pressure, it is possible to determine the possibility of wear of the surfaces of the hydraulic cylinder, rod and groundbox. It was found that the contact stress, reaching one third of the tensile strength, with complete safety of the rod from bending, can cause a significant acceleration of wear of friction surfaces. This makes it possible to clarify the cause of the identified wear patterns and the specifics of their identification.

In the paper [11] it is found that when creating new promising designs of hinge joints, it is necessary to apply an integrated approach to scientific and technical solutions to take into account a significant number of parameters that affect their performance. As a result, it is possible to create new design solutions that provide increased performance of hinge joints of logging machine manipulators. They can significantly improve the mechanical and tribotechnical characteristics, as well as optimize the thermal operation of the assembly.

The authors of [12] specified that the usage of plastics as an antifriction material eliminates the need for periodic supply of lubricant to the gap of a hinge joint. As a result, the need for oil channels disappears. In addition, the metals used to make the shaft and the enclosing lug are mated to a softer sliding material, so that wear on the surface layers of the mating parts due to elastic and plastic deformation will occur primarily in the sliding sleeve and be transmitted to the pin and enclosing lug to a lesser extent. Antifriction materials can significantly increase the service life of hinge joints.

The research paper [3], by means of the regression analysis usage, identified a dependence that describes and allows predicting the dynamics of garbage trucks' wear and tear in the Khmelnytskyi region as a whole, as well as planning the infrastructure (composition and renewal of garbage trucks, production facilities for maintenance and repair) of municipal enterprises, which is necessary to solve the problem of solid waste management.

The paper [13] presents the results of the analysis of the designs of the grippers of body manipulators of garbage trucks. The results of a study of the reliability of garbage trucks are shown. A calculation scheme of a garbage truck as an oscillating system is developed. The type of oscillations of the garbage truck frame in the operating mode is determined. The regularities of force formation in the grab-tank-grab system are determined. It is established that the maximum loads occur on the traction rod and rod of the hydraulic cylinder, which increase with the increase in the mass of the container. Changes in the mass of the garbage truck do not affect the magnitude and amplitude of the loads, but only their frequency response changes. Observations of garbage trucks can determine that the largest number of failures occurs due to wear and corrosion of the working surfaces of the working equipment parts. 32% of all failures of hydraulic drive parts are caused by hydraulic cylinder failures caused by wear of the working surfaces of the mating surfaces, deformation of the rod and cylinder during operation, which is caused by uneven loading of the body, as well as abrasive wear of the working surfaces in hard conditions of the garbage truck. The main reason is the wear of the working surfaces of the main parts in the hydraulic drive structure, in particular – spools and hydraulic distributor housings, hydraulic cylinder rods, etc., as well as water-abrasive damage due to untimely replacement of the working hydraulic fluid and the use of poor-quality or worn sealing parts such as hydraulic cylinder seals, which causes dust particles and wear products to enter the sliding zone, accelerating the wear process of the working surfaces of the parts. In order to produce chrome coatings with high deposition quality and performance, cold self-regulating electrolyte chrome plating is proposed as one of the most promising methods of restoring worn parts.

However, the authors did not find any specific mathematical regularities describing the wear of friction units of the garbage truck loading mechanism depending on the properties of antifriction materials as a result of the analysis of known publications.

Aims of the article

Determination of the regression dependence of wear of friction units of the garbage truck loading mechanism on the properties of antifriction materials.

Methods

The regression dependence of wear of friction units of the garbage truck loading mechanism on the properties of antifriction materials was determined by planning a first-order experiment with first-order interaction effects using the Box-Wilson method [14]. The coefficients of the regression equations were determined using the developed computer program "PlanExp", which is protected by a certificate of copyright registration for the work and is described in [15].

Results

Preliminary processing of the results of experimental research [12] showed that the wear of friction units of the garbage truck loading mechanism is a function of the following 4 main parameters:

$$u = f(f, HB, v, p), \tag{1}$$

where f – the friction coefficient of a pair of steel - antifriction material; HB – the Brinell hardness of the antifriction material; v – the sliding velocity, m/s; p – the pressure in the friction zone, MPa.

Investigating the influence of the above factors on the wear of friction units of the garbage truck loading mechanism when processing the results of single-factor experiments by regression analysis is associated with significant difficulties and amount of work. Therefore, in our opinion, it is advisable to conduct a multifactorial experiment to obtain a regression equation for the response functions – wear of friction units of the garbage truck loading mechanism by planning a multifactorial experiment using the Box-Wilson method [14].

The wear values of the friction units of the garbage truck loading mechanism during reverse motion for different values of the properties of antifriction materials are given in Table 1 [12].

Table 1

Values of wear of the friction units of the garbage truck loading mechanism for different values of the properties of antifriction materials [12]

Friction coefficient of a pair of steel - antifriction material f	Hardness HB of the antifriction material according to Brinell	Sliding velocity v, m/sec	Pressure in the friction zone p, MPa	Wear amount in reverse motion u, μm
0.1	250	0.08	1.06	127
0.1	250	0.13	1.7	170
0.08	235	0.08	1.06	63
0.08	235	0.13	1.7	67
0.1	170	0.08	1.06	117
0.1	170	0.13	1.7	150

Based on the data in the Table 1, using the planning of a first-order experiment with first-order interaction effects, using the developed software, which is protected by a certificate of copyright law, after rejecting insignificant factors and interaction effects by the Student's criterion, the regularity of wear of friction units of the mechanism for loading a garbage truck on the properties of antifriction materials was determined:

$$u = 458.2f + 0.1696HB + 4366v - 546.2p + 33782fv \text{ [μm]}. \tag{2}$$

Fig. 1 shows the response surfaces of the target function – wear of the friction units of the garbage truck loading mechanism u and their two-dimensional sections in the planes of the influence parameters, plotted using the regularity (2), which allows us to clearly illustrate this dependence.

It was found that according to the Fisher's criterion, the hypothesis about the adequacy of the regression model (2) can be considered correct with 95% confidence. The coefficient of multiple correlation was $R = 0.99857$, which indicates the high accuracy of the obtained results.

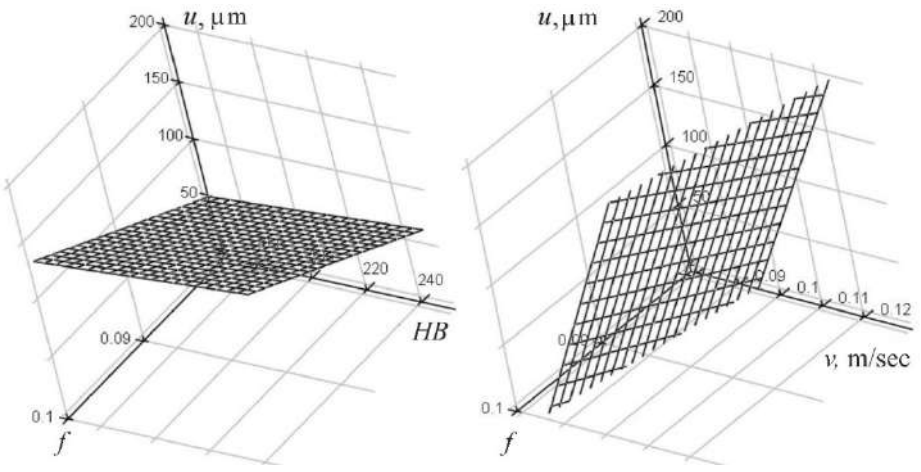

a) **b)**

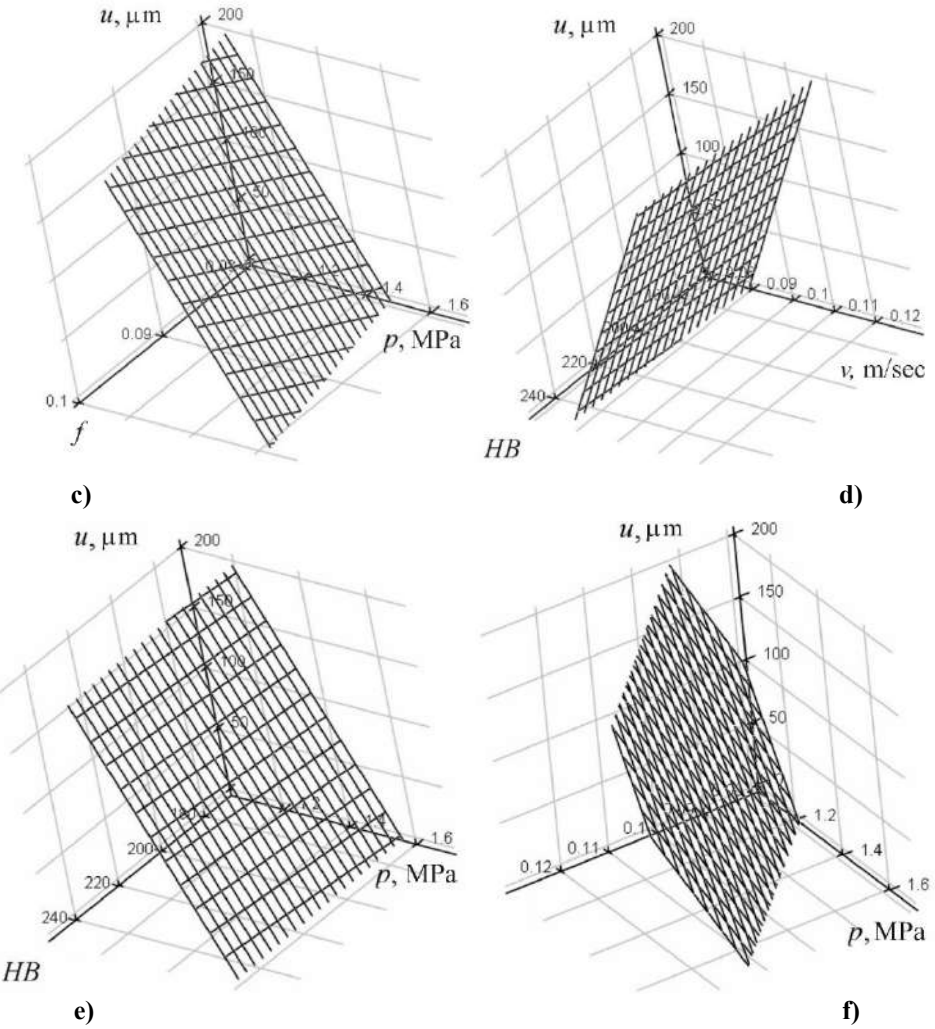

Fig. 1. Response surfaces of the objective function - wear of the friction units of the garbage truck loading mechanism *u* in the planes of influence parameters: a) $u = f(f, HB)$; **b)** $u = f(f, v)$; **c)** $u = f(f, p)$; **d)** $u = f(HB, v)$; **e)** $u = f(HB, p)$; **f)** $u = f(v, p)$

According to the Student's criterion, it was found that among the studied factors of influence, the pressure in the friction zone has the greatest impact on the wear of the friction units of the garbage truck loading mechanism, and the Brinell hardness of the antifriction material has the least.

It has been established that an increase in the pressure in the friction zone and sliding speed by 60% leads to an increase in the wear of friction units of the garbage truck loading mechanism during reverse motion by 6.3...34%, depending on the properties of antifriction materials.

The determination of the ways to further improve the wear resistance of the friction units of the mechanism for loading solid household waste into a garbage truck requires further research.

Conclusions

An adequate dependence of the wear of friction units of the mechanism for loading garbage trucks on the properties of antifriction materials has been determined according to the Fisher criterion. It is established that, according to the Student's criterion, among the studied factors of influence, the wear of friction units of the garbage truck loading mechanism is most affected by the pressure in the friction zone, and the hardness of the antifriction material is the least. The response surfaces of the objective function – wear of friction units of the garbage truck loading mechanism and their two-dimensional sections in the planes of the influence parameters are shown, which allow to clearly illustrate the specified dependence of this objective function on individual influence parameters. It has been established that an increase in the pressure in the friction zone and sliding speed by 60% leads to an increase in the wear of friction units of the garbage truck loading mechanism during reverse motion by 6.3...34%, depending on the properties of antifriction materials. To determine the ways to further increase the wear resistance of friction units of the mechanism for loading municipal solid waste into a garbage truck, further research is required.

References

1. Khomenko IM, Kindrachuk MV, Kobrynets AK (2010) Hranychnodopustymyi znos mashyn [Maximum permissible wear of machines]. Problems of friction and wear, 52, 28-37.

2. Dykha O.V.(2018) Rozrahunkovo-eksperymentalni metody keruvannja procesami granychnogo zmashhuvannja tehnichnyh trybosystem [Computational and experimental methods of controlling processes of boundary lubrication of technical tribosystems]: monograph. Khmelnytskyi: KhNU

3. Bereziuk O.V., Savulyak V.I., Kharzhevskyi V.O. (2022) Dynamics of wear and tear of garbage trucks in Khmelnytskyi region. Problems of Tribology, 27(3/105), 70-75.

4. The Cabinet of Ministers of Ukraine (2004) Resolution No. 265 "Pro zatverdzhennia Prohramy povodzhennia z tverdymy pobutovymy vidkhodamy" ["On Approval of the Program for Solid Waste Management"]. URL: http://zakon1.rada.gov.ua/laws/show/265-2004-%D0%BF.

5. Kot T., Bobovský Z., Vysocký A., Krys V., Šafařík J., Ružarovský R. (2021) Method for robot manipulator joint wear reduction by finding the optimal robot placement in a robotic cell. Applied Sciences, 11(12), 5398.

6. Kovalevskyi S.V., Zaluzhna G.V., Vladimirov E.O. (2017) Doslidzhennia sharniriv reversyvnoho tertia mashyn promyslovoho transportu z metoiu pidvyshchennia yikh dovhovichnosti [Study of reversible friction joints of industrial transport machines in order to increase their durability]. Scientific Bulletin of Donbass State Machine-Building Academy, 2, 36-45.

7. Bereziuk O.V., Savulyak V.I., Kharzhevskyi V.O., Yavorskyi V.Ye. (2023) The influence of hinges wear on the dynamic load of the articulated boom of a garbage truck's manipulator. Problems of Tribology, 28(3/109), 18-24.

8. Serebryanskii A. (2014) Except the negative reverse effect and automatically compensate for wear in the hinge manipulators. DOAJ - Lund University: Concept: Scientific and Methodological e-magazine, 4 (Collected works, Best Article).

9. Chernik D.V., Chernik K.N. (2020) Mathematical model of a combined manipulator of a forest machine. In IOP Conference Series: Materials Science and Engineering, 5(919), 052037.

10. Baybatshaev M., Beysembaev A. (2014) Synthesis of manipulation robot programme trajectories with constraints in the form of obstacles. Informatyka, Automatyka, Pomiary w Gospodarce i Ochronie Środowiska, 1, 21-23.

11. Evelson L.I., Zakharov S.M., Pamfilov E.A., Rafalovskaya M.Y. (2000) PC-process of analysing and synthesising friction units using databases and expert systems. Journal of Friction and Wear, 21(4), 380-385.

12. Serebryansky A.I., Kanischev D.A., Kaptsov V.N. (2013) Constructive exception of friction reversibility based on the analysis of the operating characteristics of joint manipulators. Europaische Fachhochschule, 5, 21-24.

13. Kargin R.V., Yakovlev I.A., Shemshura E.A. (2017) Modelling of workflow in the grip-container-grip system of body garbage trucks. Procedia Engineering, 206, 1535-1539, https://doi.org/10.1016/j.proeng.2017.10.727.

14. Andersson O. (2012) Experiment!: planning, implementing and interpreting. John Wiley & Sons.

15. Bereziuk O.V. (2016) Modeliuvannia kompresiinoi kharakterystyky tverdykh pobutovykh vidkhodiv u smittievozi na osnovi kompiuternoi prohramy PlanExp" [Modelling the compression characteristics of solid household waste in a garbage truck based on the computer programme "PlanExp"]. Visnyk of Vinnytsia Polytechnic Institute, 6, 23-28.

Березюк О.В., Савуляк В.І., Харжевський В.О., Сердюк О.В., Яворський В.Є. Залежність зносу пар тертя механізму завантаження твердих побутових відходів у сміттєвоз від характеристик антифрикційних матеріалів

Стаття присвячена встановленню регресійної закономірності зносу вузлів тертя механізму завантаження сміттєвоза від властивостей антифрикційних матеріалів. За допомогою використання планування експерименту першого порядку з ефектами взаємодії першого порядку методом Бокса-Уілсона визначено адекватну закономірність зносу вузлів тертя механізму завантаження сміттєвоза від властивостей антифрикційних матеріалів. Встановлено, що за критерієм Стьюдента серед досліджених факторів впливу найбільше на знос вузлів тертя механізму завантаження сміттєвоза впливає тиск в зоні тертя, а найменше – твердість антифрикційного матеріалу за Бринелем. Показано поверхні відгуку цільової функції – зносу вузлів тертя механізму завантаження сміттєвоза та їхні двомірні перерізи в площинах параметрів впливу, які дозволяють наглядно проілюструвати вказану залежність даної цільової функції від окремих параметрів впливу. Встановлено, що підвищення тиску в зоні тертя та швидкості ковзання на 60% призводить до зростання зносу вузлів тертя механізму завантаження сміттєвоза при реверсивному русі на 6,3...34% в залежності від властивостей антифрикційних матеріалів. Показано доцільність проведення наступних досліджень з визначення шляхів подальшого підвищення зносостійкості вузлів тертя механізму завантаження твердих побутових відходів у сміттєвоз.

Ключові слова: знос, вузли тертя, механізм завантаження, сміттєвоз, тверді побутові відходи, закономірність, планування експерименту.

***Problems of Tribology**, V. 29, No 3/113-2024, 31-42*

Problems of Tribology
Website: http://tribology.khnu.km.ua/index.php/ProbTrib
E-mail: tribosenator@gmail.com

DOI: https://doi.org/10.31891/2079-1372-2024-113-3-31-42

Improving the technology for restoring worn parts based on cold plastic deformation

Ya.B. Nemyrovskyi[1], V.V. Otamanskyi[1], O.L. Melnik[1], I.V. Shepelenko[2], N.I. Posviatenko[3]

[1]Zhytomyr Polytechnic State University, Zhytomyr, Ukraine
[2]Central Ukrainian National Technical University, Kropyvnytsky, Ukraine
[3]National Transport University, Kyiv, Ukraine
E-mail: kntucpfzk@gmail.com

Received: 20 June 2024: Revised:25 July 2024: Accept: 15 August 2024

Abstract

Technological control scheme for forming worn parts during their restoration by deforming broaching is proposed. Particular attention is paid to the study of the stress-strain state, which provided the conditions for creating the necessary plastic flow of the product material towards the worn areas and made it possible to compensate the wear amount in these areas of the product and provide an allowance for subsequent machining. Taking into account the peculiarities of parts restoration technological process, the relationship between the required circumferential strain of the outer surface and the total tension on the hole is established. The influence of the number of deforming elements that perform the required deformation on the accumulated strain on the inner surface of the part was investigated. This made it possible to establish that the maximum accumulated strain of the inner surface is provided by the maximum number of elements with a minimum tension on the element. On the outer surface, the value of the accumulated strain does not depend on the number of deforming elements, but is determined only by the total tension and the workpiece thickness. Based on the simulation of deforming broaching in a wide range of changes in operating parameters, tool geometry and workpiece thickness, an analytical dependence was obtained to determine the angle that ensures the absence of axial strains when the workpiece is deformed. The necessary broaching modes and tool geometry were determined, which will ensure the required dimensions of the machined or restored part.

Key words: parts restoration, deforming broaching, stress-strain state simulation, forming scheme, machining modes, tool geometry.

Introduction

Currently, it is important to introduce advanced technologies into the industry that save material, fuel and energy, and raw materials. One of these technologies is the technology of worn parts restoration, the prospects of which are due to the use of significant resources in their production, which can reach up to 30% of labor and technological equipment in general industrial production [1]. The use of parts restoration technology is an important reserve for increasing the efficiency of modern production. Its economic feasibility is due to the possibility of reusing up to 80% of working parts. The cost of restoring worn parts is significantly lower than the cost of new ones (not exceeding 60%) due to the savings in product material and energy costs for its production [2]. Existing restoration technologies use numerous technological methods that take into account the shape, materials of the worn surfaces and other features of the worn surfaces [3]. For the same part, several variants of restoration technologies can be developed, and then the most effective one can be selected. To make an objective choice of restoration technologies, it is necessary to evaluate the advantages and disadvantages of each technology. One of the most basic requirements when choosing a restoration technology is to ensure that the quality parameters of the restored part are not lower than the new one. In this regard, the use and implementation of waste-free

technological processes for restoring the dimensional accuracy of worn parts, especially those whose production is mass or large-scale, is extremely relevant. Such parts include the piston pin. The annual program for its production in the European automotive industry alone is more than 30 million pins. The overall dimensions of the part have the following range: diameter 20-58 mm, length 45-220 mm, its weight varies between 0.2-1.8 kg depending on the engine brand, and, for example, for diesel locomotives and marine diesel engines, the weight of piston pins is quite significant and can reach 4.5 kg [4].

Literature review

Let's consider the existing technologies for restoring piston pins. All pins, regardless of their size, have the same design (Fig. 1) and represent an axisymmetric hollow cylinder with chamfers, which has a wear-resistant outer surface hardened to *HRC* 60-62 and a fairly plastic core [5]. Worn pins can be restored in various ways. The most common of them are: grinding to the repair size, hardening, thermoplastic and electrohydraulic distribution, and electrocontact heating [6].

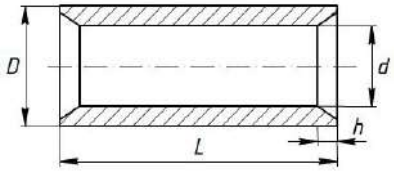

Fig. 1. Typical piston pin design [6]

Grinding the piston pin to a repair size (reducing the outer diameter compared to the nominal diameter) ensures that the worn surface is free of marks, scratches, and macro irregularities. However, the use of such piston pins requires pistons with reduced hole sizes in the bosses. For this reason, the considered method of restoring piston pins is limited in use [7].

The restoration of piston pins by ironing and chromium plating [7], despite its high efficiency and productivity, as well as the ability to build up a metal layer 2-3 mm thick, is not currently widespread. This is due to the low mechanical properties of iron, both in terms of strength and wear resistance, and requires the use of additional thermal operations.

There is also a thermoplastic distribution method [6], which is used to restore worn piston pins. It is realized as follows. Worn piston pins are heated by high-frequency currents above the temperature of pearlite-asthenite transformation. Depending on the cooling technology, the liquid is passed either through the pin hole or by counter or parallel flows through the pin hole and the outer surface with a time shift. This cooling creates a difference in the cooling rates of the inner and outer layers, which, by fixing the volumetric expansion of the metal, ensures an increase in the outer diameter. According to the authors of [6-8], the process of pin distribution simultaneously involves heat treatment of hardening and low tempering. However, it should be noted that the process of hydrothermal distribution causes a heterogeneity of diameter increase along the length of the pin and thus a type of dimensional error such as corsetry occurs. After that, the pins are subjected to five times of grinding and polishing. It should be noted that the unevenness of the machining allowance along the outer diameter of the part leads to uneven and increased metal removal, a decrease in the depth of the cemented layer, and the appearance of areas with reduced hardness and wear resistance. In addition, during thermoplastic distribution, the increase in the outer diameter of the worn pins is due to the presence of internal stresses arising from cooling and the phase transition of austenite to martensite.

According to [9], simultaneously with the distribution of the pin, its heat treatment is carried out – hardening and low tempering. However, in the process of thermoplastic distribution, there are no conditions for low-temperature tempering. Moreover, as studies [8] have shown, the presence of harsh water cooling conditions for alloyed cemented steels of the 12KHN3A type when they are heated above the pearlite-austenite transformation temperatures can lead to cracks in the cemented layer. This is evidenced by Fig. 2, which shows the surface of the piston pin of a D-240 diesel engine restored by hydrothermal distribution, where the appearance of cracks in the cemented layer can be clearly seen.

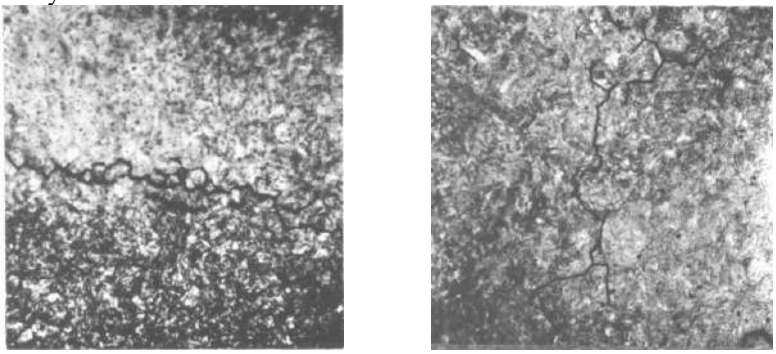

Fig. 2. Microstructure of piston pin cemented layer made of 12KHN3A steel restored by thermoplastic distribution [10]

As proof of low-temperature tempering absence in the process of thermoplastic distribution, and therefore of structures present in the pins restored in this way, which tend to move to a more equilibrium state, the following experiment was conducted by the author [10]. The pin, restored by the thermoplastic distribution method, was annealed in a protective environment. In this case, the outer diameter of the annealed pin decreased by an unacceptable amount (Fig. 3) as a result of internal stress relaxation.

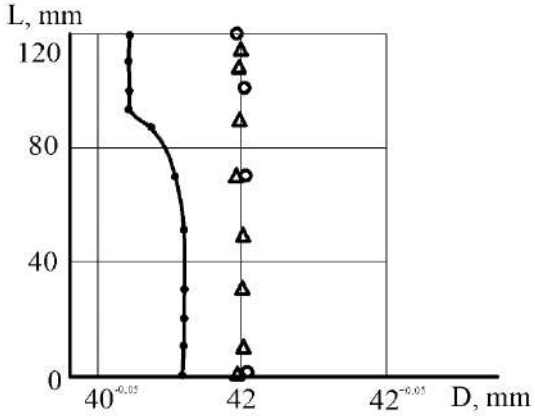

Fig. 3. Changes in the size of the pin generatrix restored by different methods after annealing: ● – after hydrothermal distribution and annealing; Δ – after deforming broaching; ○ – after deforming broaching and annealing [10]

A similar fact can occur during the operation of the pins, since the operating conditions of an internal combustion engine are characterized by the presence of high temperatures and alternating loads. This can cause a reduction in the strictly regulated outer diameter of the pin, which can lead to engine failure.

According to [4], the restoration of piston pins by the method of electrocontact heating and combined spray cooling is more advanced than hydrothermal distribution, but also has a number of disadvantages typical to the methods of restoring parts based on the use of thermal strains. The microstructure of the quenched cemented layer of the restored pins is martensite with the inclusion of cementite, residual austenite, and troostite [7]. This indicates non-compliance with the basic requirements for the technological process of cemented steels heat treatment during heat treatment and leads to the appearance of defective features in the restored pins (the presence of residual austenite).

As follows from the analysis of works [4, 7] related to the dimensional accuracy restoration of worn piston pins by heating and subsequent cooling, they all have common disadvantages. The most significant of them is the lack of allowance on the outer surface of the restored pin for subsequent machining, the presence of areas with reduced hardness and wear resistance, the possible appearance of cracks in the cemented layer, and the mismatch of the restored pin microstructure with technical requirements. All of this leads to a significant percentage of restored products rejects and does not ensure the stability of the operational parameters of the restored piston pin quality. In addition, these methods are energy-intensive, require special equipment and are not environmentally friendly.

At the same time, the use of cold plastic deformation (CPD) methods, as noted in works [11, 12], allows to ensure the required level of products working surface quality parameters.

The undoubted advantages of CPD methods are [11, 12]:

– maintaining material integrity by redistributing the product material to the worn areas;

– improving the physical and mechanical properties of the processed product material;

– the possibility of combining thermal and chemical-thermal operations makes it possible to create hybrid technologies;

– improved technological inheritance makes it possible to maintain the quality parameters of parts, even when using additional finishing operations;

– ensuring that the process does not have a negative impact on the environment;

– the ability to automate the process, which ensures the use of CPD in mass production.

According to a number of works [13-15], the development of a technology for the restoration of worn parts should be based on the study of the stress-strain state (SSS). This will provide the conditions for creating the necessary plastic flow of the product material towards the worn areas, which will compensate for the amount of wear in these areas of the product and provide allowance for subsequent machining.

The Institute of Superhard Materials of the National Academy of Sciences of Ukraine created a highly efficient technological process for restoring piston pins based on deforming broaching [8, 16], which made it possible to solve the problems of ensuring the dimensional accuracy of the pin's outer surface, as well as to develop a new scheme for deforming the pin with a change in the bearing face [17]. Based on this scheme, the installation design for pin distribution in mass and large-scale production was developed. The pins restored by deforming broaching do not have the same disadvantages as the pins restored by thermoplastic distribution (Fig. 3). Regarding the choice of the forming scheme, the authors of [8, 16] conducted experimental studies on the basis of which the

required geometric parameter of the tool was selected. However, the absence of a definite relationship between the strain of the pin hole and the strain of its outer surface will not allow optimizing the workpiece forming scheme by selecting the necessary broaching modes and tool geometry.

Purpose

The aim of the work is to develop a methodology for technological control of worn parts shape formation during their restoration by deforming broaching. Achieving this goal requires solving the following tasks:

– to develop a methodology and study the SSS in the deformation zone during deforming broaching and its influence on the change in processed workpiece dimensions;

– to establish the relationship of operating parameters and tool geometry to changes in processed workpiece dimensions;

– to develop a methodology for technological control of workpiece forming, with the help of which to determine the necessary modes of broaching and tool geometry, which ensure the required processed part dimensions.

Research Methodology

To analyze the SSS of the workpiece material and study the change in machined part dimensions, a finite element model (FEM-Model) of the deforming broaching process (DBR) was developed according to the following scheme (Fig. 4). The SSS simulation of an axisymmetric workpiece made of plastic material during deforming broaching was carried out using the DEFORM 2D/3D^{TM}V 11.0 software package [18].

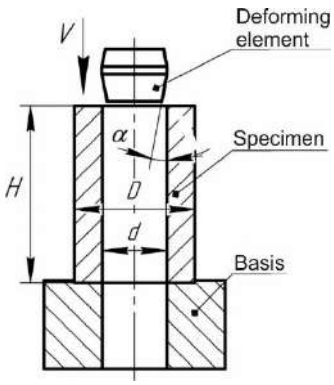

Fig. 4. Scheme of deforming broaching

To analyze the influence of the tool's geometric parameters on the characteristics of the SSS and the workpiece's geometric dimensions, the angle of the working cone inclination of the deforming element α was changed and amounted to 2°, 4°, and 8°, respectively.

Taking into account the above conditions, a finite element model of the considered process was built (Fig. 5).

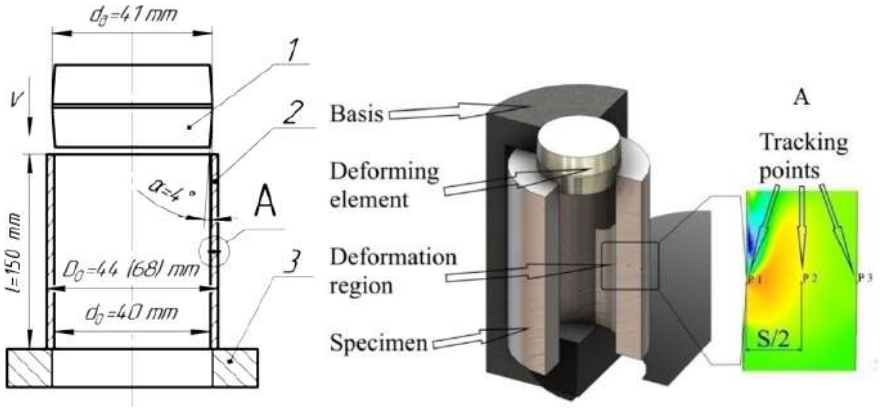

a) b)

Fig. 5. FEM model construction: a) workpiece with dimensions: 1 – deforming element; 2 – the studied axisymmetric workpiece; 3 – base; b) model scheme

The simulation process considered the machining of two workpieces with the same internal diameter. The inner diameter of the workpieces is d_0 = 40 mm, the outer diameter of the first workpiece is D_{01} = 44 mm, the

second is D_{02} = 68 mm, and the length is l = 150 mm. The deforming element is made with the angle of the working and return cone α = 4°. The diameter of the working element is equal to d_e = 41 mm, i.e., a nominal tension of 1 mm is created during its passage. The movement speed of the deforming element is V = 0.5 mm/s.

As the material for the study, we chose 12KHN3A steel, the chemical composition and mechanical properties of which are presented in Table 1. The DEFORM material library [18] contains an analog of the above material, DIN 14NiCr14, which has similar mechanical characteristics. It was used in the simulation of the SSS. In the DEFORM software, the flow curve for this material is defined by points (Table 2). The analysis of SSS was carried out in the middle of the length of the workpiece at three points (Fig. 5, b).

Table 1

Chemical composition and mechanical properties of 12KHN3A steel [19]

Chemical composition, %					Mechanical properties			
C	Mn	Si	Cr	Ni	*HB* hardness, MPa	Tensile strength σ_B, MPa	Poisson's ratio, μ	Elastic modulus, $E \cdot 10^5$, MPa
0.09-0.16	0.3-0.6	0.17-0.37	0.6-0.9	2.75-3.15	220 – 230	930	0.28	2

Table 2

Flow curve points of 14NiCr14 steel

e_i	0	0.05	0.1	0.2	0.3	0.4	0.5	0.6	0.7	0.8	0.85
σ_i	356.8	506.4	648.8	780.8	824.6	835.6	835.0	830.2	825.4	818.4	814.5

At each point, the strain intensity e_i, hydrostatic pressure σ_0, stiffness coefficient of the stress state, axial stress σ_z, axial strain e_z, and circumferential strain e_φ were determined.

The obtained FEM-model of the process was used to study the SSS of each of the deformation zone areas in the DBR simulation of a workpiece made of plastic material.

Results

Let us consider the results of the simulation. Fig. 6 shows the change in the accumulated strain during the simulation of the deformation process of thin-walled and thick-walled workpieces.

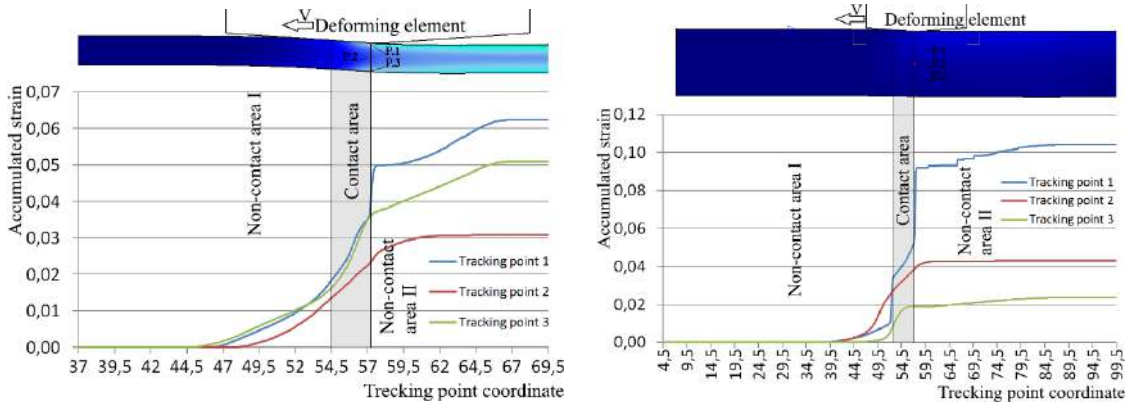

Fig. 6. Variation of the parameter ei in the deformation zone when simulating the deformation process of 12KHN3A steel workpieces by a deforming element with tension a/d_0 = 0.025 and thickness t_0/d_0 = 0.025: a) 0.05; b) 0.35

Fig. 6 shows that strain accumulation begins in noncontact zone I, then the main part of the deformation occurs in contact zone II, and in noncontact zone III, the deformation in the deformation zone is completed. It should be noted that the values of the accumulated strain in noncontact zones I and III are approximately equal to each other. Comparing Fig. 6 *a* and *b*, it follows that the changes in the accumulated strain for thin-walled and thick-walled workpieces are similar, but there are differences. In both cases, the value of the maximum accumulated strain corresponds to the inner surface of the workpiece. It decreases as the workpiece radius increases. But thin-walled workpieces have their own peculiarities. On the outer surface (Tracking point 3), the accumulated strain is greater than on the middle surface (Tracking point 2). This is not the case for thicker-walled workpieces. There, the strain gradually decreases with increasing thickness and its minimum value corresponds to the outer surface (Tracking point 3). This can be explained by the following. In a thin-walled workpiece, the strain along the wall thickness is almost through and uniform. The hydrostatic pressure (Fig. 7) for thin-walled workpieces varies from –1000 MPa in the contact zone to a value of 400 MPa, and for thick-walled workpieces from –1600 MPa to 400 MPa.

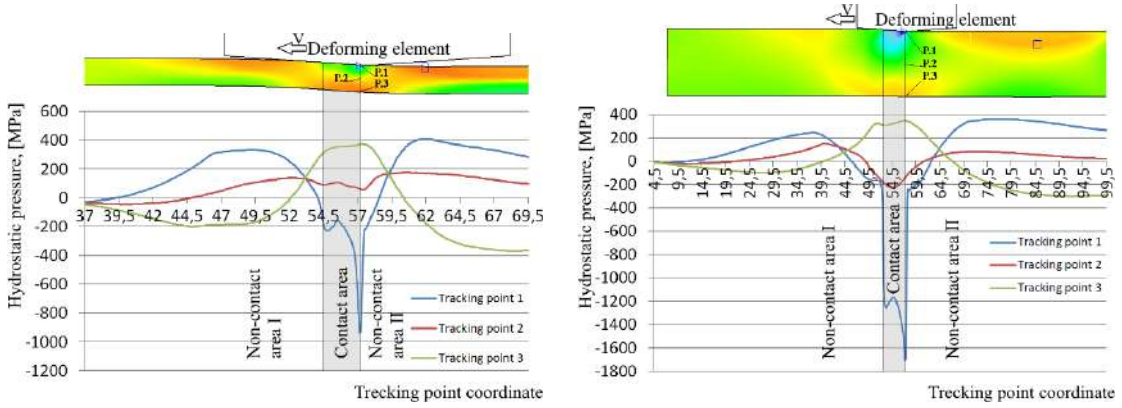

Fig. 7. Changes in hydrostatic pressure σ_0 in the deformation zone when simulating the deformation process of 12KHN3A steel workpieces by a deforming element with tension $a/d_0 = 0.025$ and thickness $t_0/d_0 = 0.025$: a) 0.05; b) 0.35

The stress state coefficient in both cases (Fig. 8) is $\eta = +2$ on the outer surface corresponding to the contact zone, and $\eta = -5$ (Fig. 8, a) and $\eta = -8$ (Fig. 8, b) on the inner surface where the maximum strain occurs.

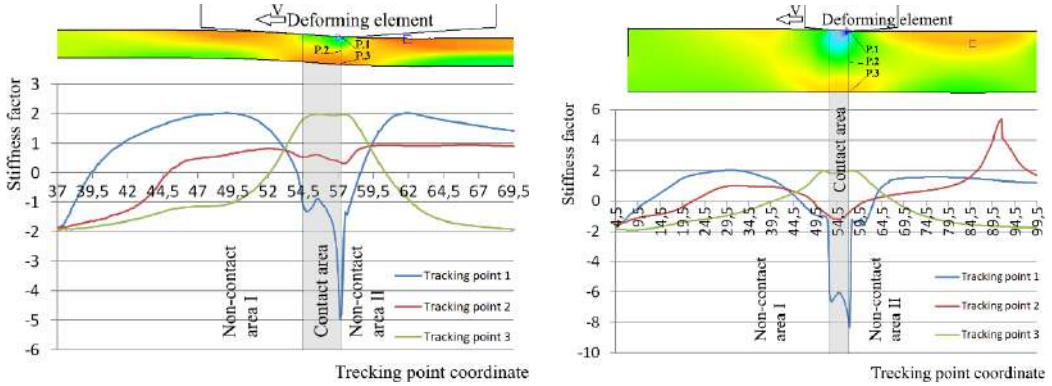

Fig. 8. Changes in the value of the stress state coefficient η in the deformation zone when simulating the deformation process of 12KHN3A steel workpieces by a deforming element with tension $a/d_0 = 0.025$ and thickness $t_0/d_0 = 0.025$: a) 0.05; b) 0.35

For thick-walled parts, the hydrostatic pressure at the middle surface (Tracking point 2) is zero, the stress value is also close to zero, and the accumulated strain is greater than Tracking point 3. At the same time, the thin-walled workpiece has a positive value of hydrostatic pressure at points 2 and 3, and at point 3 it is greater and causes the appearance of a stress state close to biaxial tension, as evidenced by the value of the stress state coefficient $\eta = +2$.

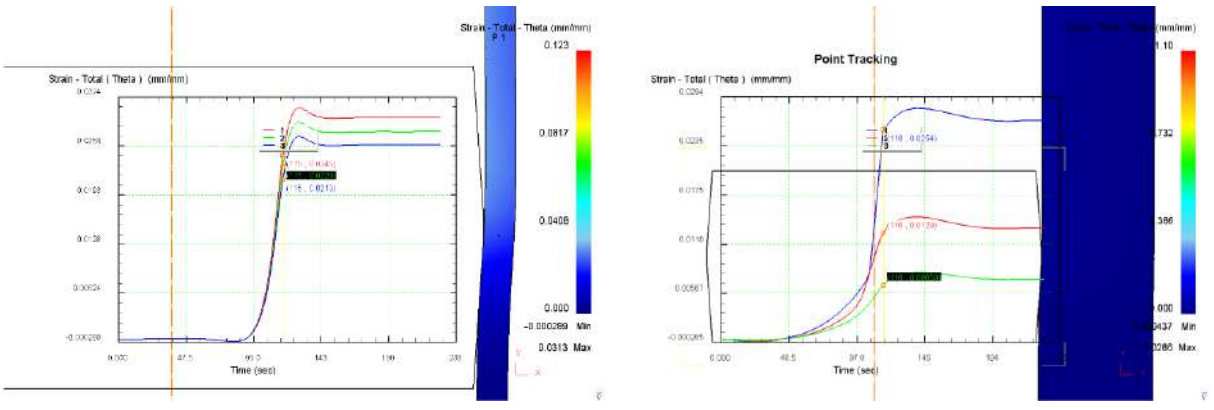

Fig. 9. Changes in the value of the circumferential component of the strain tensor e_φ in the deformation zone when simulating the deformation process of 12KHN3A steel workpieces by a deforming element with tension $a/d_0 = 0.025$ and thickness $t_0/d_0 = 0.025$: a) 0.05; б) 0.35

Consider a change in the circumferential component of the strain tensor, which determines the increase in the outer diameter of the workpiece. In Fig. 9 shows the results of simulating the deformation of thin-walled and

thick-walled workpieces.

The nature of the change in this parameter does not depend on the thickness of the workpiece, although the difference between the e_φ values for Tracking point 1, 2, 3 is insignificant for thin-walled workpieces, indicating a through homogeneous strain in this case (Fig. 9, *a*). For thick-walled ones, this difference is significant. The maximum value corresponds to the inner surface of the workpiece, and the minimum value to the outer surface (Fig. 9, *b*). The maximum value of the circumferential strain occurs in the contact zone. In non-contact zones, the value of e_φ is insignificant.

The influence of technological factors and tool geometry on the circumferential strain on the outer surface is characterized by Fig. 10.

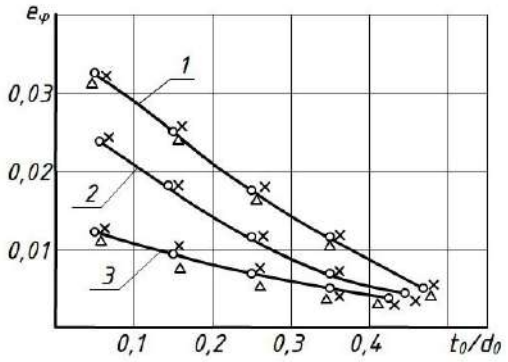

Fig. 10. Dependence of the circumferential strain e_φ on the thickness of the workpiece t_0/d_0 when simulating the workpiece strain with tension on the element a/d_0: 1 – 0.0375; 2 – 0.025; 3 – 0.0125 with different angles α: ○ – 4°; × – 8°; Δ – 2°

As can be seen from Fig. 10, the circumferential strain of the outer surface practically does not depend on the angle α, but is determined only by the thickness of the workpiece and the tension on the element. The approximation of the data shown in Fig. 10, made it possible to obtain a dependence by which it is possible to determine the required tension depending on the required circumferential strain:

$$e_\varphi = 0,95a / d_0 - (1,95a / d_0) t_0 / d_0 . \quad (1)$$

The required total strain of the inner surface is determined by the equation:

$$\Sigma a / d_0 = \frac{e_\varphi^*}{0,95 - 1,95 t_0 / d_0} . \quad (2)$$

When designing a workpiece restoration process, the circumferential strain required to compensate for wear and provide allowance for subsequent machining is determined. Then, according to dependence (1), the required total tension is determined to ensure that this circumferential strain is obtained for a specific workpiece thickness. If there is a need to perform several deformation cycles, the total tension is divided into several transitions, whereby:

$$\Sigma a / d_0 = a_1 / d_0 + a_2 / d_0 . \quad (3)$$

Studies [11] have shown that assessing the plasticity utilization rate is important when plastic strain is followed by thermal or chemical-thermal treatment. In this case, the properties of the prestrengthened material largely depend on the plasticity reserve utilization rate accumulated during previous operations. The authors of works [10, 11] recommend limiting the value of the used plasticity resource within the limits:

$$\psi_{max} \le [\psi]^*, \quad (4)$$

where $[\psi]^* = (0,25 \div 0,3)[\psi]$, $[\psi]$ – maximum deformation of the workpiece corresponding to a specific stress state coefficient.

After determining the required strain of the outer surface and the corresponding total hole tension, the workpiece must be checked for the remaining plasticity on the outer and inner surfaces of the workpiece.

Consider how the number of deforming elements that perform the required total strain of the hole affects its strain intensity. Let us consider three cases in which the same total strain $\sum a/d_0 = 0.075$ is performed. In the first case, the strain is performed by 6 deforming elements with a tension on the element $a/d_0 = 0.0125$. In the second case, it is performed by 3 deforming elements with a tension on the element $a/d_0 = 0.025$. And in the third case, it is performed by 2 deforming elements with a tension on the element $a/d_0 = 0.0375$. As follows from Fig. 11, the maximum accumulated strain $e_0 = 0.76$ occurs when deformed by 6 deforming elements. A smaller strain $e_0 = 0.27$ is observed when the total tension is applied by 3 deforming elements. And the smallest strain on the inner surface of the hole $e_0 = 0.18$ is observed when deformed by 2 elements.

At the same time, no such significant difference in the values of the accumulated strain from the number of deforming elements is observed on the outer surface. The number of deforming elements practically does not affect its value and on the outer surface of the part is in all three cases $e_0 = 0.06, 0.07, 0.072$, respectively.

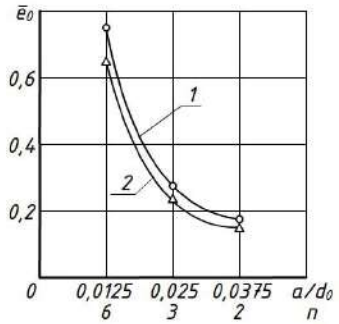

Fig. 11. Dependence of the accumulated strain on the inner surface of a 12KHN3A steel workpiece during simulation of its strain by working elements with an angle of α = 4° on the tension on the element and the number of deforming elements that perform the total strain, workpiece thickness t_0/d_0: 1 – 0.35; 2 – 0.2

The change in the accumulated strain at the thick-walled state t_0/d_0 = 0.2 has a similar character, i.e., the wall thickness has practically no effect on the nature of the change in the accumulated strain depending on the number of broached elements. Therefore, taking into account the significant effect of the number of deforming elements on the value of the accumulated strain on the inner surface of the part, we check the used plasticity resource on the deformed hole surface.

After determining the number of elements and the tension on them according to dependence (3), we select the deformation scheme. It can be compression, tensile, or schemes with a change in the supporting face [17].

Further, according to the thickness of the workpiece and the tension on the element determined by dependence (1), which provides the required increase in the outer diameter of the workpiece, we determine the angle α, which will provide the required axial deformation of the workpiece. As is known from scientific works [11, 12] on determining the workpiece strain, deforming broaching causes shortening of parts, i.e., during the dispensing of the inner hole, the outer diameter of the workpiece increases and its length decreases. However, some works [20, 21] note that in addition to shortening the workpiece, it can be lengthened, which can be used to restore the worn axial dimension of the part. Therefore, we considered the possibility of changing the axial strains of the workpiece. To do this, we simulated the deformation process of a 12KHN3A steel workpiece to determine its axial dimensions in a wide range of changes in the part thickness, element tension, and angle α. Examples of simulation results are shown in Fig. 12.

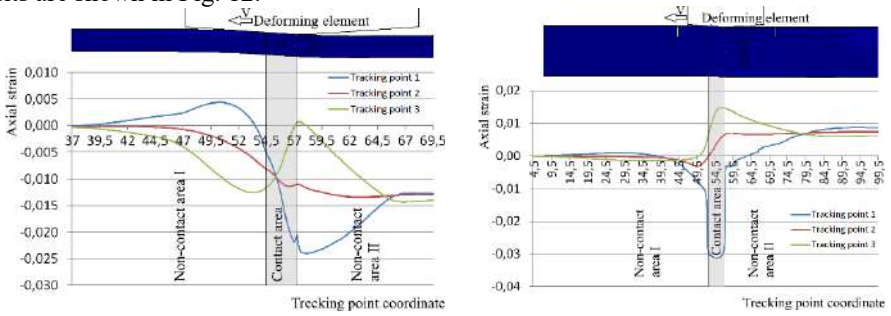

a) b)

Fig. 12. Variation of the axial component of the strain tensor e_z in the deformation zone when simulating the deformation process of 12KHN3A steel workpieces by a deforming element with tension a/d_0 = 0.025 and thickness t_0/d_0 = 0.025: a) 0.05; b) 0.35

Fig. 12 shows that when thin-walled parts are deformed (Fig. 12, *a*), the workpiece is shortened. At the same time, when thick-walled parts are deformed, the workpiece is elongated. If there is shortening and lengthening, then there should be a zero change in the axial dimension of the workpiece. The simulation results, which indicate the presence of a zero size of the machined workpiece depending on its thickness and tension on the element, are shown in Fig. 13.

The approximation of the data shown in Fig. 13, allowed us to obtain an analytical dependence for determining the angle α, which ensures the absence of axial strains depending on the thickness of the workpiece and the tension on the element:

$$\alpha^* = \frac{0,35\left(1+100a/d_0\right)}{t_0/d_0}. \tag{5}$$

The process of controlling the forming for a given workpiece thickness is as follows. First, the circumferential deformation required to compensate for wear and provide an allowance for further processing is determined. Then, according to the dependence (1) obtained as a result of simulation, the required total tension on the element ∑a is determined according to dependence (2).

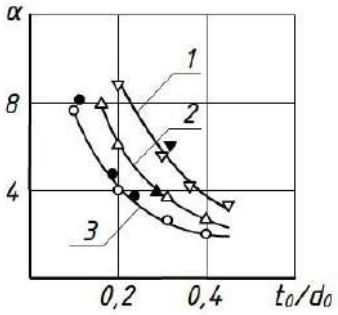

Fig. 13. The dependence of the angle α, which ensures the absence of axial strains on the thickness of the workpiece, was obtained by simulating the deformation process of a 12KHN3A steel workpiece with different tensions: 1 – 0.0375; 2 – 0.025; 3 – 0.0125; ●, ▲, ▼ – used experimentally obtained data [16]

If the part is subjected to thermal or chemical-thermal operations during processing, it is mandatory to check the used plasticity resource on the restored surface of the part.

Then, based on a given thickness and a certain tension, which is responsible for obtaining the required outer diameter size, we determine the angle α, which ensures a zero change in the length of the workpiece. This is done according to the previously obtained experimental dependence (5) obtained from the simulation results.

Subsequently, depending on the requirements for the workpiece, we fulfill the conditions under which the workpiece either elongates $\alpha > \alpha^*$, shortens $\alpha < \alpha^*$, or its axial dimension remains unchanged $\alpha = \alpha^*$.

The conducted studies made it possible to build an algorithm for technological control of workpiece forming (Fig. 14).

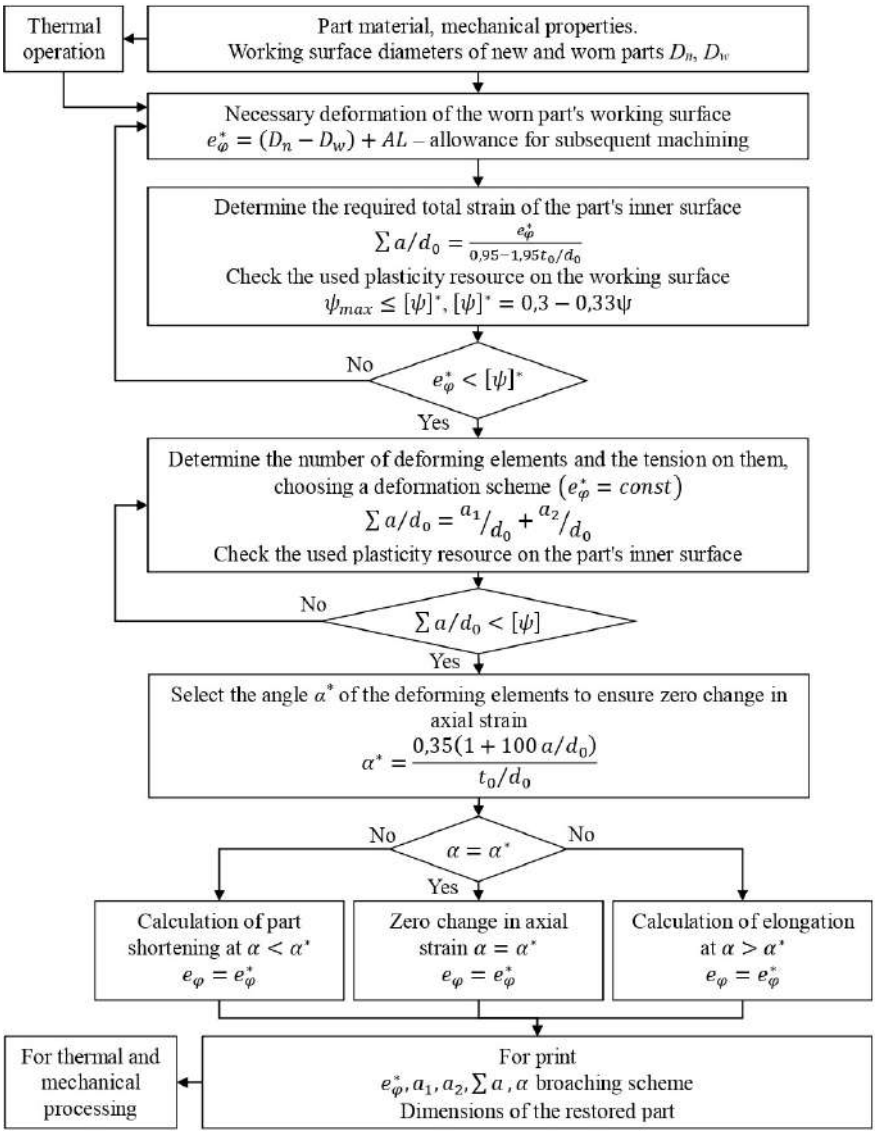

Fig. 14. Algorithm scheme of the technological process for restoration or processing using plastic strain of a hollow axisymmetric part

The developed scheme of the algorithm for constructing a technological process for restoring a hollow axisymmetric part using plastic strain has been successfully tested during the design of such technological processes for restoring worn parts:

– worn piston pins of 10D100 diesel locomotive engines at the Dnipro Locomotive Repair Plant. During the restoration of 10D100 piston pins, the recommendations presented in the forming scheme (Fig. 14) provided a zero change in length, i.e., the length of the pin did not change after increasing the outer diameter. The dimensions of the 10D100 pins are $t_0/d_0 = 0.4$, the length of the pin is 182 mm, the outer diameter of the pin is 80 mm, and the weight of the pin is 4.5 kg. Material of the pins – 12KHN3A steel;

– restoration of the dimensions L and D_1 geometric accuracy of the cardan joint worn crosspieces (Fig. 15) [20] at the Institute of Superhard Materials of the National Academy of Sciences of Ukraine. During their strain, there is a simultaneous increase in the outer diameter and an increase in the original axial dimension h to h_1, which made it possible to finishing the worn faces to the required size.

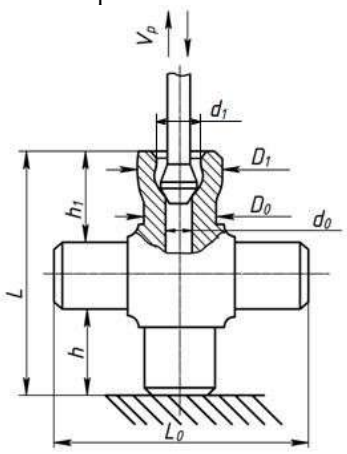

Fig. 15. Scheme of a worn crosspiece deformation [20]

Conclusions

Controlling the parts forming scheme is an important aspect of developing a technological process for restoring worn parts and machining new parts using CPD. This allows to obtain the required dimensions of the parts after their deformation. When machining new parts, the required allowances for subsequent machining are obtained, and when restoring worn parts, the dimensions of the worn surface are obtained to compensate wear and provide allowances for subsequent machining.

The conducted studies allowed us to draw the following conclusions:

– developed methodology for studying the SSS by simulating the deformation process of workpieces with different thicknesses in a wide range of changes in the broaching modes and tool geometry using the DEFORM 2D/3D^{TM}V 11.0 software package;

– based on the study of SSS, the relationship between the required circumferential strain of the outer surface e_φ and the total tension on the hole is established. It is shown that the parameter e_φ does not depend on the angle α, but is determined by the thickness of the workpiece and the total tension. The dependence for determining the required tension, which ensures the desired value of the parameter e_φ, is obtained;

– the influence of the number of deforming elements that perform the required circumferential strain on the accumulated strain on the inner surface of the part is determined. It is shown that the maximum accumulated strain of the inner surface is provided by the maximum number of elements with minimal tension on the element. On the outer surface, the value of the accumulated strain does not depend on the number of deforming elements, but is determined only by the total tension and thickness of the workpiece;

– the necessity of checking the obtained dimensions of the part after plastic strain by the parameter of the used plasticity is proved;

– it is shown that after obtaining the required value of the circumferential strain, it is necessary to determine the angle α, which will ensure a zero change in its axial strain. Based on the process of simulating strain in a wide range of changes in operating parameters, tool geometry, and workpiece thickness, an analytical dependence is obtained for determining the angle α, which ensures the absence of axial strains during workpiece deformation. To obtain the required axial dimensions of the processed workpiece, we choose an angle α from the following conditions: to obtain a zero change in length – angle $\alpha = \alpha^*$, to obtain a shortening $\alpha < \alpha^*$, to obtain an elongation $\alpha > \alpha^*$;

– an algorithm for technological control of the hollow axisymmetric part forming was developed, which allowed determining the necessary broaching modes and tool geometry to ensure the required dimensions of the machined or restored part.

References

1. Chernovol, M.I., Permyakov, O.A, Nemyrovskyi, Ya.B., Shepelenko, I.V., Gorbulik, V.I. (2023). Methodology of technological design of the process of parts recovery. Bulletin of the National Technical University 'KhPI'. Series: Technologies in mechanical engineering. 2 (8). P.10-16. https://doi.org/10.20998/2079-004X.2023.2(8).02 [Ukrainian]

2. Khitrov, I.O., Gavrish, V.S., Kononogov, Yu.A., Fastovets, P.M. (2013). Technological support of the quality of restoration of the landing holes of body parts. Rivne, NUVGP, 127 p. [Ukrainian]

3. Luzan, S.A. (2015). Determination of methods of restoration of parts of agricultural machines, providing their resource at the level and exceeding the level of new ones. Visnik KhNTUSG P. Vasilenka. 158. P.93-98. [Russian]

4. Kapelyushny, F.M. (2001). Influence of operational factors on the wear of diesel engine pins. Proceedings of the Tauride State Agrotechnical Academ. 2(17). P.113-117. [Ukrainian]

5. Nemyrovskyi, Ya.B., Shepelenko, I.V., Krasota, M.V. (2022). Estimation of strength of piston pins restored by means of internal bore distribution. Central Ukrainian Scientific Bulletin. Technical Sciences. 5 (36) I. P.14-22. https://doi.org/10.32515/2664-262X.2022.5(36).1.14-22 [Ukrainian]

6. Kuleshkov, Y.V., Krasota, M.V., Rudenko, T.V. (2021). Restoration of piston pins by hot plastic deformation. Central Ukrainian Scientific Bulletin. Technical Sciences. 4(35). P.54-62. https://doi.org/10.32515/2664-262X.2021.4(35).54-62 [Ukrainian]

7. Kapelyushny, F.M. Improvement of the technology of heat treatment of piston pins of diesel engines during their restoration [thesis abstract of the candidate of technical sciences]. 2005. 18 p. [Ukrainian]

8. Nemyrovskyi, Ya.B., Derevets, L.I. (2003). Restoration of piston pins on the basis of deforming broaching. Mechanisation and electrification of agriculture. 87. P. 269-278. [Russian]

9. Nemyrovskyi, Ya.B., Shepelenko, I.V., Chernovol, M.I., Zlatopolskiy, F.Y. (2022). Development of a technological process for the restoration of piston pins using deforming broaching. *Problems of Tribology*, *27*(3/105), 41–48. https://doi.org/10.31891/2079-1372-2022-105-3-41-48

10. Nemyrovskyi, Ya.B. Scientific basis for ensuring precision in deformable broaching [thesis abstract of the doctor of technical sciences]. 2018. 40 p. [Ukrainian]

11. Rosenberg, A.M. (1990). Mechanics of plastic deformation in cutting and deforming broaching processes. Kyiv, Naukova dumka, 320 p. [Russian]

12. Posvyatenko, E.K., Nemyrovskyi, Ya.B., Sheikin, S.E., Shepelenko, I.V., Chernyavsky O.V. (2021). Engineering of parts processed by broaching. Publisher Lysenko V.F., 466 p. [Ukrainian]

13. Nemyrovskyi, Y.; Shepelenko, I.; Storchak, M. Plasticity Resource of Cast Iron at Deforming Broaching. Metals 2023, 13, 551. https://doi.org/10.3390/met13030551 [English]

14. Shepelenko, I., Nemyrovskyi, Y., Lizunkov, O., Vasylenko, I., Osin, R. (2023). The Stress-Deformed State of the Cylinder Liner's Working Surface. In: Ivanov, V., Trojanowska, J., Pavlenko, I., Rauch, E., Piteľ, J. (eds) Advances in Design, Simulation and Manufacturing VI. DSMIE 2023. Lecture Notes in Mechanical Engineering. Springer, Cham. pp. 347-355. https://doi.org/10.1007/978-3-031-32767-4_33 [English]

15. Shepelenko, I., Nemyrovskyi, Y., Chernovol, M., Kyrychenko, A., Vasylenko, I. (2022). Deformation Zone Scheme Clarification During Deforming Broaching. In: Ivanov, V., Trojanowska, J., Pavlenko, I., Rauch, E., Peraković, D. (eds) Advances in Design, Simulation and Manufacturing V. DSMIE 2022. Lecture Notes in Mechanical Engineering. Springer, Cham, pp. 302-311. https://doi.org/10.1007/978-3-031-06025-0_30 [English]

16. Nemyrovskyi, Ya.B., Gerovskiy, A.I., Natalenko, V.A., Kopiev, O.A. (1993). Restoring piston pins. Electric and diesel locomotive traction. 11. P.22-23. [Russian]

17. Nemyrovskyi, Ya.B. (2014). Influence of base conditions on the accuracy of parts processed by deforming broaching. Bulletin of Ternopil National Technical University. 3(75). P.144-157. [Ukrainian]

18. Deform-User Manual SFTC-Deform V11.0.2, Columbus (OH), USA, (2014). *DEFORM* [Electronic resource]. Access mode www URL: https://www.deform.com

19. Sushko, O.V., Posvyatenko, E.K., Kurchev, S.V., Lodyakov, S.I. (2019). Applied materials science. Forwarpress, 352 p. [Ukrainian]

20. Krivosheya, V.V. (2015). Influence of the working cone angle of the deforming element on the process of deforming broaching of cylindrical holes. LAMBERT Academic Publishing. – Saarbrucken, Deutchland, 127 p. [Russian]

21. Posvyatenko, E.K., Nemyrovskyi, Ya.B, Shepelenko, I.V. (2020). Broaching and broaching tools. Publisher Lysenko V.F., 298 p. [Ukrainian]

Немировський Я.Б., Отаманский В.В., Мельник О.Л., Шепеленко І.В., Посвятенко Н.І. Удосконалення технології відновлення зношених деталей на основі холодного пластичного деформування

Запропоновано схема технологічного управління формоутворенням зношених деталей при їх відновленні деформуючим протягуванням. Особливу увагу приділено дослідженню напружено-деформованого стану, що забезпечило умови для створення необхідної пластичної течії матеріалу виробу по направленню до зношених ділянок та дозволило компенсувати величину зносу на цих ділянках виробу та забезпечити припуск під наступну механічну обробку. З врахуванням особливостей технологічного процесу відновлення деталей встановлено зв'язок необхідної окружної деформації зовнішньої поверхні з сумарним натягом на отвір. Досліджено вплив кількості деформуючих елементів, які виконують необхідну деформацію, на накопичену деформацію на внутрішній поверхні деталі. Це дозволило встановити, що максимум накопиченої деформації внутрішньої поверхні забезпечується максимальним числом елементів з мінімальним натягом на елемент. На зовнішній поверхні значення накопиченої деформації не залежить від кількості деформуючих елементів, а визначається тільки сумарним натягом і товстостінністю заготовки. На основі симуляції деформуючого протягування в широкому діапазоні зміни режимних параметрів, геометрії інструменту та товстостінності заготовки отримана аналітична залежність для визначення кута, який забезпечує відсутність осьових деформацій при деформуванні заготовки. Визначенні необхідні режими протягування і геометрію інструменту, які забезпечать отримання необхідних розмірів обробленої або відновленої деталі.

Ключові слова: відновлення деталей, деформуюче протягування, моделювання напружено-деформованого стану, схема формоутворення, режими обробки, геометрія інструменту.

Problems of Tribology, V. 29, No 32/113-2024, 43-55

Problems of Tribology
Website: http://tribology.khnu.km.ua/index.php/ProbTrib
E-mail: tribosenator@gmail.com

DOI: https://doi.org/10.31891/2079-1372-2024-113-3-43-55

Finite-element analysis of contact characteristics and friction modes of the "valve-guide" of the internal combustion engine

K.E. Holenko, A.A. Vychavka, M.O. Dykha*, V.O. Dytyniuk

Khmelnytskyi national University, Ukraine
**E-mail: tribosenator@gmail.com*

Received: 25 June 2024: Revised 25 July 2024: Accept 25 August 2024

Abstract

Modeling the performance of the "valve-guide" engine pair using modern software is an effective tool both for identifying weak points in the design and for predicting the behavior of the friction unit in operation. In this study, the method of finite element analysis was chosen as a tool to study the contact and antifriction parameters of the friction pair of the internal combustion engine "directional valve". Using the FEM application program, the raw data on the material, surface dimensions, loads, and motion kinematics are described. Based on the constructed finite-element model of the "valve-guide" conjugation, an analysis of the influence of determining tribological factors: sliding speed in contact, temperature, skew angle, friction coefficient on contact stresses both for each part of the friction pair and in the process of contact interaction was carried out. A consolidated matrix of the results of the numerical experiment was built, and the conclusions regarding the influence of each factor on the tribological characteristics were substantiated. Algorithms of influence on the design, technological and operational factors for prolonging the resource of the friction pair of the internal combustion engine "klpapn-napramna" are outlined.

Keywords: internal combustion engine, valve guides, finite element model, contact parameters, friction coefficient, stressed surface state

Introduction, analysis of research

Modeling the performance of the "valve-guide" engine pair using modern software is an effective tool both for identifying weak points in the design and for predicting the behavior of the friction unit in operation. This issue has received considerable attention in the scientific literature. In the article [1], filling materials are considered to reduce the weight of intake or exhaust valves of an internal combustion engine. Micro-computed tomography was used to reverse engineer the original component and assess the valve's internal geometry and material integrity. The valve has been redesigned using Finite Element Analysis (FEA) to select a lightweight weighted design that provides weight savings over the original equipment valve. The article [2] describes the concept of a non-invasive method of diagnosing the value of valve gaps in internal combustion engines, based on the analysis of engine surface vibration signals using artificial neural networks. The method uses as diagnostic signals the readings of vibration sensors, which record the acceleration of the engine head depending on the angle of rotation of the crankshaft, with pre-set values of the valve clearances measured in the cold state. In article [3], a study of the causes of engine intake valve damage was conducted, during which the intake valve heads were overheated and deformed as a result of material creep. On the example of a malfunction detected in the analyzed engine, it was established that traditionally known causes, such as a failure of the combustion process, cannot cause the described damage. The performed calculations showed that with an increase in the rotation frequency, the failure of the control system leads to an increase in temperature higher than recommended for the materials used. Based on the conducted research, the authors have developed recommendations for increasing the reliability of intake valves with variable gas distribution phases. In [4], a methodology for the analysis of valve wear of internal combustion engines is proposed, which is the result of the combined use of numerical and experimental methods. Numerical solutions are obtained using a specialized finite element method where a solution contact algorithm is used to model the flexible-flexible contact along with the adhesive wear law. Experimental results are obtained on a wear

test rig specially designed to evaluate wear parameters under valve operating conditions. A good agreement was found between the experimental wear profiles and the numerical calculations of the wear on the contact surfaces. In [5], engine reliability was improved using Al-Sic composites for engine guide valves. Finite element analysis of Al-Sic composite with titanium alloy,copper-nickel silicon alloys and aluminum bronze alloy as an alternative material for the engine valve guide was carried out using Ansys 13.0 software. The finite element method is one of the most widely used methods for analyzing mechanical load characteristics in modern engineering components. The directional valve model was modeled as shown in Fig. 15. A finite element model was built to perform the analysis of the guide valve. The stress analysis of the engine valve guide at different pressures and temperatures was carried out. It was found that the stresses were significantly lower than the allowable for all materials, but the Al-Sic composites were found to be the most optimal. The purpose of the work [6] was to determine the main parameters affecting this wear. The approach was based on the tribological triplet and material flows within the contact, using both numerical and experimental approaches. A dynamic model and valve train test bench showed that wear flows can be activated by the architecture of the valve opening system. Therefore, limiting these flows can be achieved by controlling the geometry of the system without changing the properties of the materials. In the same way, the finite element model of the local response of the seat-valve contact emphasized the influence of the "local" contact geometry. As noted in [7], intake and exhaust valves are important engine components used to control intake and exhaust gas flow in internal combustion engines. They are used to seal the working space inside the cylinders and are opened and closed by means of a valve mechanism. The study is devoted to various types of failure of internal combustion engine valves: due to fatigue, exposure to high temperature, shock load. In works [8-9] it was shown that sliding in the valve sealing area is one of the main causes of wear. Sliding wear is expected to play an even more important role in modern engines. Experimental data obtained using a special technique on a test stand are presented. Experimental data are supplemented by FEM modeling. The simulation involves checking the sliding behavior of the valve seal area on a test bench and investigating how different parameters affect the sliding length. These parameters include combustion pressure, contact angle, contact length, valve head thickness, friction coefficient, run-in wear, and change in modulus due to temperature variations.that stresses were significantly lower than allowable for all materials, but Al-Sic composites were recognized as the most optimal. The purpose of the work [6] was to determine the main parameters affecting this wear. The approach was based on the tribological triplet and material flows within the contact, using both numerical and experimental approaches. A dynamic model and valve mechanism test bench showed that wear flows can be activated by the architecture of the valve opening system. Consequently, limiting these flows can be achieved by controlling the geometry of the system without changing the properties of the materials. In the same way, the finite element model of the local response of the seat-valve contact emphasized the influence of the "local" contact geometry. As noted in [7], intake and exhaust valves are important engine components used to control intake and exhaust gas flow in internal combustion engines. They are used to seal the working space inside the cylinders and are opened and closed by means of a valve mechanism. The study is devoted to various types of failure of internal combustion engine valves: due to fatigue, exposure to high temperature, shock load. In works [8-9] it was shown that sliding in the valve sealing area is one of the main causes of wear. Sliding wear is expected to play an even more important role in modern engines. Experimental data obtained using a special technique on a test stand are given. Experimental data are supplemented by FEM modeling. The simulation involves checking the sliding behavior of the valve seal area on a test bench and investigating how different parameters affect the sliding length. These parameters include combustion pressure, contact angle, contact length, valve head thickness, friction coefficient, run-in wear, and change in modulus due to temperature variations.that stresses were significantly lower than allowable for all materials, but Al-Sic composites were recognized as the most optimal. The purpose of the work [6] was to determine the main parameters affecting this wear. The approach was based on the tribological triplet and material flows within the contact, using both numerical and experimental approaches. A dynamic model and valve train test bench showed that wear flows can be activated by the architecture of the valve opening system. Therefore, limiting these flows can be achieved by controlling the geometry of the system without changing the properties of the materials. In the same way, the finite element model of the local response of the seat-valve contact emphasized the influence of the "local" contact geometry. As noted in [7], intake and exhaust valves are important engine components that are used to control the flow of intake and exhaust gases in internal combustion engines. They are used to seal the working space inside the cylinders and are opened and closed by means of a valve mechanism. The study is devoted to various types of failure of internal combustion engine valves: due to fatigue, exposure to high temperature, shock load. In works [8-9] it was shown that sliding in the valve sealing area is one of the main causes of wear. Sliding wear is expected to play an even more important role in modern engines. Experimental data obtained using a special technique on a test stand are given. Experimental data are supplemented by FEM modeling. The simulation involves checking the sliding behavior of the valve seal area on a test bench and investigating how different parameters affect the sliding length. These parameters include combustion pressure, contact angle, contact length, valve head thickness, friction coefficient, run-in wear, and change in modulus due to temperature variations.They are used to seal the working space inside the cylinders and are opened and closed by means of a valve mechanism. The study is devoted to various types of failure of internal combustion engine valves: due to fatigue, exposure to high temperature, shock load. In works [8-9] it was shown that sliding in the valve sealing area is one of the main causes of wear. Sliding wear is expected to play an even more important role in modern engines. Experimental data obtained using a special technique on a test bench are presented.

Experimental data are supplemented by FEM modeling. The simulation involves checking the sliding behavior of the valve seal area on a test bench and investigating how different parameters affect the sliding length. These parameters include combustion pressure, contact angle, contact length, valve head thickness, friction coefficient, run-in wear, and change in modulus due to temperature variations.They are used to seal the working space inside the cylinders and are opened and closed by means of a valve mechanism. The study is devoted to various types of failure of internal combustion engine valves: due to fatigue, exposure to high temperature, shock load. In works [8-9] it was shown that sliding in the valve sealing area is one of the main causes of wear. Sliding wear is expected to play an even more important role in modern engines. Experimental data obtained using a special technique on a test stand are presented. Experimental data are supplemented by FEM modeling. The simulation involves checking the sliding behavior of the valve seal area on a test bench and investigating how different parameters affect the sliding length. These parameters include combustion pressure, contact angle, contact length, valve head thickness, friction coefficient, run-in wear, and change in modulus due to temperature variations.

Output data for modeling and calculation

Valves in automotive and industrial applications are usually made of materials that can withstand high temperatures, pressures and active corrosive environments. The choice of material largely depends on the specific application and operating conditions. Stainless steel is widely used because of its resistance to corrosion and strength at high temperatures. Grades such as AISI 304 (UNS S30400) and AISI 316 (UNS S31600) are common in the chemical and food industries. For applications at higher temperatures, such as engine exhaust valves, heat-resistant stainless steels such as AISI 347 (UNS S34700) or AISI 321 (UNS S32100) are used.

Titanium-based alloys are alternative materials for the manufacture of valves - they are most often found in the cylinder heads of sports and "custom" car engines with increased requirements for reliability at high speeds and temperatures. The last indicator is primarily influenced by the coefficient of thermal expansion, which is a measure of how much the material expands for one degree of temperature increase. A specific example of a titanium alloy commonly used for high-performance engine valves is Ti-6Al-4V, also known as grade 5 titanium. This alloy is known for its excellent combination of strength, light weight and corrosion resistance, making it a popular choice in aerospace, automotive and the medical industry.

Valve guides, which are critical to maintaining proper alignment, positioning, and clearance of the valve stem as it moves through the cylinder head, are typically made from materials that offer high wear resistance and improved thermal conductivity. The choice of material for guide valves largely depends on the operating conditions and requirements of the engine or mechanism. Manganese bronze is a group of high-strength, hard bronzes that are typically used in assemblies that require a combination of high strength, wear resistance, and corrosion resistance. Such alloys provide excellent durability and heat dissipation properties.

The object of research is a prefabricated solid model of the valve together with a guide (Fig. qe a, b) as part of the head of the Brodix 10X cylinder block (Fig. qe c, d, g). The 10X modification belongs to the line of high-performance cylinder heads produced by Brodix, which is well-known in the field of automotive auto parts, including heads, blocks and manifolds. Brodix 10X cylinder heads are designed for installation in high-performance and frequently modified Chevrolet (General Motors) "Small-Block" racing gasoline engines. Introduced back in 1955, the Chevrolet Small-Block V8 engine has become a staple of GM vehicles thanks to its versatility and performance, and remains the most widely produced in the world. Displacement can vary between 262–400 cubic inches (4.3–6.6 L). Brodix 10X heads have a modified valve mechanism: stronger valve springs and rocker arms for reliable high-rpm operation, valves made of titanium-containing stainless steel (such as AISI 321 steel with the formula X6CrNiTi18-10) or directly titanium alloys such as Ti-6Al- 4V. Such heads have gained particular popularity among tuning enthusiasts for street racing (Drag Racing) or professional wheel racing, but remain reliable and adaptable enough for daily use. The Ansys model of the valve guide is made of C86300 bronze.

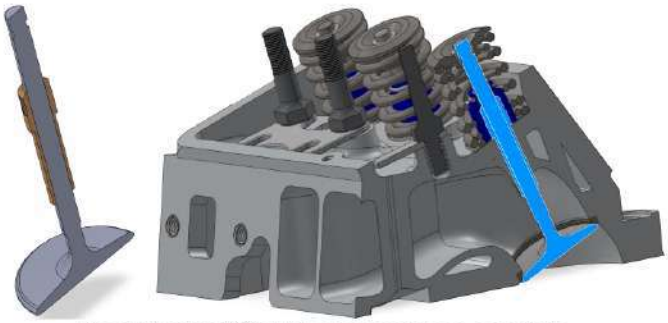

Fig. 1. Brodix 10X guide valve and head assembly

Additionally, for the contact surfaces between the valve stem and the guide, the detailing of the grid has been increased with the maximum element length Element size = 1.0 mm. The type of contact is Frictional with successive application of different friction coefficients: = 0.1 and 0.2 according to the boundary conditions, the

summarized data for which are presented below. To achieve convergence of forces in the contact area, the Normal Stiffness > Factor parameter is set to 0.1 for some of the test modes μ_v .

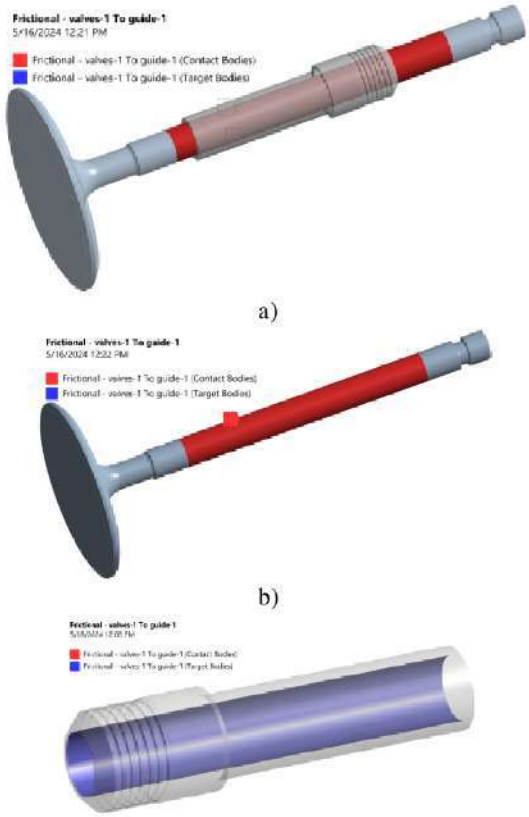

Fig. 2. Frictional contact: a) valve stem with a guide; b) contact surface of the valve stem; c) target (Target) surface of the guide.

Statistics of the grid of finite elements (Fig. 3): 153399 nodes; 91621 elements.

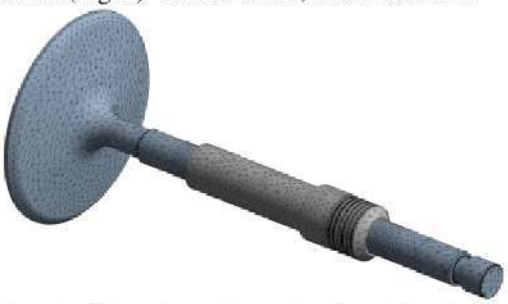

Fig. 3. FEM mesh of the valve with a guide (Ansys Coupled Field Static)

The surface temperature of the exhaust valve can reach 600-900°C, while the intake valve usually operates at lower temperatures as it is cooled by the incoming air or fuel mixture. During the fourth and final exhaust stroke, the valve opens to allow the exhaust gases to leave the combustion chamber– it is during this period that the highest temperature on the surface of the valve head (Valve Surface Temperature) of the Ansys model is reached (600°C in Fig. 4). The following calculations will consider both temperature cases: 600 and 900°C T_{vs}

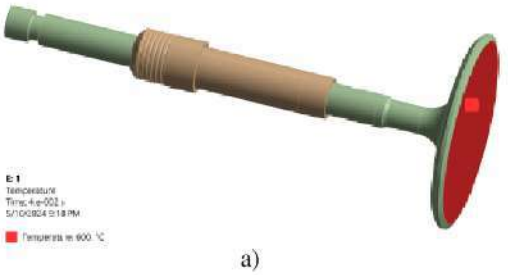

b)

Fig. 5 Temperature model a) and application of convection b)

For the Chevrolet V8 engine, which is a typical liquid-cooled engine, the valve stems are primarily cooled by engine oil and the surrounding material of the cylinder head with additional heat transfer to the coolant. The convective heat transfer coefficient of the valve guide where the stem operates will depend on the oil film (or lack thereof) that lubricates the contact area, typically ranging from 100 to 500 W/(m²·K). Apply the value of 300 W/(m²·°C) to our calculation model. Other surfaces are set to a convection value of 100W/(m²·K) for the same temperature loads on the valve surface:600 or 900°C (depending on the mode).

In order to fix the model, we will apply restraints with restriction of movements and rotations relative to all three axes (hard clamping, corresponding to the type of Fixed Support in Ansys) to the following surfaces of the valve guide in accordance with its attachment in the body of the cylinder head (Fig. . 6).

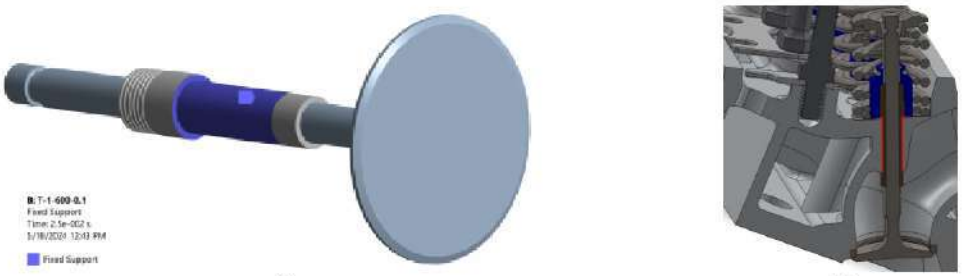

and) b)

Fig. 6. Attaching the Fixed Support type yokes to the valve guide: a) selected surfaces; b) cross-section of the block head with marking of guide mounting surfaces (red lines)

To form the boundary conditions of the kinematics and dynamics of the movement of the "valve–directional" in Ansys, we will analyze the main processes of the exhaust stroke): at the beginning or just before the start of the stroke, the exhaust valve is opened, controlled by the camshaft, which has cams designed to press on the valve pushers, effectively opening them at the right moment.

The exhaust valve moves down as the cam presses against the valve tip. The kinematics of this process is determined by the valve guide– a cylindrical part that ensures smooth and precise movement of the valve stem without lateral movement or rotation. In fact, there is a gap between the valve stem and the inner cylindrical surface of the guide, which in the studied model of the Brodix 10X block head is 0.03358 mm (Fig. 7) and is symmetrical about the longitudinal axis of the valve.

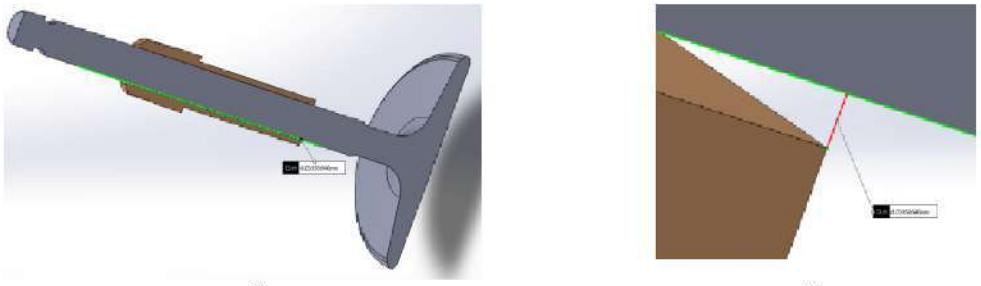

and) b)

Fig. 7. The gap between the valve stem and the guide: a) longitudinal section; b) enlarged view of the Solid model

In the next step, we will form the boundary conditions regarding the kinematics of the valve movement:

- the valve opening duration is = 0.04 s, which approximately corresponds to the idle speed of a low-speed enginet_{vo}"Small-Block" Chevrolet V8 (600-800 rpm);
- the stroke of the rod is linear from 0 to 10 mm within = 0.04 s (Fig. 8);$s_{vo}t_{vo}$

- the skew angle during the stroke of the rod is stepwise and is analyzed for two variants of its intensity (curve #1 and #2 in Fig. 8)$a_{vo}s_{vo}$
- step-by-step application and (Number of Steps = 3): 0 – 0.01 c; 0.01 - 0.025 c; 0.025 - 0.04 c;$s_{vo}a_{vo}$

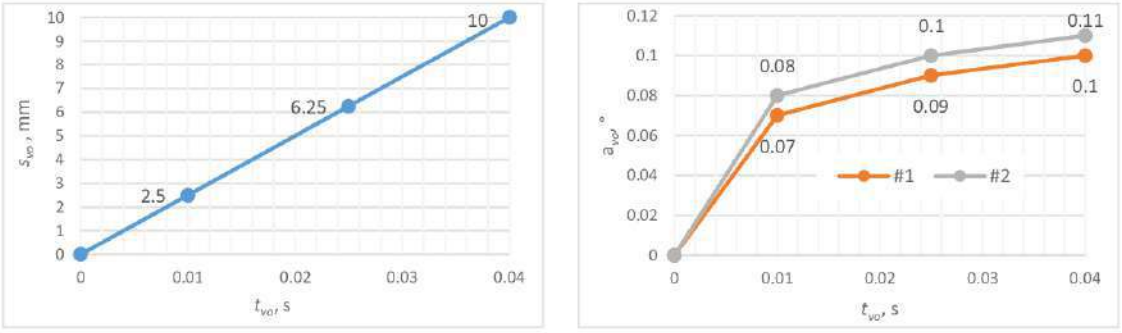

a) b)

Fig. 8. Kinematics of valve movement: a)stroke of the rod; b) skew angles$s_{vo}a_{vo}$

It should be noted that the misalignment angle occurs as a result of the pressure of the cam on the valve tip: turning, the camshaft in addition to the normal forces that actually ensure the strokea_{vo}rod, also creates tangential ones. The stabilizing factors of the valve are the upper support plate of the spring and directly the valve guide with a gap. At the same time, the lower part of the valve (the base) is in a relatively free position during the opening stage (out of the seat) and exhibits oscillations during the opening time, which will be demonstrated below in the discussion of the research results. We consolidate the boundary conditions of the Ansys model in Fig. 8 and in table. qg and consider the following designations using T-1-600-0.1-0.04 as an example:$s_{vo}t_{vo}$.

- T–valve manufacturing material (T–Ti-6Al-4V or A–AISI 321);
- 1– skew angle curve number (#1 or #2 according to the graph in Fig. 8);a_{vo}
- 600– temperature on the surface of the valve head (600 or 900°C);T_{vs}
- 0.1– coefficient of friction between the rod and the guide (0.1 or 0.2);μ_v
- 0.04– valve opening duration (0.04 or 0.01 s).t_{vo}

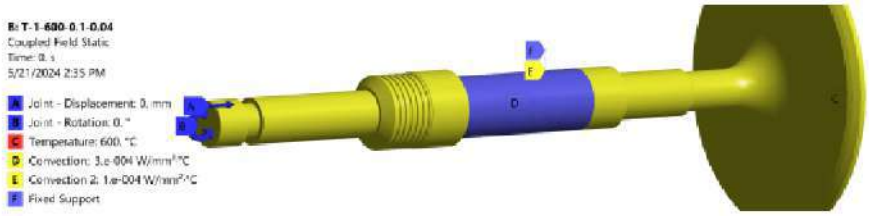

Fig. 9. Consolidated boundary conditions on the example of mode T-1-600-0.1-0.04

Table 1

Legend of calculation modes of the Ansys model

Name of the mode	Material	a_{vo}, #	t_{vo}, c	T_{vs},°C	μ_v	The purpose of the regime's tasks
T-1-600-0.1-0.04	Ti-6Al-4V	1	0.04	600	0.1	influence of the material
A-1-600-0.1-0.04	AISI 321	1	0.04	600	0.1	
T-2-600-0.1-0.04	Ti-6Al-4V	2	0.04	600	0.1	influence of the angleskew
A-2-600-0.1-0.04	AISI 321	2	0.04	600	0.1	
T-2-900-0.1-0.04	Ti-6Al-4V	2	0.04	900	0.1	effect of temperature
A-2-900-0.1-0.04	AISI 321	2	0.04	900	0.1	
T-2-900-0.2-0.04	Ti-6Al-4V	2	0.04	900	0.2	the effect of the coefficient friction
A-2-900-0.2-0.04	AISI 321	2	0.04	900	0.2	
T-2-900-0.1-0.01	AISI 321	2	0.01	900	0.1	influence of engine revolutions
A-2-900-0.1-0.01	AISI 321	2	0.01	900	0.1	

Temperature distribution by model

Application of temperature load$T_{vs}$to the surface of the valve head(Fig. 10) made it possible to obtain a map of the temperature distribution on the surface of his body. The dynamics of the temperature drop along the length of the valve significantly depends on the intensity of the applied convection. So, for an engine under low load and active cooling due to the oil film.

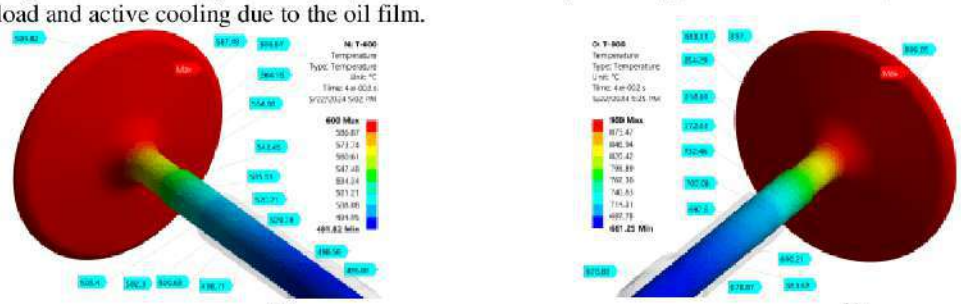

a) b)

Fig. 10. Temperature distribution along the length of the titanium valve (Ti-6Al-4V): a) = 600T_{vs}°C; b)T_{vs}= 900°C

The temperature near the end of the rod (valve tip) can drop to 150-200°C. Under the conditions of increased operating revolutions (over 2500-3000 rpm) and weaker cooling, the temperature can rise to 450-720 °C.

The influence of the material

We will begin the analysis of the stress state of the model with modesT-1-600-0.1-0.04 and A-1-600-0.1-0.04in accordance withtasks formedintable 1. "Equivalent (von-Mises) Stress" stress maps in Ansys of valves and guides (cross section in Fig. 11):

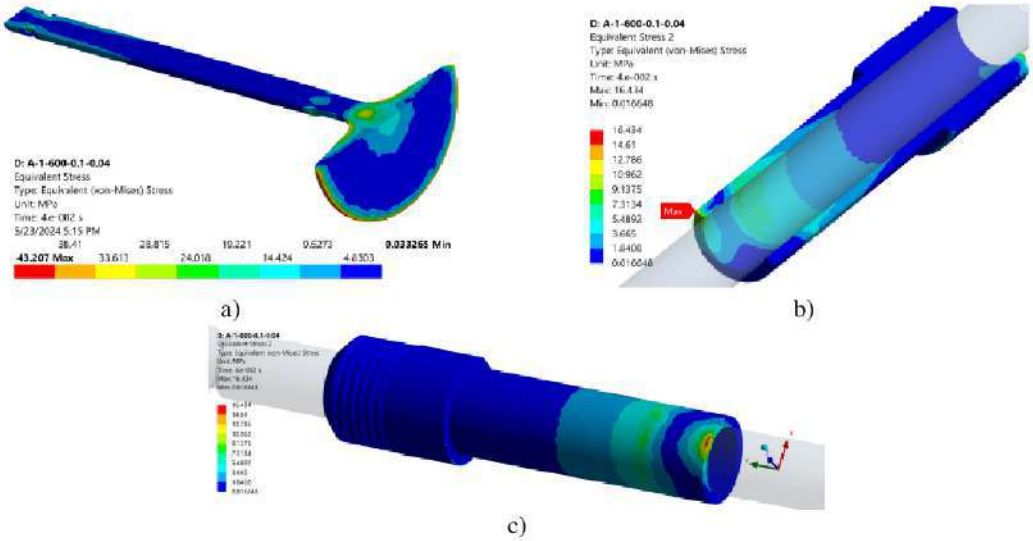

a) b)

c)

Fig. 11. Mises stress maps of the valve and guide

As of = 0.04 c, the maximum and average stresses are: 22.46 MPa in the titanium valve and 43.21 MPa in the steel valve. In both cases, they are "thermal" and fixed on the edge of the valve head, where no mechanical interactions occur according to the set boundary conditions. The result shows that the steel sample is almost twice as heat-resistant, which is also reflected in the results (6.83 vs, 3.34 MPa for the titanium valve). guides are 13.98 MPa in combination with a titanium valve and 16.43 MPa – with a steel valve, respectively. The regularities here are as follows: 1) higher valve stresses provoke higher guide stresses (combination$t_{vo}\sigma_{max}\sigma_{ave}\sigma_{ave}\sigma_{max}$AISI 321–Bronze C86300); 2) guide demonstrated on the inner surface (zone of contact with the titanium valve), and when in contact with the steel one - on the outer surface; 3) as a result of valve misalignment, the maximum stresses in the body of the guide are observed along the diagonal of its opening. The average stresses in the body of the guide are 0.745 and 0.398 MPa when interacting with a steel and titanium valve, respectively.$\sigma_{max}\sigma_{ave}$.

Let's analyze the situation with the contact surface of the valve stem (Fig. 12). The more ductile steel sample of the valve received significantly higher stresses at the moment of first contact = 0–0.0005 s, where sliding occurred, and showed a peak stress of 16.09 MPa (= 0.00031). At that time, the titanium valve received only 2.73

MPa (= 0.00043 s). After the end of the first step of distortion (angle) at = 0.013 s, the steel valve receives the next peak of maximum stresses = 13.99 MPa, which is clearly visible on the stress map in Fig. 12. In measure$t_m t_m t_m a_{vo} t_m \sigma_{max}$of the stroke of the stem and changes, the titanium valve changes the side of contact with the guide closer to the tip (the steel valve shows a similar behavior). As of the end of the experiment, titanium and steel valves acquire values of 5.21 and 9.41 MPa, respectively.$s_{vo} a_{vo} \sigma_{max}$

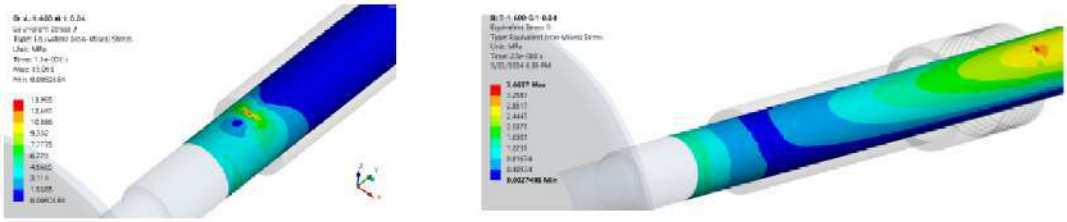

and) b)

Fig. 12. Mises stress map of the contact surface of the rod: a) steel (c); b) titanium (c)$t_m = 0.013\ t_m = 0.025$

Let's examine the indicators and the contact surface of the guide (mode$\sigma_{max} \sigma_{ave}$A-1-600-0.1-0.04). At the moment of time = 0.00023 s, the first contact of the rod with the guide occurs - it is 6.47 MPa (Fig. 13 a). Thus, having a free end (according to the design of the engine head in Fig. 12 $t_m \sigma_{max}$), the guide received an impulse and shows jump-like stresses. Further, the contact stabilizes and as the angle increases by = 0.01 s, the maximum stresses are 5.88 MPa (Fig. 13b). At the end of the experiment (= 0.04 s), the stresses move to the edge of the contact surface and increase to 12.35 MPa.$a_{vo} t_m t_m$

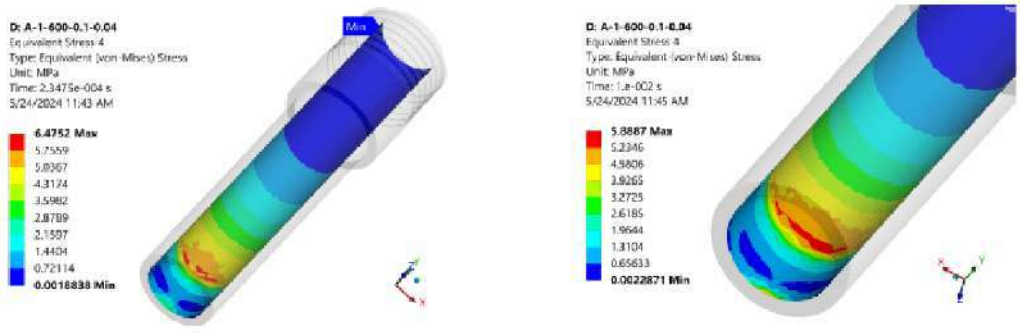

a) b)

Fig. 13. Stress map of the contact surface of the guide at the moment of time: a) 0.00023 s; b) 0.01 st_m

The behavior of the guide in the conditions of the regimeT-1-600-0.1-0.04 is very close to the steel valve model.

Effect of angleskew

According to the boundary conditions of the table. qg the following two modes were simulated, similar to those described above, but with a different graph of the skew angle. In fact, the difference between the skew angle is 0.01° at each of the 3 steps. Thus, curve #2 is more intense and in theory should cause higher stress values in the modesa_{vo}T-2-600-0.1-0.04 and A-2-600-0.1-0.04. INthe influence of the angle change in the case of a steel rod begins to appear from c, where the curves of maximum stresses diverge and, as of the end of the experiment, the difference is 3.63 MPa (9.41 and 13.1 MPa in the mode of curve #1 and #2, respectively). In contrast to mode A-1-600-0.1-0.04, where oscillations with the corresponding peak stress of 16.09 MPa were recorded in the first 0-0.0005 s, a more intensive change in angle stabilizes the valve better. The situation with the titanium valve is more obvious - a systematic growth is observed until the end of the experiment = 0.04 s, when the stresses are 7.14 and 5.21 MPa for modes with curve #2 and #1, respectively.$t_m = 0.025 \sigma_{max} a_{vo} \sigma_{max} t_{vo}$. Voltage at characteristic moments of time is shown in fig. 14. Of interest is the change in the shape of the contact spot in a very short period of time (s) and the change in stress from 2.69 to 2.87 MPa.$t_m t_m = 0.0094 - 0.01$.

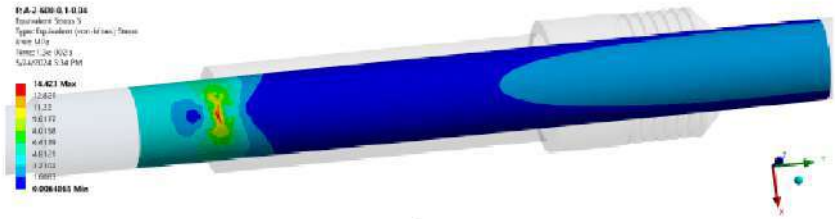

a)

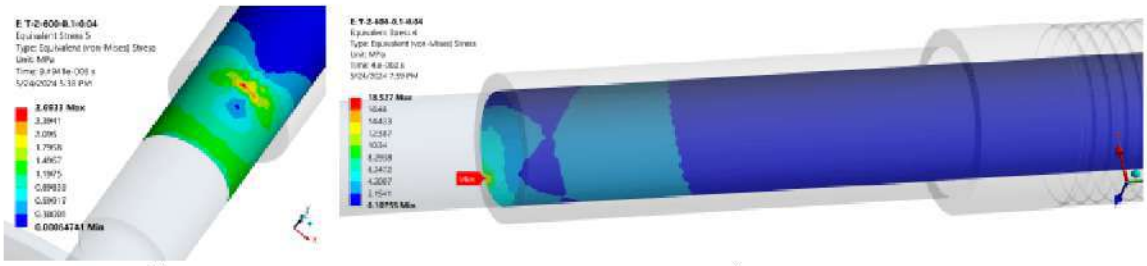

b) c)

Fig. 14. Stress maps in the regimes with the skew angle curve #2: a) steel valve in c; b) titanium valve in c; c) guide (modet_m = 0. 013 t_m = 0. 0094 T-2-600-0.1-0.04) at the momentt_m = 0. 04with

Thus, the preliminary hypothesis regarding the growth of stresses attransitions from curve #1 to #2 were confirmed. For example, (increase in average stresses) is 24-30% for the valve surface and 28-41% for the guide.$\Delta\sigma_{ave}$

Effect of temperature

The next iteration of calculations is devoted to the effect of temperature on the stress state of the models. So, to the previous modes with curve #2 (T-2-600-0.1-0.04 and A-2-600-0.1-0.04) apply a temperature of 900°C (to the surface of the valve head - Fig. 14) and analyze the obtained results. Titane models almost coincide with each other in values (7.14 and 7.16 MPa at 600 and 900σ_{max}°C, respectively), which are fixed as oft_m = 0.04with. The largest difference in maximum stresses between them is 1.57 MPa and was recorded at the time oft_m = 0.014Thus, it can be stated that the titanium alloy is resistant to temperature loads. The situation is different with a steel valve–= 50.3% (increase from 14.42 to 21.67 MPa) at the peak moment c, which came earlier than that of the titanium model (c). Steel turned out to be more sensitive to temperature changes in the valve. The bronze guide when interacting with the titanium valve almost did not feel changes in its temperature during stress analysis$\Delta\sigma_{max}$ t_m = 0.013t_m = 0.014 σ_{max}increased from 18.5 to 18.7 MPa.

This testifies to the positive influence of the titanium alloy on the thermodynamics of the guide and its working conditions– in fact, the titanium valve is as gentle as possible to the surface of the guide when heated.The steel valve as a result of the experiment (= 0.04 s) creates lower maximum stresses in the guide (14.02 and 14.5 MPa at 600 and 900t_{vo}°C, respectively), than titanium. WITHordinary tensionsσ_{ave}guide in combination with a steel valve are higher by more than 24% and when it is heated from 600 to 900°C show fluctuations.

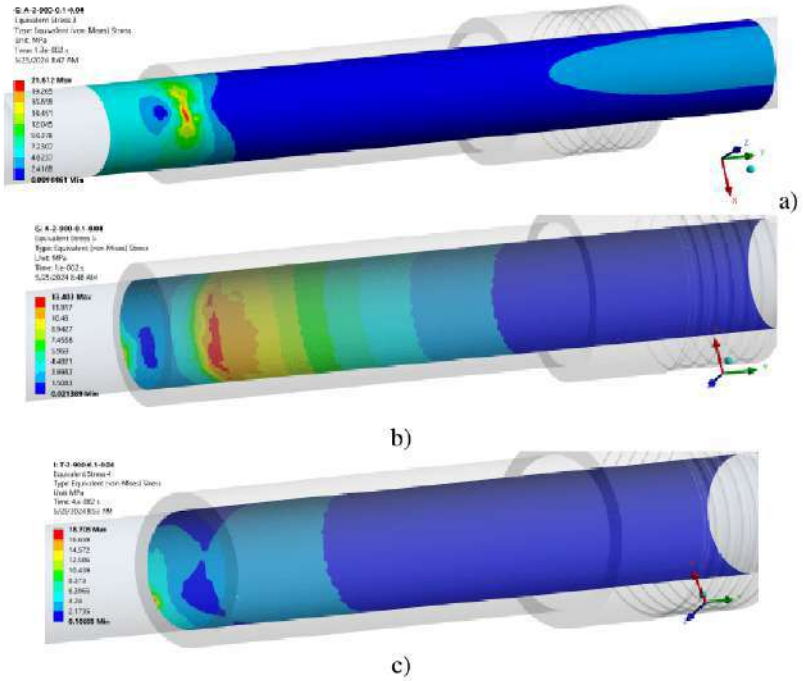

a)

b)

c)

Fig. 15. Stress maps at key moments of time: a) 0.013 s – steel rod; b) 0.01 s – guide in a complex with a steel valve; c) 0.04 s – a guide in a complex with a titanium valvet_m

The influence of the coefficient of friction

The next step and change the coefficient of friction in the previous modes$\mu_v$from 0.1 to 0.2. The modes will receive the following designations, respectively: T-2-900-0.2-0.04 and A-2-900-0.2-0.04. Magnification $\mu_v$from 0.1 to 0.2minimally reducedσ_{max} steel valve: 21.67 vs, 21.42 MPa as oft_m= 0.013 s. At the end of the experiment(= 0.04 s) the mode with greater friction showed a 25% higher value: 16.56 vs 13.19 MPa. The titanium sample is much less sensitive to changes due to higher surface hardness – the curves of the graphs almost coincide, and at the final moment = 0.04 s the difference is only 12.2% (7.16 vs, 8.03 MPa in the regimes with = 0.1 and 0.2, respectively),$t_{vo}\sigma_{max}\mu_v t_{vo}\mu_v$.

The maximum stresses of the guide body increased from 16.43 MPa (regσ_{max}A-1-600-0.1-0.04 on Fig. 16) up to 26.26 MPa (Fig. 16 a) when interacting with a steel valve, which in turn received 67.4 MPa as a result of temperature loading (edge of the head in Fig. 16 b). Titanium valve in current modeT-2-900-0.2-0.04 showed only 34.97 MPa (Fig. 16 b), and the corresponding guideline is 21.07 MPa.

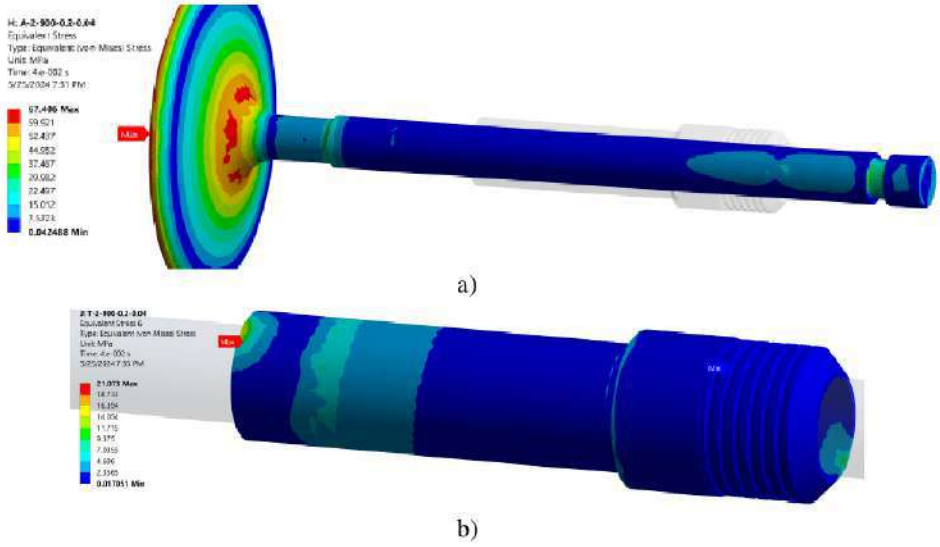

a)

b)

Fig. 16. Mises stress maps of valve and guide models in the mode: a)A-2-900-0.2-0.04; b) T-2-900-0.2-0.04

As a result, we get the following paradox: in general, the guide model receives lower maximum stresses when interacting with a titanium valve than in a complex with a steel one, but its contact surface, on the contrary, is more stressed precisely in the mode of interaction with a titanium valve.σ_{max}

Effect of engine speed

We will perform the next iteration of the calculation - we will determine the effect of engine revolutions (valve opening time) on the stress state of the model in modes T-2-900-0.1-0.01 andA-2-900-0.1-0.01 ($\mu_v = 0.1$), where the last component notation is just responsible forvalve opening duration =0.01 s. We will approximately calculate the frequency of rotation of the crankshaft for the given value.$t_{vo}t_{vo}$

The exhaust valve in a 4-stroke engine usually starts to open before reaching bottom dead center (BDC) on the intake stroke and finishes opening when it reaches top dead center (TDC) on the exhaust stroke. The total angle to which the exhaust valve is open is about 240-280° of crankshaft rotation, since it opens before the start of the exhaust stroke (about 40-60° before TDC) and closes after it ends (later 10-20° after TDC).

So, to determine the engine speed at which the valve opening time for 130° is 0.01 s, we will use the following approach: determine how long it takes for 1 full revolution of the crankshaft (360°); calculate the engine speed in revolutions per minute (rpm).

The time for a 130-degree rotation is 0.01 s. Let's determine the time for one complete revolution (360°): ; s, where: – time for one complete revolution, c.

$$\frac{130°}{360°} = \frac{0.01}{t_{ft}} t_{ft} = 0.0277 t_{ft}$$

Engine speed (rpm):

$$rmprmp = \frac{1}{t_{ft}} \cdot 60 = \frac{1}{0.0277} \cdot 60 = 2166 \frac{1}{min}.$$

So, the engine rotates at a frequency of approximately 2166 rpm, if the valve opening time (corresponding to 130° rotation of the crankshaft) is =0.01 s.t_{vo}

We update the boundary conditions - we update the graphs in Fig. 17, reducing the time along the abscissa axis to 0.01 s: graph$t_{vo}$of the stroke of the rod and the skew angle correspond to the step-by-step of the previous modes, only the values themselves are reached 4 times faster $s_{vo}a_{vo}$

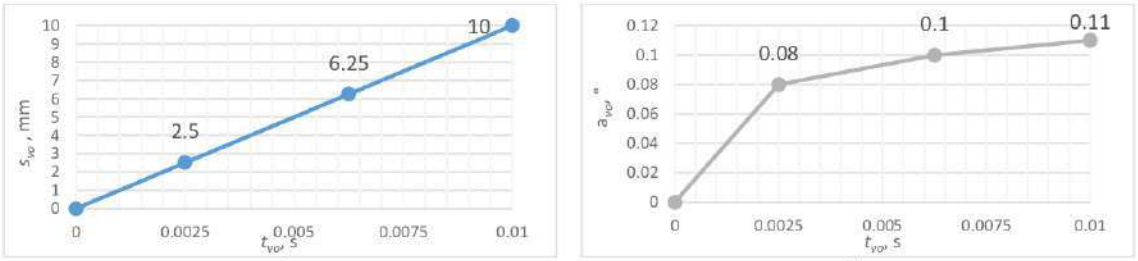

a) b)

Fig. 17. Kinematics of valve movement at: a)$rmp = 2166\frac{1}{min}$stroke of the rod; b) skew angles$s_{vo}a_{vo}$

All values of □□□□ and □□vereached at the end of the experiment =0.01 s. The exception is the modet_{vo}T-2-900-0.1-0.01, at whichσmaxin the guidefixed as of =0.0099 s and ist_m14.16 MPa.σmax and σaveat =0.01 s were always higher than the compared regimest_{vo}A-2-900-0.1-0.04 and A-2-900-0.1-0.04 witht_{vo}= 0.04 s except for the case with the guide in contact with the titanium valve: □□□□decreased from 18.71 to 14.16 MPa with decreasing time$t_{vo}$from 0.04 to 0.01 s (Fig. 18 a). The dimensions of this location on the edge of the guide are so small (0.3 mm) that the titanium valve literally "flies" past the contact spot when the engine revs increase. At the same time, □□vein the guide grew on171.5% (with1.44 to 3.91 MPa). The situation is similar in the A-2-900-0.1-0.01 mode –$\Delta\sigma_{ave}$guide folded111.9%, and 74.7%. Thus, the overall behavior of a titanium valve with a bronze guide is unique - increased revolutions go to the lower contact surface of the guide due to the reduction of maximum stresses and almost a 2-fold difference$\Delta\sigma_{max}\sigma_{ave}$(3.91 MPa in mode T-2-900-0.1-0.01and 7.5MPa in A-2-900-0.1-0.01).

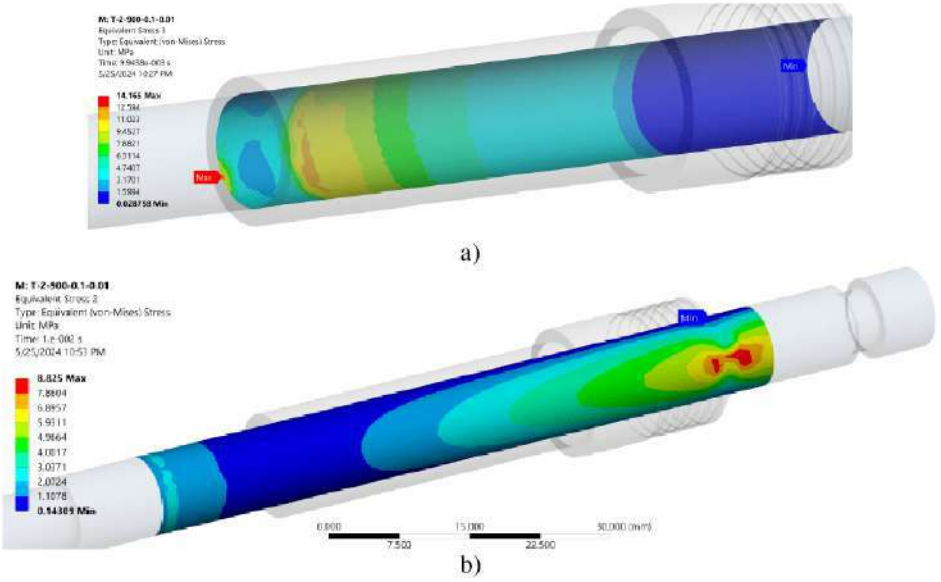

a)

b)

Fig. 18. Map of stresses according to Mises in modes z = 0.01 s: a) directionalt_{vo}T-2-900-0.1-0.01; b) titanium valvet_m= 0.01 s

Consolidated data

Let's summarize the array of results obtained above for each of the test modes in the table. 2: and – maximum and average stresses; and – stress difference in percentage between the current and previous mode of the same material;$\sigma_{max}\sigma_{ave}\Delta\sigma_{max}\sigma_{ave}t_{\sigma_{max}}$and is the time to reach the maximum and average stresses and .$t_{\sigma_{ave}}\sigma_{max}\sigma_{ave}$.

Table 2

Summary results for stresses and for Ansys model modes$\sigma_{max}\sigma_{ave}$

Contact surface of the valve						
Regime	σ_{max}, Mpa	$\Delta\sigma_{max}$, %	$t_{\sigma_{max}}$, p	σ_{ave}, Mpa	$\Delta\sigma_{ave}$, %	$t_{\sigma_{ave}}$, p
T-1-600-0.1-0.04	5.21	–	0.04	1.38	–	0.04
A-1-600-0.1-0.04	16.09	+208.8	0.00031	2.79	+102.2	0.04
T-2-600-0.1-0.04	7.14	+37.0	0.04	1.80	+30.4	0.04
A-2-600-0.1-0.04	14.42	-10.4*	0.013	3.47	+24.4	0.04
T-2-900-0.1-0.04	7.16	+0.3	0.04	1.91	+6.1	0.04
A-2-900-0.1-0.04	21.67	+50.3	0.013	3.99	+15.0	0.04
T-2-900-0.2-0.04	8.03	+12.2	0.04	1.91	0	0.04
A-2-900-0.2-0.04	21.42	-1.2	0.013	4.01	+0.5	0.04
T-2-900-0.1-0.01	8.82**	+23.22	0.01	1.92	+0.5	0.01
A-2-900-0.1-0.01	24.21**	+11.7	0.01	4.29	+7.5	0.01
The contact surface of the guide						
Regime	σ_{max}, Mpa	$\Delta\sigma_{max}$, %	$t_{\sigma_{max}}$, p	σ_{ave}, Mpa	$\Delta\sigma_{ave}$, %	$t_{\sigma_{ave}}$, p
T-1-600-0.1-0.04	13.98	–	0.04	0.95	–	0.04
A-1-600-0.1-0.04	12.35 p.m	- 11.7	0.04	2.23	+134.7	0.04
T-2-600-0.1-0.04	18.52	+32.5	0.04	1.34	+41.1	0.04
A-2-600-0.1-0.04	14.02	+13.5	0.04	2.85	+27.8	0.04
T-2-900-0.1-0.04	18.71	+1.0	0.04	1.44	+7.5	0.04
A-2-900-0.1-0.04	14.50	+3.4	0.04	3.54	+24.2	0.04
T-2-900-0.2-0.04	21.076	+12.7	0.04	2.32	+61.1	0.04
A-2-900-0.2-0.04	17.01	+17.3	0.04	4.81	+35.9	0.04
T-2-900-0.1-0.01	14.16**	-24.3	0.0099	3.91	+171.5	0.01
A-2-900-0.1-0.01	25.33**	+74.7	0.01	7.50	+111.9	0.01

Conclusions

Mode A-2-600-0.1-0.04 demonstrated$\Delta\sigma_{max} = -10.4\%$relativelyA-1-600-0.1-0.04, where oscillations with a corresponding peak stress of 16.09 MPa were recorded in the first 0-0.0005 s. The next stress peak = 13.99 MPa in mode A-1-600-0.1-0.04 (curve #1) occurs already at the moment of c. Thus, without taking into account the specified jump, the value +3.1% will be more balanced, as the difference between 13.99 and 14.42 MPa.$\sigma_{max}t_m = 0.013\Delta\sigma_{max} =$

Reference

1. Cooper, D., Thornby, J., Blundell, N., Henrys, R., Williams, MA, Gibbons, G., Design and Manufacture of high performance hollow engine valves by Additive Layer Manufacturing, Materials and Design (2014), doi: http://dx.doi.org/10.1016/j.matdes.2014.11.017.

2. Jedliński, Ł., Caban, J., Krzywonos, L., Wierzbicki, S., & Brumerčík, F. (2015). Application of vibration signal in the diagnosis of IC engine valve clearance. Journal of vibration engineering, 17(1), 175-187.https://www.extrica.com/article/15446

3. Dmitriev, SA, & Khrulev, AE (2019). Thermal Damage of Intake Valves in ICE with Variable Timing. International Journal of Automotive and Mechanical Engineering, 16(4), 7243-7258.http://journal.ump.edu.my/ijame/article/view/1600

4. Cavalieri, FJ, Zenklusen, F., & Cardona, A. (2016). Determination of wear in internal combustion engine valves using the finite element method and experimental tests. Mechanism and machine theory, 104, 81-99.https://doi.org/10.1016/j.mechmachtheory.2016.05.017

5. Srivastava, H. , Chauhan, A. , Kushwaha, M. , Raza, A. , Bhardwaj, P. and Raj, V. (2016) Comparative Study of Different Materials with Al-Sic for Engine Valve Guide by Using FEM . World Journal of Engineering and Technology, 4, 238-251. doi:10.4236/wjet.2016.42023.

6. Crozet, M., Berthier, Y., Saulot, A., Jones, D., & Bou-Saïd, B. (2021). Valve-seat components in a diesel engine: a tribological approach to limit wear. Mechanics & Industry, 22, 44. https://doi.org/10.1051/meca/2021043

7. Kumar, GU, & Mamilla, VR (2014). Failure analysis of internal combustion engine valves by using ANSYS. American International Journal of Research in Science, Technology, Engineering & Mathematics.document (psu.edu)

8. Forsberg, P., Debord, D., & Jacobson, S. (2014). Quantification of combustion valve sealing interface sliding—A novel experimental technique and simulations. Tribology International, 69, 150-155.https://doi.org/10.1016/j.triboint.2013.09.014

9. Muzakkir, SM, Patil, MG, & Hirani, H. (2015). Design of innovative engine valve: background and need. International Journal of Scientific Engineering and Technology, 4(3), 178-181.indianjournals.com/ijor.aspx?target=ijor:ijset1&volume=4&issue=3&article=013

Голенко К.Е. Вичавка А.А., Диха М.О., Дитинюк В.О. Скінчено-елементний аналіз контактних характеристик і режимів тертя пари «клапан-напрямна» двигуна внутрішнього згорання

Моделювання працездатності пари двигуна «клапан-напрямна» за допомогою сучасних програмних засобів є дієвим інструментом як для виявлення слабких місць в конструкції, так і прогнозуваняя поведінки вузла тертя в експлуатації. В даному дослідженні для дослідження контактних і антифрикційних параметрів пари тертя двигуна внутрішнього згорання «клапан-напрямна» як інструмент вибраний метод скінчено-елементного аналізу. За використання прикладної програми FEM описані вихідні дані по матеріалу, розмірам поверхонь, навантаженням, кінематиці руху. На основі побудованої скінчено-елементної моделі спряження «клапан-напрямна» проведений аналіз впливу визначальних трибологічних факторів: швидкості ковзання в контакті, температури, кута перекосу, коефіцієнту тертя на контактні напруження як для кожної деталі пари тертя, так і в процесі контактної взаємодії. Побудована консолідована матриця результатів чисельного експерименту, обгрунтовані висновки щодо впливу кожного фактора на трибологічні характерстики. Окреслені алгоритми впливу на конструкторсько технологічні і експлуатаційні фактори для подовження ресурсу пари тертя двигуна ДВЗ «клпапн-напрямна».

Ключьові слова: двигун внутрішнього згорання, напрямні клапанів, скінчено-елементна модель, контактні параметри, коефіцієнт тертя, напружений поверхневий стан

Problems of Tribology, V. 29, No 32/113-2024, 56-64

Problems of Tribology
Website: http://tribology.khnu.km.ua/index.php/ProbTrib
E-mail: tribosenator@gmail.com

DOI: https://doi.org/10.31891/2079-1372-2024-113-3-56-64

Adhesive built-up edge on tool steels due to friction and wear

O.M. Makovkin*, O.V. Dykha, I.K. Valchuk

Khmelnytskyi national University, Ukraine
**E-mail: makovkin@ukr.net*

Received: 05 July 2024: Revised 30 July 2024: Accept 05 September 2024

Abstract

When processing metals by cutting, there are a number of materials prone to growth. This phenomenon leads to a change in the geometry of the cutter, cutting forces and surface quality, final dimensions of the part. In friction nodes: shaft-sleeve, piston-sleeve, etc. this phenomenon causes jamming. In this work, experimental studies of the processes of dry friction of tool steels with coatings were carried out to evaluate the effectiveness of reducing the growth process. As a result, it was established that the nature of formation, destruction and size of growth of materials prone to growth depends on the chemical composition of the material and modes of friction. High-strength chromium-manganese steels are most prone to growth and microseizures. It is shown that the well-known recommendation of increasing speed cannot always be used to prevent build-up, but it can be achieved by using single-layer and multi-layer coatings with a defect-free structure and moderate friction modes. It was found that electrolytic single-layer nickel and chromium coatings contribute to the formation of growth on the studied materials and this phenomenon does not depend on the modes of friction, while the same chemical coatings, which have an almost defect-free structure, are almost not prone to growth formation.

Key words: adhesion, build-up, friction, wear, contact pressure, tool steels, chemical and electrolytic coatings.

Introduction

Under certain conditions of friction in air, in a vacuum and in environments that do not contain enough oxygen for the formation of secondary structures with its participation, wear of the contact surfaces is observed, which is associated with their direct destruction due to the development of the adhesion process.

From the practice of cutting metals, it is known that there are a number of materials prone to growth. This phenomenon is undesirable, because in the process of metal cutting, it leads to a change in the geometry of the cutter, cutting forces and surface quality, and the final dimensions of the part. In closed systems (shaft-sleeve, piston-sleeve, etc.), this phenomenon causes jamming. In the practice of metal cutting, this phenomenon is overcome by changing the cutting modes, and in mechanical engineering, as a rule, they try not to use such materials. But such an approach is irrational, since materials that are likely to be prone to growth can exhibit quite attractive mechanical, physical, and tribological properties.

In addition, the data provided in the literature about materials prone to build-up formation do not contain information about the behavior of the build-up in the friction process, and if the behavior of the material under certain operating conditions (modes) is unknown, the possibility of their use becomes problematic.

Therefore, in order to study the nature of this phenomenon, it became necessary to conduct a series of studies to identify materials that are prone to growth, study the nature of this phenomenon, and recommend prevention of growth. To identify the propensity of materials to build up, it is necessary to conduct a series of complex experimental studies.

Review of known studies

Buildup can affect tool wear and surface integrity when machining ductile metals. The main purpose of the work [1] is to study the close relationship between the formation of growth and the tribological behavior at the

interface between the tool and the working material during the processing of plastic metals. Machining of AA2024-T351 aluminum alloy with WC–Co carbide tool is considered as a practical example. A new method is proposed, based on the introduction of a time-dependent friction coefficient at the interface between the tool and the working material. Two cases were considered, which correspond, respectively, to a sharp change and a gradual development of friction at the tool-work material interface.

When turning SAE 1045 carbon steel with uncoated carbide cutting tools at a cutting speed of 50 m/min–150 m/min , the wear is characterized by crater wear [2]. In the mode of low cutting speed, the formation of a built-up edge (BUE) is visible. BUE structures are unstable in the cutting process and lead to deterioration of the surface of the workpiece. Laser surface texturing was applied to texturize the front surface of the cutting tool with different textures to change the adhesion tendency of the growth to the cutting tool. The process is accompanied by better wear behavior compared to a non-textured cutting tool with respect to corner radius wear. It is shown that the adhesion of the workpiece material on the front surface can be changed in relation to the non-textured cutting tool made of hard alloy in the process of dry metal cutting by applying laser textures.

The work [3] presents a study of the formation of a raised edge during the machining of S32750 stainless steel. The BUE structures obtained at different cutting speeds were studied. The growth geometries were determined using a scanning electron microscope and white light interferometry. Analysis of the growth structure revealed a high level of grain refinement and elongation for both ferritic and austenitic structures. The effect of growth on the machining process from the point of view of chip formation and surface integrity was studied. It is shown that it is possible to significantly improve the friction conditions and the integrity of the workpiece surface at low cutting speeds.

When processing titanium alloys, the task remained to find an effective technology to increase tool life during machining using surface treatment tools. It was found that in the case of turning, this can be achieved by applying a self-lubricating TiB2 PVD coating. TiB2 coating has been shown to increase tool life by more than 60% compared to an uncoated tool. An analysis [4] of the wear resistance of the coated and uncoated cutting tool was carried out using the methods of optical 3D imaging. The coating also showed less impact on the substrate, as it did not indicate better protection of the coated tool surface. The TiB2 coating is shown to combine beneficial micromechanical characteristics and self-lubricating properties due to the formation of tribofilms on the tool surface during operation.

A feature when cutting many alloys is that workpiece material adheres to the cutting tool at the sliding contact surfaces, between the work material and the tool [6]. This built-up material formed during cutting is of fundamental importance in machining operations, because it may significantly affect the surface roughness, tool wear, workpiece dimensions and tolerances, tool forces, and chip form. The agglomeration of the work material to the tool appears to be analogous to cold welding, metal transfer in tribology and dead zone in extrusion. In machining terminology this phenomenon is often called "built-up edge" (BUE). Several important factors affect the built-up material formation, e.g. cutting temperature, cutting speed, strain hardening, adhesion between the work material and the tool, micro-crack formation, plastic flow of the work material in the vicinity of the cutting edge, etc.

Tool wear is one of the main parameters employed for evaluating tool life, due to its influence in the loss of quality of the manufactured parts [7]. Different mechanisms can cause the tool wear in a specific machining process. Adhesion wear is one of the tool wear mechanisms that can be present in a wider range of cutting temperatures. This type of tool wear can be produced by the direct adhesion wear is caused by the incorporation of tool particles to the chips. Tool geometry changes by the material incorporation. In a second place, when these fragments are removed, they can drag out tool particles causing tool wear. This study has been developed using aerospace aluminium alloys. Results is formed by mechanical adhesion mechanism. On the other hand, BUL is initially formed by thermo-mechanical causes. Obtained results have confirmed that BUE changes the tool position angle giving rise to a reduction of Ra.

Built-up edge has been noted as a major cause for surface finish deterioration in micromachining processes—even a trace formation of hardened and brittle structure on the tool edge alters the chip load, creates ad hoc and irregular material flow patterns, and results in deposits and smeared regions on the machined surface. To date, few investigations have addressed the formation and effects of BUE in micromachining. The paper [8] is one of the first experimental investigations of the BUE effects on surface quality and its prediction in micromachining. The experiments consisted of micromilling 12mm long thin channels on 316L stainless steel plates (30mm×40mm×0.5mm) using uncoated tungsten carbide micromills at 16 different settings of carefully selected combination of cutting speed and chip load with minimum quantity lubrication (MQL). These metrics capture, respectively, the extent and dispersion of BUE on the surface. We also conducted empirical studies to assess the extent to which these quantifiers can determine the variation in surface finish (Sa). Results suggest that the BUE is the major determinant of surface finish besides the chip load effect in micromachining.

Titanium alloys are widely used in aerospace industries due to their excellent physical and mechanical performances, however, their poor machinability always induce fast tool wear. In [9] design of experiments was used towards analyzing pertinent effects involved in machining Ti6Al4V. Uncoated carbide inserts were artificially treated with different initial flank wear (VB) in order to decouple the effects involved in progressive wear condition from rake and flank faces. Dry cutting, flood cutting with emulsion and cryogenic cutting with liquid nitrogen (LN2) were used as different cooling strategies. The results show that initial VB presents significant

contributions to BUEs formation, diffusion wear and cutting forces fluctuation, especially under aggressive cutting conditions.

Research methodology

The research was carried out on a modernized universal friction machine UMT 2168 with data fixation and recording (linear wear, average temperature in the friction zone and friction moment) in automatic mode without stopping the friction process [10]. The samples were used with a spherical friction surface, the counterbody is made of AISI G51320 HRC 55 steel. Experiments were performed with a constant force of pressing the sample to the counterbody (from 20 to 60 N) in the range of speeds from 0.6 to 1.5 m/s. Since the shape of the surface of the sample is hemispherical with a radius of R=2.5 mm, according to Hertz's formula, high (1300-2000 MPa) contact stresses occur in the contact zone at the initial stage of friction.

The dependence of the size of the contact area on the stress is shown in Fig. 1.

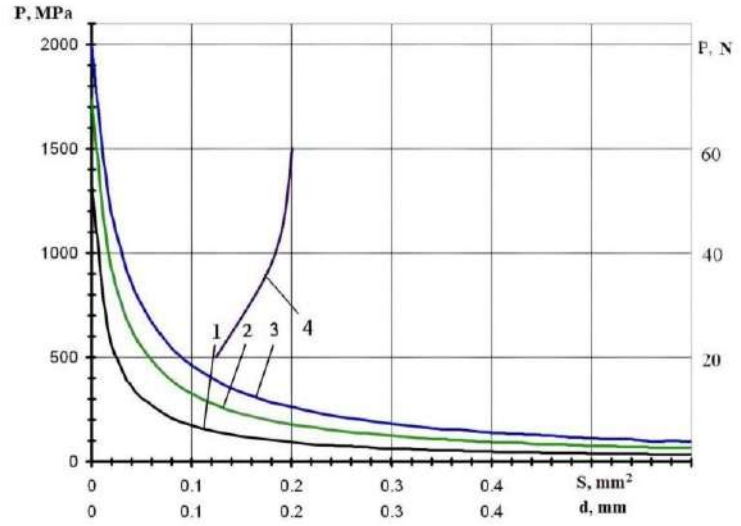

Fig. 1. Dependence of the diameter of the contact spot on stress at different pressing forces (P) (1 – 20 N, 2 – 40 N, 3 – 60 N) of contacting bodies. Dependence of the size of the initial area of the contact spot (4) on the pressing force

Friction modes are given in table. 1, which were chosen from conditions close to the parameters that occur when cutting metals (in particular, stress) and from the requirements of mathematical planning.

Table 1

Modes of friction

Mode No	Friction parameters		
	Pressing force, N	Initial stress, MPa	Cutting speed, m/min
1	60	2000	80
2	20	1300	40
3	60	2000	80
4	20	1300	40

Tool alloy steels (AISI 9262, AISI T31507) and high-speed AISI M3 in the heat-hardened state were used as the object of the study, the mechanical characteristics of which are given in the table. 2.

Table 2

Mechanical characteristics of tool steels

Material	HRC	Endurance limit σB, MPa
AISI 9262	55	1760
AISI T31507	52	1850
AISI M3	60	1300

To increase the tribological parameters and prevent the formation of growth, chromium and nickel coatings were used, as well as composite coatings based on Ni and dispersed particles of Cu, Al2O3 (the thickness of the coating was 10...15 microns). At the same time, the coating technology was used [11].

Research results and their discussion

After conducting a number of test experiments on different steels AISI M3, AISI 9262, AISI T31507 and under different test conditions, it was found that the tendency of AISI T31507 and AISI 9262 steels to form growth, which manifested itself in an increase in the initial linear dimensions of the sample at the first stages of the experiment. Moreover, this phenomenon was observed only at the initial stages, and therefore our calculations will reflect the characteristics of friction and wear of the studied materials at the initial stage, that is, during a fairly short period of time of the study (for 200...300 m of the tested path). We will not provide data on changes in tribological parameters (moment of friction, temperature in the contact zone, intensity of wear) in this message.

As shown by the results (Fig. 2), at the first stage of research on AISI T31507 steel, at friction modes 2, 3, 4, the first wear zone is distinguished, where an increase in the linear size of the sample by 0.02-0.05 mm is observed when passing 25 m of the friction path and its gradual reduction to the initial dimensions at 150 m of the traveled friction section, intensive wear of the sample occurs in mode 1.

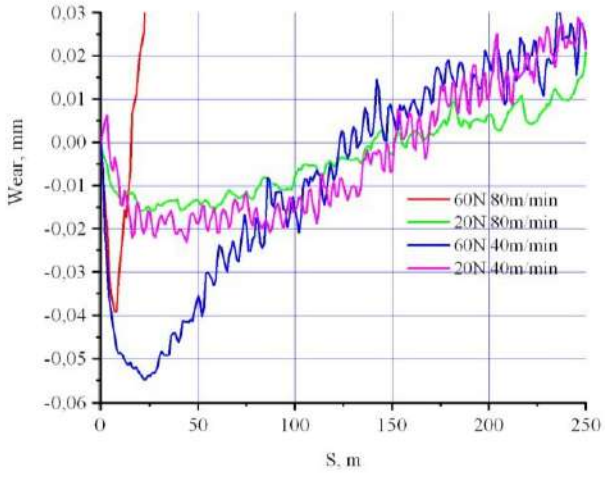

Fig. 2. Effect of friction modes on linear wear of AISI T31507 steel

The increase in the linear size of the growth is accompanied by a rapid increase in temperature and friction moment and depends on the modes of friction - the amount of contact stress and the speed of sliding (larger growth sizes corresponded to higher contact stress). Moreover, only at the maximum contact stress and the maximum sliding speed (Fig. 2, curve 1) is there a chipping of the growth and a sharp change in the linear size of the sample under study, for all other modes (Fig. 2, curves 2, 3, 4.) - smooth monotonic reduction of growth. This is clearly shown on the graphs when the scale is increased along the ordinate axis (traveled path). By reducing the discreteness of the measurement of the amount of wear to 0.5 s, the nature of wear of the material is clearly marked on the wear curves and, as can be seen from fig. 2, the wear process takes place, in our opinion, by periodic seizure of contacting micro-areas, destruction of the bridge, removal of wear products from the contact zone. This is evidenced by the dust-like wear curves. To verify such assumptions, it is necessary to carry out fine studies of the friction surface, which will allow us to judge the mechanism of wear.

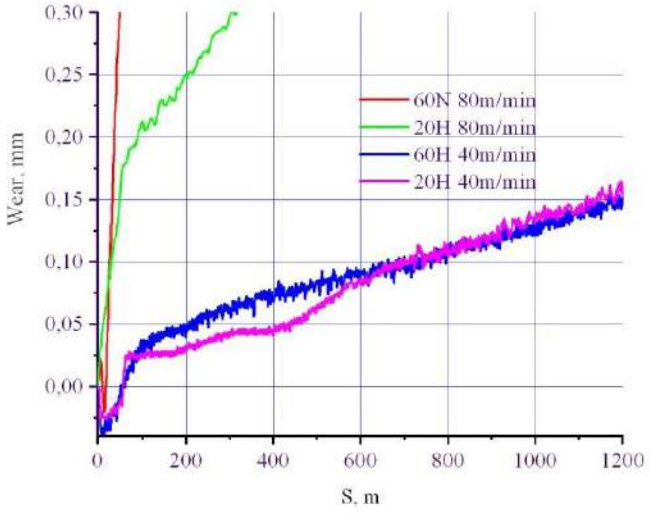

Fig. 3. Linear wear of AISI T31507 nickel-plated steel

It is known that all materials can be divided into materials that are not prone to or prone to growth. Technological methods of applying wear-resistant coatings were used to prevent growth.

After testing the electrolytic nickel coating of Fig. 3 for friction and wear, it was established that under the same regimes growth occurs again, and in general, the general pattern of wear has not changed, and in some cases the amount of wear has increased. The growth disappears after 100 m of the traveled path, while on the samples without coating the growth stops after 150 m of the traveled path. The wear process is carried out in the same way as the sample without coating.

Analysis of the above studies of the tribobehavior of AISI T31507 steel with a two-layer coating (sublayer of copper (Cu) and nickel (Ni)), which is presented in Fig. 4, indicates that the conditions for growth formation are created on the surface of this coating. A growth was formed, but the linear size of the growth was insignificant, the maximum size was equal to 0.035 mm. Moreover, this value was obtained according to test mode 4.

In other research modes, growth formation was not observed. In addition, after wear to a certain limit, there is a sharp decrease in the moment of friction, which, in our opinion, is a manifestation of the effect of copper on the change in the coefficient of friction.

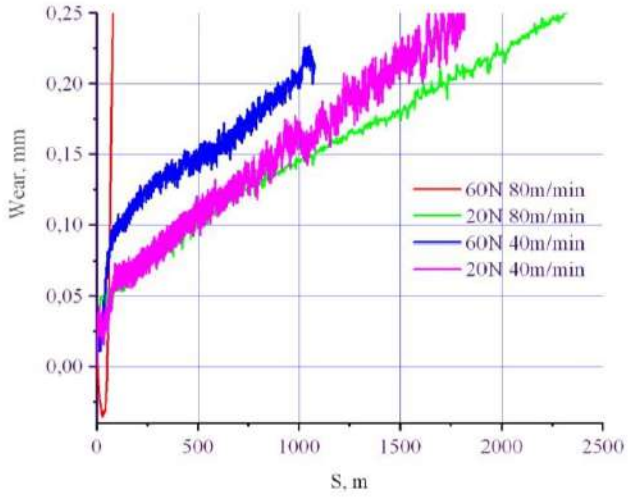

Fig. 4. Linear wear of steel AISI T31507 with two-layer copper-nickel coating

After a relatively successful attempt to solve the problem of build-up formation by applying a two-layer copper-nickel coating, the modes of build-up formation of a combined coating based on nickel (Ni) with particles of corundum (Al2O3) were determined, fig. 5, which was applied to the surface of AISI T31507 steel according to the technology proposed by the authors [11].

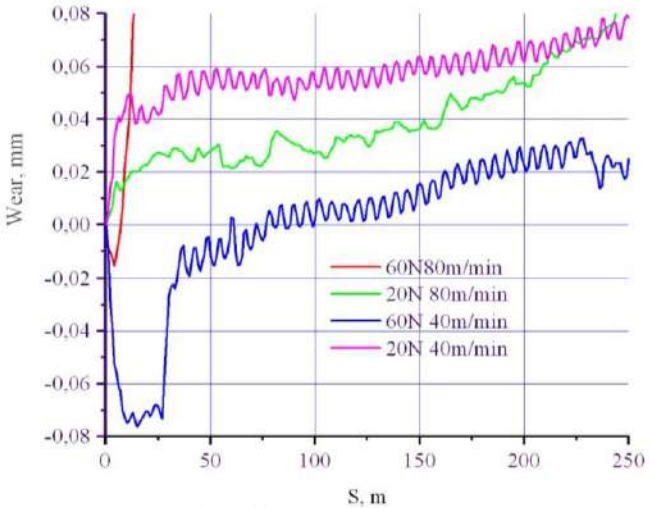

Fig. 5. Linear wear of T31507 steel with combined Al2O3-Ni coating

It was established that the growth process does not occur at all during experimental studies in modes 2, 4, but at the same time, an increase in the moment of friction, temperature, and more intense wear compared to the original material is noted.

Since nickel coatings, complex coatings based on nickel, copper and corundum on AISI T31507 steel are insufficiently effective against scale formation, the aim was to test the influence of chromium on the process of scale formation. For this, electrochemical and chemical chromium coatings were used, differing among themselves in the defectiveness of the surface layer. When a coating was applied to the base by chemical deposition of chromium and during the further study of tribological characteristics on a friction machine, no build-up was recorded (Fig. 7) in any mode, and the friction moment and average temperature in the friction zone also decreased.

For comparison, a chrome coating was applied using the electrolytic method. During tribological studies, intensive growth was established on friction modes 1, 2, 3; the intensity of growth formation depended on the modes of friction (Fig. 6).

From our observations and as a result of the analysis, it was established that the greater the force of clamping the sample, the greater the linear size of the growth.

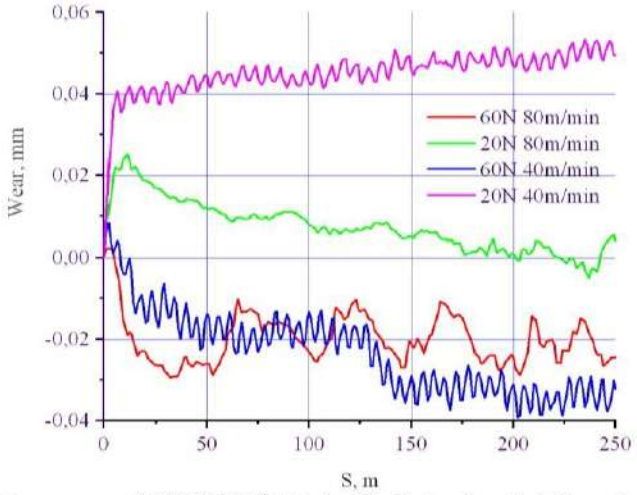

Fig. 6. Linear wear of AISI T31507 steel with electrochemical chromium coating

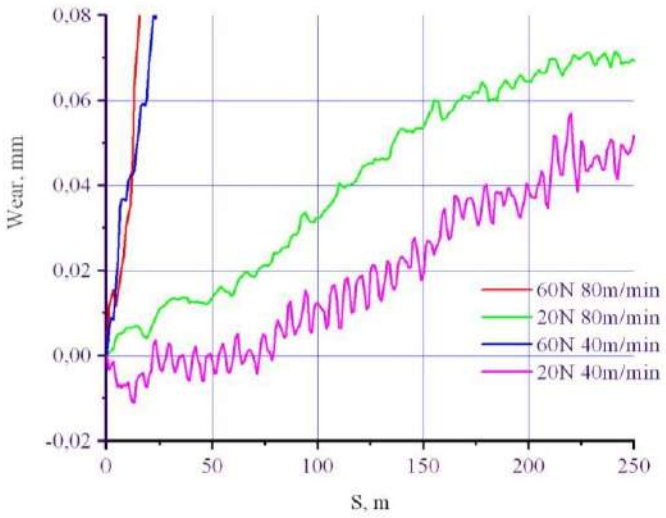

Fig. 7. Linear wear of steel AISI T31507 with chemical chromium coating

Since the active formation of growth with chromium coating applied by the electrolytic method and its almost absence on samples with chemically deposited chromium was detected, we decided to investigate its behavior on siliceous spring steels with different structural states of the matrix (steel AISI 9262, tempering temperature 200, 300, 400 0C), high-speed steel AISI M3.

During experimental studies, it was established that on the surface of a sample of AISI 9262 steel with a tempering temperature of 2000C and a chrome electrolytic coating, growth was not formed only on the fourth mode of friction (Fig. 8) curve 4. It should be noted that on friction modes 2, 4 wear curves 6, 8 was 0.05 mm per 2,000 m of travel, while, using a clean sample, the wear was already 0.4 mm after 200 m of travel.

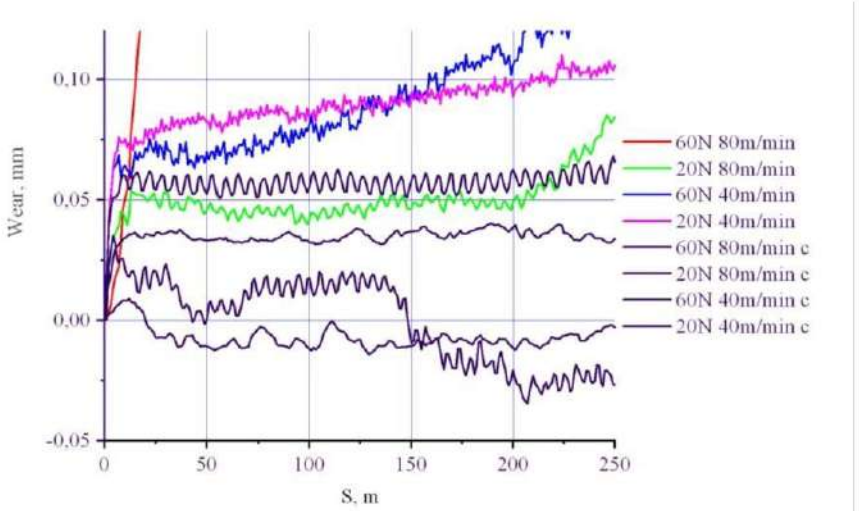

Fig. 8. Linear wear of steelAISI9262, tempering temperature 200 0C wear lines 1, 2, 3, 4 - material without coating; 5, 6, 7, 8 - with chrome electrolytic coating

Chromium electrolytic coating on AISI 9262 steel with a tempering temperature of up to 300 0C (martensite structure of tempering) behaved in a completely different way - at the same time, growth formation was observed in all modes of friction; moments and temperature jumps, which are interrelated, but with intense friction modes, the wear line fluctuates in the range of 5...6 μm, at 2000 m of the traveled path, while the wear of the uncoated sample when reaching 200 m was 0.2 mm (Fig. 9, mode 3, curve 3).

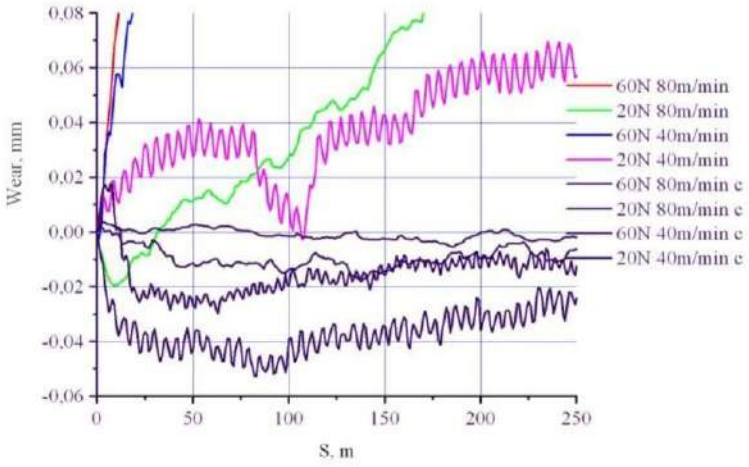

Fig. 9. Linear wear of steelAISI9262, tempering temperature 300 0C wear lines 1, 2, 3, 4 - material without coating; 5, 6, 7, 8 - with chrome electrolytic coating

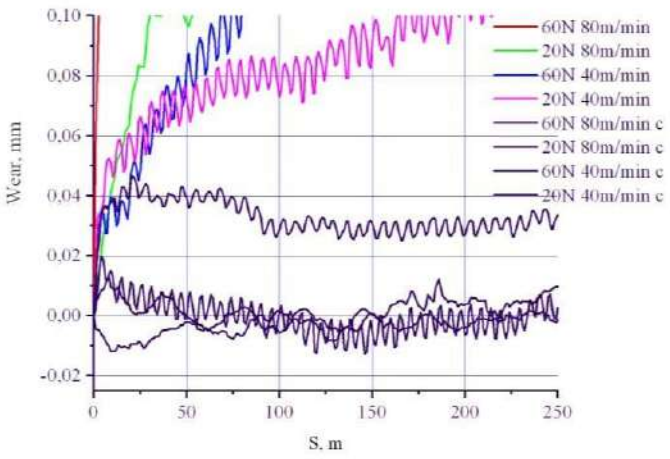

Fig. 10. Linear wear of steelAISI9262, tempering temperature 400 0C, wear lines 1, 2, 3, 4 material without coating, 5, 6, 7, 8 - with chrome electrolytic coating

When using AISI 9262 steel with a tempering troostite structure (tempering temperature 400 0C) for electrolytic chromium coating, growth formation is observed in all modes of friction, but wear decreased by 3-5 times, depending on the mode of friction when using this coating (Fig. 10).

Research on the wear resistance of AISI M3 steel (Fig. 11) showed that on the regimes (1-4 wear curves 5 - 8) growth formation is observed, but the wear of AISI M3 steel decreased by 2...3 times.

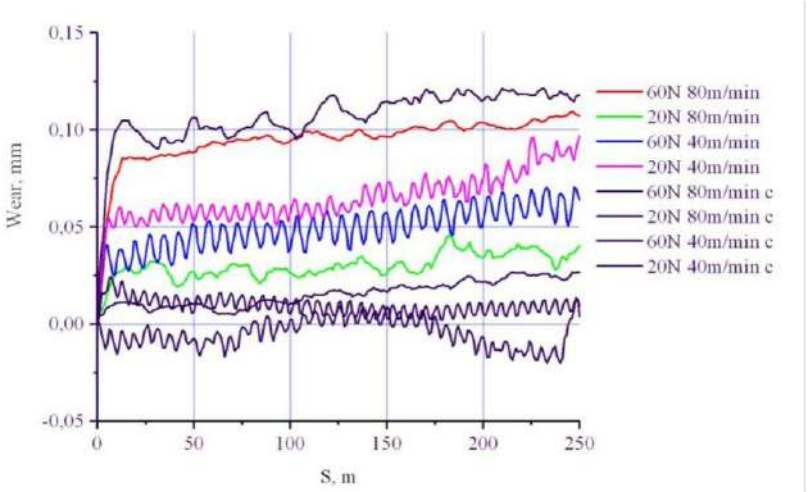

Fig. 11. Linear wear of M3 steel, wear lines 1, 2, 3, 4 - material without coating, 5, 6, 7, 8 - with chrome electrolytic coating

Conclusions

The technique of continuous, automatic recording of tribological characteristics allows to detect not only the tendency of materials to form growth, but also the microseizure of surfaces during the tests.

The nature of formation, destruction, and growth size of materials prone to growth depends on the chemical composition of the material and friction modes. High-strength chromium-manganese steels are most prone to growth and microseizures.

In order to prevent growth, it is not always possible to use the well-known recommendation - to increase the speed, but to achieve it by using single-layer and multi-layer coatings with a defect-free structure and moderate modes of friction.

It was found that electrolytic single-layer nickel and chromium coatings contribute to the formation of growth on the studied materials and this phenomenon does not depend on the modes of friction, while the same chemical coatings, which have an almost defect-free structure, are almost not prone to growth formation.

References

1. S. Atlati, B. Haddag, M. Nouari, A. Moufki,Effect of the local friction and contact nature on the Built-Up Edge formation process in machining ductile metals,Tribology International,Volume 90, 2015, Pages 217-227, https://doi.org/10.1016/j.triboint.2015.04.024.

2. Johannes Kümmel, Daniel Braun, Jens Gibmeier, Johannes Schneider, Christian Greiner, Volker Schulze, Alexander Wanner, Study on micro texturing of uncoated cemented carbide cutting tools for wear improvement and built-up edge stabilisation, Journal of Materials Processing Technology, Volume 215, 2015, Pages 62-70, https://doi.org/10.1016/j.jmatprotec.2014.07.032.

3. Yassmin Seid Ahmed, Jose Mario Paiva, Bipasha Bose, Stephen Clarence Veldhuis, New observations on built-up edge structures for improving machining performance during the cutting of superduplex stainless steel, Tribology International, Volume 137, 2019, Pages 212-227,https://doi.org/10.1016/j.triboint.2019.04.039.

4. M.S.I. Chowdhury, S. Chowdhury, K. Yamamoto, B.D. Beake, B. Bose, A. Elfizy, D. Cavelli, G. Dosbaeva, M. Aramesh, G.S. Fox-Rabinovich, S.C. Veldhuis, Wear behaviour of coated carbide tools during machining of Ti6Al4V aerospace alloy associated with strong built up edge formation, Surface and Coatings Technology, Volume 313, 2017, Pages 319-327, https://doi.org/10.1016/j.surfcoat.2017.01.115.

5. Dong Zhang, Xiao-Ming Zhang, Guang-Chao Nie, Zheng-Yan Yang, Han Ding, In situ imaging based thermo-mechanical analysis of built-up edge in cutting process, Journal of Manufacturing Processes, Volume 71, 2021, Pages 450-460,

6. Tomac, N., Tønnessen, K., Rasch, F.O., Mikac, T. (2005). A Study of Factors That Affect the Build-Up Material Formation. In: Kuljanic, E. (eds) AMST'05 Advanced Manufacturing Systems and Technology. CISM

International Centre for Mechanical Sciences, vol 486. Springer, Vienna. https://doi.org/10.1007/3-211-38053-1_17

7. A. Gómez-Parra, M. Álvarez-Alcón, J. Salguero, M. Batista, M. Marcos, Analysis of the evolution of the Built-Up Edge and Built-Up Layer formation mechanisms in the dry turning of aeronautical aluminium alloys, Wear, Volume 302, Issues 1–2, 2013, Pages 1209-1218, https://doi.org/10.1016/j.wear.2012.12.001.

8. Z. Wang, V. Kovvuri, A. Araujo, M. Bacci, W.N.P. Hung, S.T.S. Bukkapatnam, Built-up-edge effects on surface deterioration in micromilling processes, Journal of Manufacturing Processes, Volume 24, Part 2, 2016, Pages 321-327, https://doi.org/10.1016/j.jmapro.2016.03.016.

9. Hongguang Liu, Yessine Ayed, Hélène Birembaux, Frédéric Rossi, Gérard Poulachon, Impacts of flank wear and cooling strategies on evolutions of built-up edges, diffusion wear and cutting forces in Ti6Al4V machining, Tribology International, Volume 171, 2022, 107537, ISSN 0301-679X, https://doi.org/10.1016/j.triboint.2022.107537.

10. Automation of friction and wear process research Hladkyi Y.M., Taranchuk A.A., and others // Bulletin of the Khmelnytskyi National University. - 2005. - No. 1 - pp. 12-16.

11. The effect of heat treatment on the wear resistance of coatings, Hladkyi, Y.M., Pokryshko, G.A., and others // Bulletin of the Khmelnytskyi National University. – 2005. – No. 5 – Part 1, Volume 1. – p. 27-30.

Маковкін О.М., Диха О.В., Вальчук І.К. Адгезійний нарост на інструментальних сталях при терті і зношуванні

При обробці металів різанням існує ряд матеріалів схильних до наростоутворення. Це явище призводить до зміни геометрії різця, сил різання та якості поверхні, кінцевих розмірів деталі. У вузлах тертя: вал-втулка, поршень-гільза і т.д. це явище спричиняє заклинювання. В даній роботі проведені експериментальні дослідження процесів сухого тертя інструментальних сталей з покриттями для оцінки ефективності зменшення процесу наростоутворення. В результаті встановлено, що характер утворення, руйнування та розмір наросту матеріалів, схильних до наростоутворення, залежить від хімічного складу матеріалу та режимів тертя. Найбільш схильними до наростоутворення та мікросхоплювань є високоміцні хромо-марганцеві сталі. Показано, що дДля запобігання наростоутворення не завжди можна використовувати відому рекомендацію - збільшення швидкості, а досягнути шляхом використанням одношарових, та багатошарових покрить з бездефектною структурою та помірковані режими тертя. Виявлено, що електролітичні одношарові нікелеві та хромисті покриття сприяють утворенню наросту на досліджуваних матеріалах і це явище не залежить від режимів тертя, в той час, як такі ж хімічні покриття, що мають практично бездефектну структуру, майже не схильні до наростоутворення.

Ключьові слова: адгезія, нарост, тертя, зношування, контактний тиск, інструментальні сталі, хімічні та електролітичні покриття.

Problems of Tribology, V. 29, No 32/113-2024, 65-71

Problems of Tribology
Website: http://tribology.khnu.km.ua/index.php/ProbTrib
E-mail: tribosenator@gmail.com

DOI: https://doi.org/10.31891/2079-1372-2024-113-3-65-71

The effect of manganese and carbon on the mechanical properties of the welded layer of the bucket teeth of the Hadfield steel excavator

S.F. Posonskyi

Khmelnytskyi national University, Ukraine
E-mail: p.s.f@ukr.net

Received: 15 July 2024: Revised 02 September 2024: Accept 20 September 2024

Abstract

The paper investigates the effect of the surfacing composition's chemical structure (the manganese and carbon concentrations' ratio) on the mechanical properties of the surfacing layer on Hadfield steel for increasing the durability of the products made from it, namely the excavator bucket's teeth. Two criteria, namely the impact toughness and wear resistance of the coating, were chosen as optimization parameters. The assessment of the impact strength of the deposited coating was carried out on the Sharpie samples on the pendulum copra, and the wear test was carried out according to the Brinly-Haworth scheme in the conditions of samples' abrasion with quartz sand. Wear resistance of Hadfield steel, containing 1.1% *C* and 13% *Mn*, was taken as a unit of wear resistance in these experiments. To determine the optimal coating modes, the active experiment with the application of mathematical planning methods was conducted. The obtained response surfaces and graphs of equal output lines make it possible to establish the level of studied factors' influence on the optimization parameter. In order to analyze the influence of given factors on the optimization criteria, scatter plots with histograms were constructed, which make it possible to determine the rational values of the selected optimization criteria graphically - impact toughness and wear resistance of the coating.

Key words: teeth of the excavator bucket, Hadfield steel, deposited layer, manganese, carbon, impact toughness, wear resistance, optimal parameters

Introduction

Meeting the requirements for soil treatment largely depends on the efficiency and condition of the tillage machines' working bodies. Increasing their durability and ensuring proper recovery are critically important for the agro-industrial complex (AIC) of Ukraine. This task becomes especially vital taking into account the specific operating conditions of the tillage machines, which work in environments that contribute to rapid wear and huge production scales (millions of pieces).

Open pit mining is the most efficient way of extracting minerals. The most important part in the technological chain of open-pit mining is the excavation process; its continuity is largely determined by the durability of the replaceable bucket teeth of quarry excavators that experience direct interaction with the rock. When excavating a planted mass of particularly strong and abrasive rocks, the teeth of the excavator bucket work in extreme conditions of abrasive wear (a large number of favorably oriented cutting edges on the surface of planted rock's fragments, the dominant role of metal micro-cutting, intense shock loads, etc.), which causes their rapid failure. The intensity of tillage machines' wear is significantly influenced by the type of cultivated soil, its granulometric composition, stress-strain state, and the material of the tillage machines [1].

The destruction of a piece of rock occurs during collision and abrasion with the working body and they are used for the destruction of materials with a compressive strength limit of up to 125 *MPa*.

The investigation of the wear process of bucket teeth made of steel 45, 85, Hadfield steel, high-strength cast iron, showed that their outer surface (ends and side walls) perceive the impact of abrasive particles at the angle from 5 to 60°, and the working surface - at a straight angle [2].

During wear and tear, a characteristic microrelief is formed on their surface. When struck at an angle from 5 to 60°, the pits and streaks have a distinct directionality, and at 90° - a uniform bumpy appearance with traces of repeated direct introduction of abrasive particles of different weights.

In most cases, the performance of working bodies is determined by time. Therefore, the most important task for increasing labor productivity in the processing is to increase the wear resistance of parts in conditions of shock-abrasive wear. The amount of bucket tooth loss due to wear can reach up to 1/3 of its initial weight.

During the development of ferruginous quartzites, the service life of a set of bucket teeth of quarry excavators with a total weight of 1 ton makes up 2-3 days, and the weight of worn metal relative to the total weight of the teeth does not exceed 15%. Increasing their durability will give a significant economic effect and, therefore, is quite vital [2].

The bucket teeth of quarry excavators are a defining product representing a whole group of parts made of Hadfield steel, hardened to austenite and possessing a unique combination of viscosity and wear resistance. Since its creation, this steel has not found worthy substitutes in the production of solid-cast parts that work in extreme conditions of abrasive wear with shock loads.

The high wear resistance of this steel is explained by the exceptional ability of manganese austenite to undergo plastic deformation by means of homogeneous and multiple sliding and to strong hardening during slander, which occurs simultaneously with plastic deformation (without yielding). But in the conditions of the absence of dynamic or large specific static loads, the wear resistance of steels of this type is low, approximately the same as that of steel 45. Therefore, the teeth of excavators' buckets which work under weak shock loads have low wear resistance.

As for the teeth of the quarry excavators' buckets, the design and material of wear-resistant areas, in addition to their direct purpose, must provide an acceptable level of bearing capacity of the teeth of the quarry excavators' buckets as a whole.

Increasing the operational characteristics of the steel surfaces of the teeth of excavators working in difficult conditions of abrasive wear and significant shock loads can be achieved by electric arc welding of coatings with highly alloyed floatings. When developing electrode materials for surfacing, an important aspect is to ensure a chemical composition that matches the basic material as much as possible. Chromium, nickel, manganese, molybdenum are key alloying elements that help increase the hardness and wear resistance of the deposited layer. Coatings obtained by electric arc deposition have a structure consisting of solid carbide particles that provide resistance to abrasive wear. Self-strengthening of coatings (slander effect) during operation under shock loads is especially important for high-manganese steels. Prospects for the application of electric arc surfacing are the following:

- the development of the new electrode materials and improvement of surfacing technologies in order to reduce cracks and internal defects;
- optimization of the coatings' composition to improve their wear resistance with simultaneous maintaining impact toughness, which is critically important for work surfaces operating in extreme conditions.

Thus, electric arc surfacing remains the leading method in the field of surface engineering for increasing the wear resistance of steel surfaces operating under difficult conditions of abrasive wear and shock loads.

The purpose of this paper is to study the influence of manganese and carbon content on the impact toughness and wear resistance of the deposited layer on Hadfield austenitic manganese steel in order to increase the durability of the excavator bucket teeth.

Literature review

The problem of the optimal ratio of manganese and carbon concentrations specifically in the deposited layer on Hadfield steel is not fully investigated, although research in this direction was carried out by V. A. Loktionov-Remizovskyi, N. V. Kiryakova, G. E. Fedorov and their colleagues [3]. A comparative analysis of topographic projections of mechanical properties (strength limits, yield limits and impact toughness) of austenitic manganese steels with their structural diagrams has been made in the research. This allows us to understand the relationship between the structural characteristics of the material and its mechanical properties. The concentration range of Hadfield steel (in particular, the content of manganese and carbon regulated by Ukrainian standards) has been compared with the structural diagram of manganese steels. These analyzes help to evaluate how changes in the chemical composition and structure of the steel affect its performance characteristics, such as strength and toughness. It was found out that in order to increase the stability of the structure, as well as to achieve constant levels of properties of Hadfield steel (such as strength, viscosity and other important characteristics) from melting to melting, it is necessary to optimize the carbon content. In particular, it is proposed to raise the lower limit of carbon content to 0.95% and lower the upper limit to 1.25%. Meanwhile, according to DSTU (National Standard of Ukraine) 8781:2018, the carbon and manganese content can vary from 0.9 to 1.5% and from 11.5 to 15.0%, accordingly. This will ensure better repeatability of the properties of cast parts in the entire range of carbon and manganese content regulated by the Ukrainian standard.

It is considered that the most optimal materials for depositing coatings on high-manganese steel parts are those whose component composition can provide a significant amount of manganese austenite in the coating [4].

However, despite the wide selection of electrode materials, such as EN14700 T Fe 9, OK Tubrodur 14 and others, intended for the application of wear-resistant coatings by the electric arc deposition method, the range of materials suitable for operation under conditions of shock loads is quite limited. Such materials are mainly represented by alloys of the Fe-13Mn-1C system (iron-manganese alloys with a content of 13% manganese and 1% carbon). The best mechanical properties of these alloys are achieved under the conditions of formation of a single-phase austenite structure. As described in the studies [5] of the cast steel microstructure without heat treatment, the ferrite-carbide mixture is released mainly along the boundaries of austenite grains; this makes these boundaries more brittle and prone to destruction. The mixture of ferrite and carbide has a high dispersion and lamellar structure, where the interlamellar distance is 30±7 nm. This indicates that such a structure is eutectoid and is usually observed during cooling of steel, which contributes to a decrease in its plasticity. The presence of a ferrite-carbide mixture in the structure leads to a significant decrease in plasticity, and with its amount ~20 wt. %, the relative elongation decreases by 7 times.

In the research [6], in order to reduce the influence of the cementite phase on the formation of coatings of the *Fe*-12*Mn*-1.1*C* system during electric arc welding, a complex alloying of the electrode charge with vanadium (*V*) and silicon (*Si*) in amounts of 1.2% and 2 .4% by weight, accordingly. As a result, multilayer coatings were obtained, which consisted of austenite, which formed dendritic crystallites, and ferrite, which was located in the interdendritic space. Vanadium carbide (*VC*) in the amount of about 5.6% was localized in the central regions of austenitic dendrites in the form of faceted phases up to 2 μm in size. This carbide phase increased the hardness of coatings to the level of 31–34 HRC, which is 10 HRC units higher than the hardness of coatings with an unalloyed manganese austenite structure. However, a significant amount of ferrite (~28 vol. %) negatively affected the possibility of operational strengthening of coatings. The conclusion is that although alloying with carbide-forming elements such as vanadium ensures the absence of undesirable cementite phases and increases hardness, the presence of ferrite reduces the effectiveness of strain hardening. This indicates the need for further optimization of the composition to minimize the effect of the ferrite phase on the coating characteristics.

Results

In this workpaper, the influence of the chemical structure of the surfacing composition (the ratio of manganese and carbon concentrations) on the mechanical properties of the surfacing layer on Hadfield austenitic manganese steel was investigated in order to increase the durability of the products made from it, namely the teeth of the excavator bucket.

To assess the optimal ratio of manganese and carbon, and in a wider interval compared to DSTU (National Standard of Ukraine) 8781:2018, a number of laboratory tests of surfacing samples with manganese concentrations of 6.36...17.64% were carried out. The carbon content in each series was varied from 0.60 to 1.60%. For all samples, impact tests at + 20 ^{0}C were carried out, as well as wear tests according to the Brinly-Haworth scheme under the conditions of abrasion of samples with quartz sand. The wear resistance of Hadfield steel, containing 1.1% *C* and 13% *Mn*, was taken as a unit of wear resistance in these experiments.

The task of planning the experiment was mathematically formulated as follows: it is necessary to get an idea of the response surface of the factors, which can be shown in the form of a function or a mathematical model [7]:

$$M\{y\} = \eta = \varphi(x_1, x_2, x_3, ..., x_k), \tag{1}$$

where y – is the optimization parameter (in our case, the impact toughness (*KCU*) and wear resistance (*I*) of Hadfield steel, which is used to make the teeth of the excavator bucket); x_i – variable factors, that have strong impact on the response and which can be changed during the experiment (content in percent of carbon and manganese). Accordingly, the task is reduced to determining the dependence of the mathematical expectation of the process result on the parameters (factors).

Finding the functions that determine the relationship between the factors (carbon and manganese content in percentages) and the impact viscosity (*KCU*) and wear resistance (*I*) parameters, the area of homogeneity of the processes can be conveniently described by an expression in the form of a polynomial.

Since it is necessary to evaluate two factors, the task of conducting a two-factor experiment [7] arises, the factor levels are shown in Table 1.

Table 1

Levels of factors are intervals of variation

Factors	Levels				
	1,41	+1	0	– 1	– 1,41
x_1 – carbon content, %	1,6	1,45	1,1	0,75	0,6
x_2 – manganese content, %	17,64	16	12	8	6,36

According to the planning matrix, experiments are performed with provided factors. The test results are shown in Table 2.

Table 2

Experiment planning matrix in real values and test results

№	*C*, %	*Mn*, %	*KCU*, J/ cm²	*I*, relat. units
1	0,75	8	75	0,9
2	0,75	16	316	0,85
3	1,45	8	133	1,25
4	1,45	16	170	0,98
5	0,6	12	232	0,88
6	1,6	12	151	0,8
7	1,1	6,36	108	1,36
8	1,1	17,64	270	0,89
9	1,1	12	215	1,01
10	1,1	12	218	1,01

Data processing of the experiment and search for optimal values were made in the Statistica 6.0 program.

Thus, thanks to the two-factor experiment, a regression equation was obtained for the impact toughness (*KCU*) of the deposited layer depending on the carbon and manganese content, it is as follows:

$$KCU = -699{,}3 + 657{,}5C - 132{,}9C^2 + 83{,}1Mn - 1{,}1Mn^2 - 36{,}4C \cdot Mn\,. \quad (2)$$

And the regression equation for the intensity of wear of the deposited layer depending on the content of carbon and manganese is the following:

$$I = 0{,}46 + 2{,}05C - 0{,}66C^2 - 0{,}08Mn + 0{,}004Mn^2 - 0{,}04C \cdot Mn\,. \quad (3)$$

By means of the "Design Analysis of Experiments" module (experimental project) of this program, the influence of each of the factors on impact toughness (*KCU*) Picture 1 and wear resistance (*I*) Picture 2 was determined, and the optimal values of the factors were obtained.

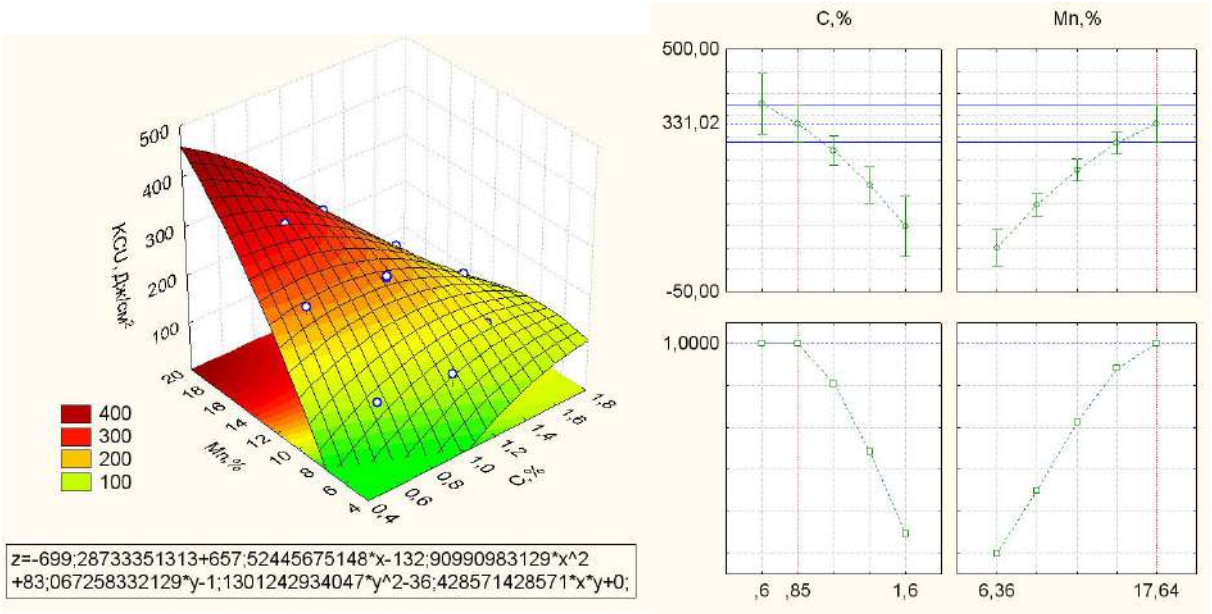

a) b)

Fig.1. The influence of the ratio of manganese and carbon on the impact toughness of the deposited layer: a) response surface of the impact toughness (*KCU*) of the deposited layer; b) dot graphs with histograms characterizing the impact of the studied factors for impact toughness

In the course of the study, it was found out that the impact toughness (*KCU*) of manganese steels depends on the carbon content and changes along a curve with a maximum. This means that for each value of the manganese content there is an optimal carbon concentration at which the impact toughness reaches its peak. In particular, for steels with a manganese content of 13%, a carbon content of 0.85...1.0% is optimal. At the same time, an increase in the manganese content in general contributes to an increase in impact toughness at all carbon concentrations,

except for the highest carbon concentrations (1.5...1.7%). The maximum values of impact toughness were obtained for steel containing 17...18% manganese and 0.6...0.7% carbon.

This indicates that the correct selection of carbon and manganese content is a key to achieving the maximum impact toughness of steel, which is an important factor in ensuring high mechanical stability of the material. It should be noted that even with a reduced manganese content (10.3...11.0% or 8.6...9.2%), the impact toughness of the samples can remain high provided that the carbon concentration is chosen correctly. In particular, with a carbon content of 1.0% for steel with 10.3...11.0% manganese and 1.3% for steel with 8.6...9.2% manganese, the impact toughness exceeds 150 J/cm². This suggests that such coatings can be economically viable for applying as cheaper materials, while maintaining the sufficiently high impact toughness required for many industrial applications.

The maximum wear resistance is observed in deposits with a manganese content of 6%. In such deposits, during abrasion, a surface martensite is formed, which significantly increases the hardness of the surface, providing increased resistance to wear. However, with a further increase in the manganese content, wear resistance begins to decrease.

On the other hand, an increase in carbon concentration has a positive effect on wear resistance, which makes the carbon content an important factor for improving the performance characteristics of surfacing. Thus, the correct ratio of manganese and carbon is a key to achieving optimal wear resistance.

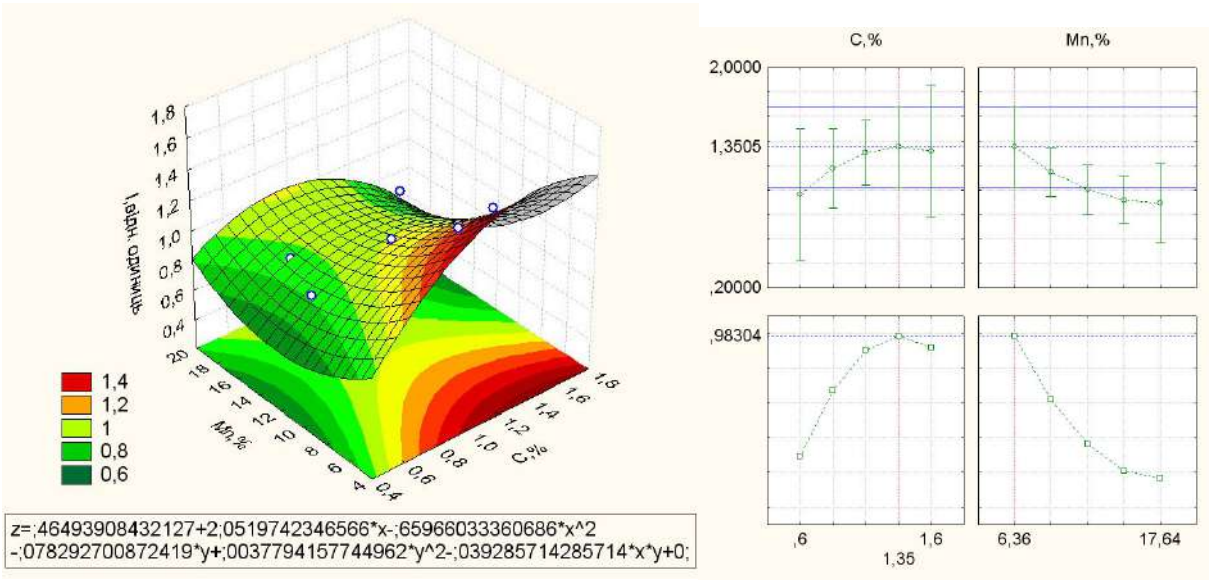

a) b)

Fig.2. The effect of the ratio of manganese and carbon on the impact wear resistance of the deposited layer: (a) response surface of the wear intensity of the deposited layer; (b) dot graphs with histograms characterizing the influence of the investigated factors on the intensity of wear

The investigation of the deposited layer's microstructure (Picture 3) showed the absence of hot cracks.

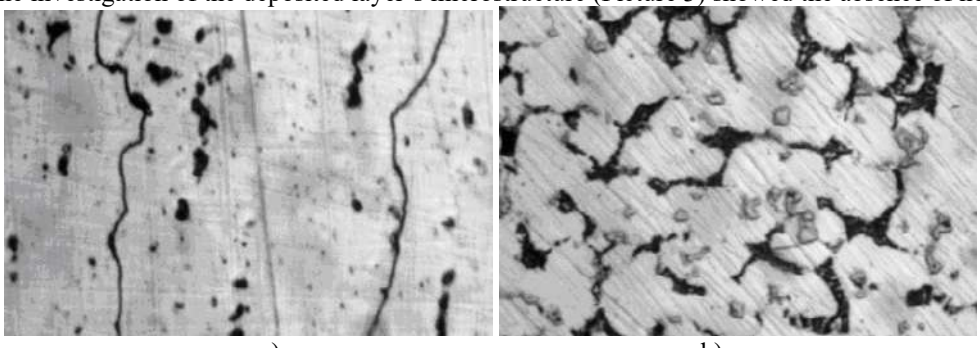

a) b)

Fig.3. Microstructure of the deposited layer: a) content: carbon – 0,85 %; manganese – 17,64 %; b) content: carbon – 1,35 %; manganese – 6,36 %.

As the manganese content decreases, hardness and wear resistance increase, but the structure tends to decrease the impact toughness.

Conclusions

By controlling the chemical composition of powder wire, it is possible to achieve different mechanical properties of the deposited layer of the excavator bucket teeth for different types of cultivated soil. So, to ensure

the highest value of the impact toughness of the deposited layer (when processing hard soil rocks), the following concentration of powder wire elements is optimal: carbon - 0.85%; manganese - 17.64%, and to ensure the highest value of wear resistance of the deposited layer (when processing soft soil rocks), the optimal concentration of elements is as follows: carbon - 1.35%; manganese - 6.36%.

References

1. Posonskyi S., Babak O. (2017). Optimization of technological parameters of induction surfacing by composite powder of made from l53 steel working units of the soil-processing machines. *Problems of tribology*. Khmelnytskyi. KhNU, 85 (3). P.82-88.

2. Zagurskyi A. (2015). Increasing the wear resistance of the teeth of single-bucket excavators. *Student's Bulletin of NUVHP*. Rivne. NUVHP, 3 (5). P. 52-55.

3. Loktionov-Remizovskyi V., Kiryakova N., Fedorov G., Grybov M., Oleksenko I. (2020). Optimization of Carbon and Magganese Content in Steel 110G13L. *Casting processes*. Kyiv. NAS, 142 (4). P. 26-33, URL: https://doi.org/10.15407/plit2020.04.026

4. Prysiazhniuk P.M. Scientific basis of formation of wear-resistant coatings of the system "high-manganese steel - refractory compounds" by electric arc surfacing [dys. ... d-ra tekhn. nauk: 05.02.01]. 2024. 384 p. [Ukrainian]

5. S.H.M. Anijdan. (2018) The effect of heat treatment process parameters on mechanical properties, precipitation, fatigue life, and fracture mode of an austenitic Mn Hadfield steel. J. Mater. Eng. Perform. 27, P. 5246–5253. URL: https://doi.org/10.1007/s11665-018-3625-y

6. Rodríguez, M., Perdomo, L., Béjar, L., Moreno, J. A., Medida, A., Soriano, J. F., & Alfonso, I. (2017). Efecto del V y el Si sobre la microestructura de depósitos realizados con electrodos tubulares revestidos de alto contenido de Mn (Hadfield). *Soldagem & Inspeção*, 22(3), P. 249-257, URL: https://doi.org/10.1590/0104-9224/si2203.03

7. Vasylkovska K., Leshchenko S., Vasylkovskyi O., Petrenko D. Improvement of equipment for basic tillage and sowing as initial stage of harvest forecasting. *INMATEH – Agricultural Engineering*. 2016. 50 (3). P. 13-20. [English]

Посонський С.Ф. Вплив марганцю та вуглецю на механічні властивості наплавленого шару зубів ковша екскаватора зі сталі Гадфілда

В роботі виконано дослідження впливу хімічного складу наплавочної композиції (співвідношення концентрацій марганцю і вуглецю) на механічні властивості наплавленого шару на сталь Гадфільда з метою підвищення довговічності виготовлених з неї виробів, а саме зубів ковша екскаватора. За параметр оптимізації обрано два критерії, ударну в'язкість та зносостійкість покриття. Оцінку ударної в'язкості наплавленого покриття проводили на зразках «Шарпі» на маятниковому копрі, а випробування на знос за схемою Брінля-Хаворта в умовах стирання зразків кварцовим піском. За одиницю зносостійкості в цих експериментах прийнята зносостійкість сталі Гадфільда, що містить 1,1 % *C* і 13 % *Mn*. Для визначення оптимальних режимів нанесення покриття проводився активний експеримент з використанням методів математичного планування. Отримані поверхні відгуку та графіки ліній рівного виходу дають можливість встановити рівень впливу досліджуваних факторів на параметр оптимізації. Для аналізу впливу заданих факторів на критерії оптимізації побудовані графіки розсіювання з гістограмами, з яких можна графічно визначити раціональні значення обраних критеріїв оптимізації – ударну в'язкість та зносостійкість покриття.

Ключові слова: зуб ковша екскаватора, сталь Гадфільда, наплавлене покриття, марганець, вуглець, ударна в'язкість, зносостійкість, оптимальні параметри

***Problems of Tribology**, V. 29, No 32/113-2024, 72-78*

Problems of Tribology
Website: http://tribology.khnu.km.ua/index.php/ProbTrib
E-mail: tribosenator@gmail.com

DOI: https://doi.org/10.31891/2079-1372-2024-113-3-72-78

The patterns of changes in the degree of lubrication of the crankshaft bearings of car engines depending on the parameters of the load-speed modes of operation

A. Gypka [1*], V. Aulin [2], O. Lyashuk [1], A. Hrynkiv [2], V. Hud [1]
1 Ternopil Ivan Puluj National Technical University, Ukraine
2 Central Ukrainian National Technical University , Ukraine
**E-mail: Gypkab@gmail.com*

Received: 20 July 2024: Revised 05 September 2024: Accept 20 September 2024

Abstract

The practice of operating machines and mechanisms indicates that bearing wear is one of the main reasons for limiting their durability. This especially applies to the sliding bearings of crankshafts of car engines, where the intensity of wear of their working surfaces significantly depends on the properties of the lubricant. An experimental study of the wear resistance of the sliding bearings of the crankshafts of car engines was carried out on the KI-5543 model break-in and braking stand. In experimental studies, BELZONA Super E-Metal insulating material was used to provide electrical isolation of the main and connecting rod bearings of the crankshaft from the cylinder block of the car engine. The experimental dependencies of the values of the criteria characterizing the degree of lubrication of the friction surfaces on the parameters of the load-speed modes (the moment of the applied force and the frequency of rotation of the crankshaft) were obtained. The ranges of values of the investigated parameters, in which the effective operation of the sliding bearings of the crankshaft of car engines is implemented, have been revealed.

Keywords: crankshaft sliding bearings, criteria for the degree of lubrication, bench tests, mode of friction, wear, lubricant.

Formulation of the problem

The most important reason for the failure of the sliding bearings of the crankshafts of cars is the wear of the friction surfaces of the liners and necks. The intensity of wear of the working surfaces of sliding bearings depends on the properties of the lubricant and the modes of the lubrication process under the conditions of vehicle operation. Wear of the friction surfaces leads to an increase in the diametric gap, ovality and conicity, destruction of the anti-friction layer of the bearing. This helps to reduce the load-bearing capacity of the lubricating layer and reduce its minimum thickness, increase the probability of destruction and, accordingly, increase the duration of the contact interaction of the friction surfaces [1,2]. It is known that violation of the liquid lubrication regime intensifies the process of wear of the main and connecting rod bearings of the crankshaft, and therefore the rate of consumption of the resource of the engine and the car as a whole.

The practice of operating cars shows that the durability of main and connecting rod bearings of crankshafts of car engines is limited by the type and intensity of wear. For automobile engines, structural and technological methods of increasing the wear resistance of crankshaft sliding bearings are used. Operational methods of increasing their wear resistance are also acceptable. The stage of operation of machines and mechanisms is the most expensive and has a significant reserve for increasing their durability.

Analysis of recent research and publications

During the operation of the car engine, the operating conditions of the crankshaft sliding bearings must be ensured in the liquid lubrication mode in the acceptable ranges of the load and speed modes of the car's operation.

The research of the wear resistance of bearings, including crankshaft sliding bearings of car engines, under different lubrication regimes, is devoted to the works of domestic scientists V.M. Pavliskyi [3], A.G. Kuzmenka

[4], O.V. Dykha. [4-6], V.V. Aulina [1,2,7], V.A. Voitova,[8] and other scientists, as well as a number of foreign scientists [9-17]

The issue of the influence of various factors on the lubrication process in crankshaft sliding bearings is considered in works [1,3,4,8,13,16,17]. At the same time, insufficient attention is paid to the criteria that characterize the degree of lubrication of the friction working surfaces during the operation of the car.

Further research is needed to identify patterns of changes in the degree of lubrication of crankshaft sliding bearings of car engines depending on the parameters of the load-speed modes of its operation.

The purpose of the work

The purpose of this work is to establish the patterns of changes in the criteria that characterize the degree and regimes of the lubrication process in the main and connecting rod bearings of the crankshaft depending on the parameters of the loading and speed regimes of their operation.

Research results

An experimental study of lubrication processes in crankshaft sliding bearings was carried out on the break-in and braking stand of the KI-5543 model of a specially prepared automobile engine with main bearings electrically isolated from the engine cylinder block. BELZONA Super E-Metal from BELZONA® (USA) was used as an insulating material. This material has high strength and dielectric properties (Table 1, Table 2), and therefore the main bearings of the car engine are electrically isolated from the cylinder block.

Table 1

General characteristics and chemical resistance of insulating material BELZONA Super E-Metal

General characteristics	Field of application	Processing time at 293 K, min	Hardening time at 293 K, min	Chemical resistance
A two-component, paste-like material that hardens quickly	For emergency repairs, sealing of leaks, obtaining long-lasting adhesives connections	5	20	Good resistance to relatively highly diluted inorganic acids, alkaline solutions and salts; special resistance to lubricants

Table 2

Physical and mechanical properties of the insulating material BELZONA Super E-Metal

Specific volume, cm3/kg	Strength limit under tensile and shear deformations, MPa, when connected to:	Strength limit at compression, MPa	Hardness by Brinell, NV	Heat resistance, T, K
450	- structural steel - 17, - stainless steel - 17, - aluminum - 12	76	15.9	Under conditions of immersion in lubricant up to 423K

A shielded wire (Fig. 1) was soldered to the liners of the crankshaft of the tested engine, which, during assembly, was led out through a drilled groove in the place of the connector of the engine cylinder block cover and the gasket of the oil sump seal to the outside of the block.

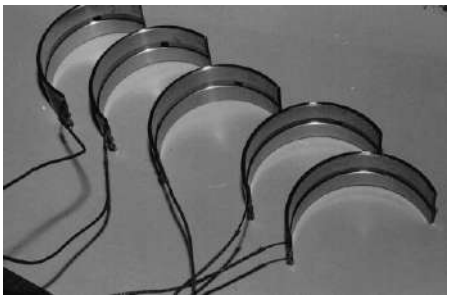

Fig. 1. Fixing the crankshaft main bearings with soldered wires

The wires were led to a five-channel connector, and a current collector was attached to the neck of the crankshaft (Fig. 2).

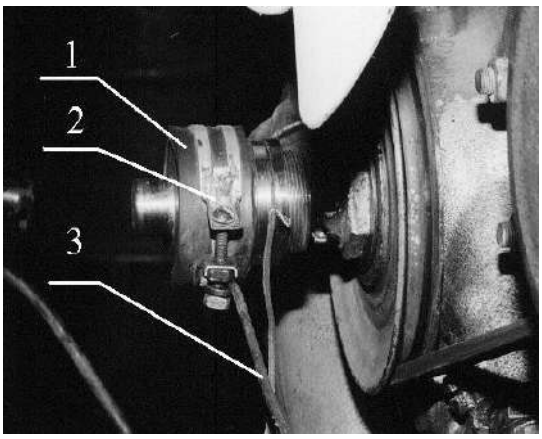

Fig. 2. Fastening the current collector on the crankshaft: 1 – rubber gasket, 2 – clamp, 3 – bracket

Through the test mode analyzer, one end of the power wire was attached to the wires of the liners, and the other - to the current collector. The value of the criterion $P_g^{m.b}$, which characterizes the relative duration of the existence of the liquid lubrication regime or the duration of the existence of the lubricating layer between the friction surfaces. When attaching the power wire to the cylinder block, the value of the criterion E_g, which characterizes the duration of the existence of the lubricating layer in the sliding bearings of the crankshaft of the car engine. In this case, the liners were electrically connected to the block of cylinder liners.

The studied engine, after applying a layer of BELZONA Super E-Metal insulating material on the original friction surfaces, corresponded to the pre-worked state. The research was conducted in two stages. The first stage is bench running of the engine according to the modes recommended by the manufacturer. The second stage is engine run-in, which consists in periodically repeating engine load modes with certain combinations of parameters of the load-speed modes of its operation: the values of the loading moment M and the frequency of rotation of the crankshaft n according to a two-factor plan built using the provisions of mathematical planning of the experiment [1,8]. The scheme for measuring the parameters of the lubrication process in the sliding bearings of the engine crankshaft is shown in Figure 3.

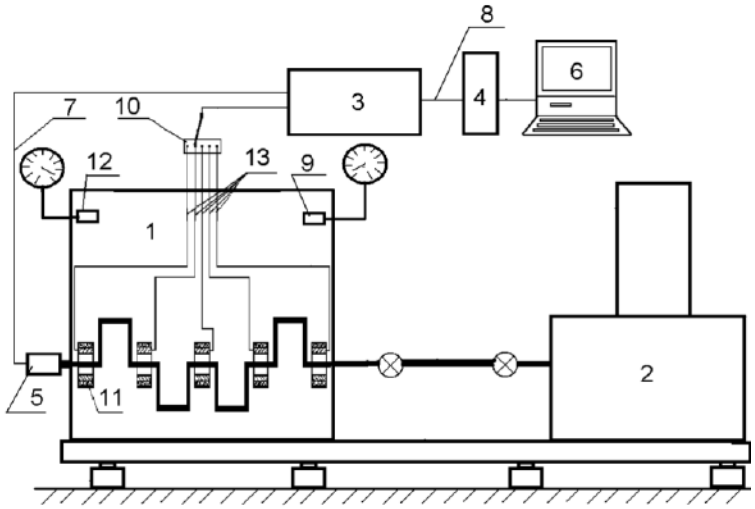

Fig. 3 - Scheme of measurement of the parameters of the lubrication process in the sliding bearings of the crankshaft of a car engine during bench tests:1 - engine; 2 – break-in and braking stand; 3 – analyzer of friction modes; 4 - connection device; 5 - current collector; 6 – computer; 7, 13 – power wires; 8 – tire; 9 – lubricant pressure sensor; 10 - connector; 11 – dielectric layer; 12 – coolant temperature sensor

Research modes: load on the crankshaft M - 0...60 N·m, speed of rotation of the crankshaft n - 1000...2600 min^{-1}.To simplify the analysis of the results of the bench tests, it was assumed that the lubrication regime of the crankshaft sliding bearings is characterized by two states: contact of the friction surfaces (dry friction or boundary lubrication), complete separation of the friction surfaces (liquid lubrication). The grouping of lubrication modes can be justified by several reasons: the difference in the intensity of wear of the friction surfaces by several orders of magnitude [1,3,8], as well as the difference in the dielectric permeability of the lubricating layers [1]. An experiment plan was drawn up for the study of the lubrication process in the main bearings of the crankshaft according to two criteria:

$$P_g^{m.b}\, i = f(M, n) \text{ and } E_g = f(M, n) \quad (1)$$

This made it possible to build appropriate regression mathematical models after the running-in process is completed, when the values of these parameters are at a stable level and characterize the balanced technical condition of the car engine.

According to the results of the analysis of the database of bench tests, graphical dependences of the change in the criterion $P_g^{m.b.}i$ (where i the serial number of the main bearing under study), from the load parameter M (Fig. 4) and the frequency of rotation of the crankshaft of the car engine n (Fig. 5).

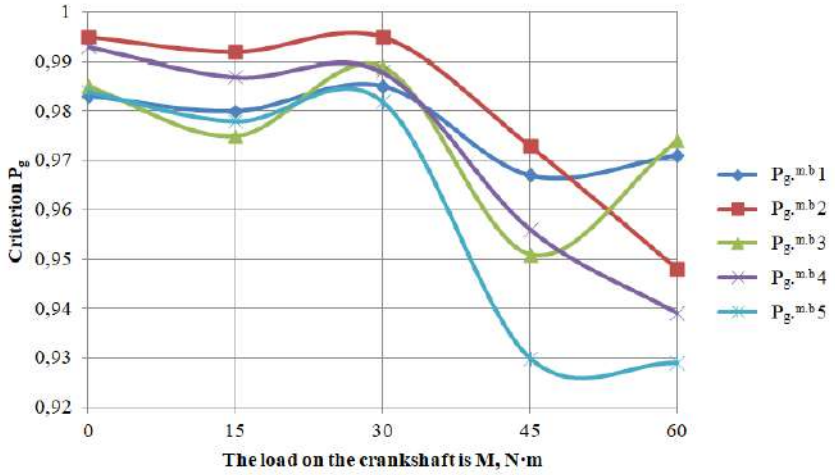

Fig. 4. Patterns of changes in the value of the $P_g^{m.b}$ at a stable level from the load parameter

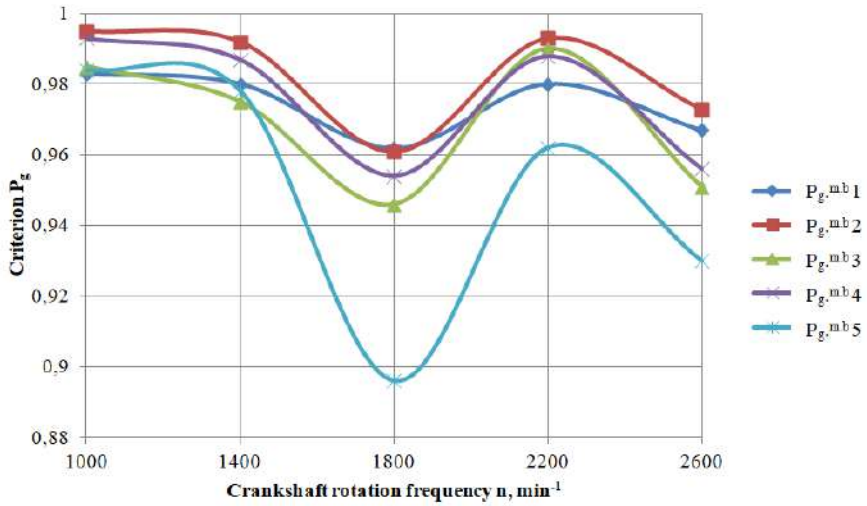

Fig. 5. Patterns of changes in the parameter $P_g^{m.b}$ at a stable level depending on the frequency of rotation of the crankshaft of the car engine

It was found that the patterns of changes in the value of the criterion $P_g^{m.b.}$ from the loading and speed parameters have a non-linear character in the presence of areas of effective operation of the car engine.

Two-factor bench tests of the engine were carried out. According to the results of the research, a regression model was built in the form of the dependence of the E_g on the parameters of the loading and speed modes of its operation:

$$E_g = 0.7951 + 2.2615\ 10^{-3} M + 1.1303\ 10^{-4} n - 5.0944\ 10^{-5} M - -4.0701\ 10^{-8} n^2 - 3.6473\ 10^{-7} M n \quad (2)$$

The regression model of the E_g with the specified parameters was obtained using application program packages on a PC with verification of its adequacy

Figure 6 shows a graphical interpretation of the regression model of the E_g.

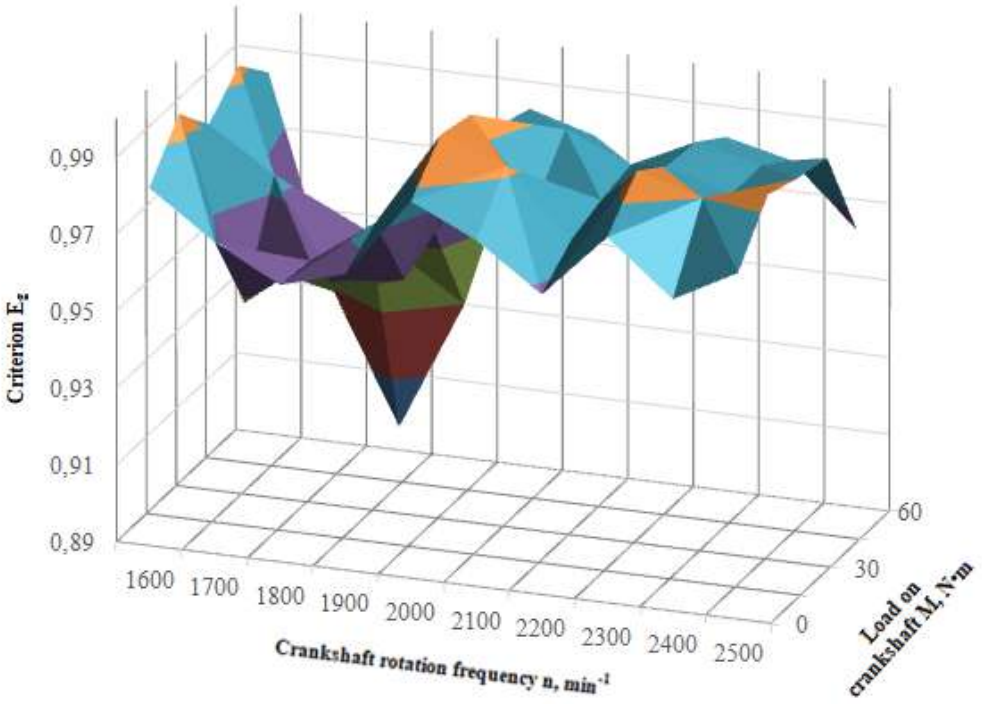

Fig. 6. The nature of the change of the E_g from the parameters of the load-speed mode of operation of the car engine

The test of homogeneity of variances of criterion E_g was carried out according to Cochran's criterion with a confidence probability of 0.95 under conditions of load M = 30 N m, n = 2000 min^{-1}. The homogeneity of variances in the equilibrium points of the factor space indicates the independence of the variance of the optimization criterion E_g from its absolute value. Fulfillment of this condition, along with others, allows you to use regression analysis when processing the obtained test results.

Conclusions

1. It was determined that to study the change in the degree of lubrication of crankshaft sliding bearings of car engines depending on the parameters of load-speed modes of operation, it is possible to use the criterion $P_g^{m.b.}$, which characterizes the relative duration of existence of the liquid lubrication regime, and the criterion E_g, which characterizes the relative duration of existence of the lubricating layer in the crankshaft sliding bearings.

2. Modes of bench tests of engines and a scheme for measuring the criteria of $P_g^{m.b.}$ and E_g, in the process of lubricating the sliding bearings of the crankshaft of the car engine.

3. Experimentally revealed patterns of changes in the criteria for the degree of lubrication of crankshaft sliding bearings depending on the load and rotation frequency during a stable mode of its operation. Areas of effective flow of lubrication processes and stable formation and duration of the existence of a film of lubricant on the working surfaces of the sliding bearings of the crankshaft of the car engine have been determined.

References

1. Methodological and theoretical foundations of ensuring and increasing the reliability of the functioning of automobile transport systems: a monograph / V. V. Aulin, D. V. Golub, A. V. Hrynkiv, S. V. Lysenko; under. general ed. Prof. V.V. Aulina. – Kropyvnytskyi: KOD, 2017. – 370 p.

2. Aulin V., Lyashuk O., Gupka A., Tson O., Mironov D., Sokol M., Leshchuk R., Yarema I. Tribodiagnosis of the surface damage of tribo-coupling parts materials during machine operation // Procedia Structural Integrity . - 2024. - Volume 59. - P. 428-435.

3. Increasing the wear resistance of tractor engines [Text]: diss... Dr. Tech. Sciences: 05.02.04 / Vasyl Mykhailovych Pavliskyi; National Agrarian University - K., 1999. - 350 p.

4. Contact, friction and wear of lubricated surfaces: monograph / A. G. Kuzmenko, A. V. Dykha. – Khmelnytskyi: KhNU, 2007. – 344 p.

5. Dykha O.V, Sorokatyi RV, Babak OP (2011). Rozrakhunky she trials on nadiinist mashyn i konstruktsii: navch. possible [Khmelnytskyi : KhNU] 151 p.

6. Dykha, O., Padgurskas, J., & Babak, O. (2021). Prediction of the life time of cylindrical tribosystems of a vehicle. In IOP Conference Series: Materials Science and Engineering (Vol. 1021, No. 1, p. 012036). IOP Publishing.

7. Aulin, V., Gypka, A., Liashuk, O., Stukhlyak, P., & Hrynkiv, A. (2024). A comprehensive method of researching the tribological efficiency of couplings of parts of nodes, systems and aggregates of cars. Problems of Tribology, 29 (1/111), 75-83. https://doi.org/10.31891/2079-1372-2024-111-1-75-83

8. Vojtov, V., Biekirov, A., & Voitov, A. (2018). The quality of the tribosystem as a factor of wear resistance. International Journal of Engineering & Technology, 7 (4.3), 25-29.

9. Bernát, R., Žarnovský, J., Kováč, I., Mikuš, R., Fries, J., & Csintalan, R. (2021). Microanalysis of Worn Surfaces

10. Al-Quraan, T.M, Mikosyanchik, O.O, Mnatsakanov, R.G, & Zaporozhets, O.I (2016). Structural-Energy characteristics of tribotechnical contact in unsteady operational modes. Modern Mechanical Engineering, 6 (3), 91-97.

11. Kučera, M., Kučera, M., & Pršan, J. (2012). Possibilities for classification of tribological processes with regard to energy.

12. Adetunla, A., Afolalu, S., Jen, TC, & Ogundana, A. (2023). The Advances of Tribology in Materials and Energy Conservation and Engineering Innovation. In E3S Web of Conferences (Vol. 391, p. 01014). EDP Sciences.

13. Ismailov , G.M, Tyurin , A.E, Gavrilin , A.N, Nevinitsyna , V.S, & Lomovskaya , SA (2020, September). Study of the identification model of tribological interaction of friction couples. In IOP Conference Series: Materials Science and Engineering (Vol. 919, No. 2, p. 022056). IOP Publishing.

14. Aleutdinova , M.I, Fadin , V.V, Kolubaev , A.V, & Aleutdinova , V.A Contact characteristics of metallic materials in conditions of heavy loading by friction or by electric current. Friction and Wear Research (FWR). 2014. No. 2. 22-28.

15. Dunaev A.V, Pustovoy I.F Experience of using electric effects on engine oils and friction in . Journal of machinery manufacture and Reliability. 2020. Vol. 49, no. 11. P. 980-989. URL: https://doi.org/10.3103/s1052618820110035.

16. A study of the effect of electrostatic processing on performance characteristics of axle oil / P. Konovalov et al. Eastern-European journal of enterprise technology. 2018. Vol. 1, no. 1 (91). P. 4–12. URL: https://doi.org/10.15587/1729-4061.2018.120977.

17. Study of electrohydrodynamic properties in insulating liquids and research of an alternative mixture to mineral oil for energy transformers / J. Rouabeh et al. Journal of electrostatics. 2022. Vol. 115. P. 103684. URL: https://doi.org/10.1016/j.elstat.2022.103684.

Гупка А., Аулін В., Ляшук О., Гриньків А., Гудь В. Закономірності зміни ступеню змащення підшипників колінчастого валу двигунів автомобілів від параметрів навантажувально -швидкісних режимів експлуатації

Практика експлуатації машин та механізмів вказує на те, що зношування підшипників є однією з головних причин обмеження їх довговічності. Особливо це стосується підшипників ковзання колінчастих валів двигунів автомобілів, де інтенсивність зношування їх робочих поверхонь істотно залежить від властивостей мастильного матеріалу.

Експериментальне дослідження зносостійкості підшипників ковзання колінчастих валів двигунів автомобілів було проведено на обкатно-гальмівному стенді моделі КІ-5543. В експериментальних дослідженнях використано ізоляційний матеріал BELZONA Super E-Metal для забезпечення електричної ізоляції корінних та шатунних підшипників колінчастого валу від блоку циліндрів двигуна автомобіля. Отримано експериментальні залежності значення критеріїв, які характеризують ступінь змащування поверхонь тертя від параметрів навантажувально-швидкісних режимів (моменту прикладеної сили та частоти обертання колінчастого валу). Виявлено діапазони значень досліджуваних параметрів, в яких реалізується ефективна експлуатація підшипників ковзання колінчастого валу двигунів автомобілів.

Ключові слова: підшипники ковзання колінчастого валу, критерії ступеню змащування, стендові випробування, режим тертя, зношування, мастильний матеріал.

***Problems of Tribology**, V. 29, No 32/113-2024, 79-88*

Problems of Tribology
Website: http://tribology.khnu.km.ua/index.php/ProbTrib
E-mail: tribosenator@gmail.com

DOI: https://doi.org/10.31891/2079-1372-2024-113-3-79-88

Tribotechnical processes of the soil environment interaction with the working bodies of soil tillage and earthmoving machines reinforced with composite materials

A.A. Tykhyi*, V.V. Aulin, M.V. Pashynskyi, A.Y. Borovik

Central Ukrainian National Technical University , Ukraine
**E-mail: a.a.tihiy@gmail.com*

Received: 30 July 2024: Revised10 September 2024: Accept 25 September 2024

Abstract

The work presents the study results of the stress-strain state of the soil, as a continuous medium filled with abrasive particles under the action of the working bodies of soil tillage and earthmoving machines. One of the main properties of the soil, which determines the specifics of the force interaction of the working surfaces of the working bodies of soil tillage and earthmoving machines with the technological environment, is taken into account, namely the tendency of the contact layer of the treated layer to compaction.

The relationship between stress in the soil and the wear of the working bodies of soil tillage and earthmoving machines has been established experimentally. A theoretical analysis is presented for the stress-strain state of the local region of the strengthened surface layer that is used in the working bodies of soil tillage and earthmoving machines, in which the filler, inclusion or strengthening phase is placed.

An analysis of the contact characteristics of the stress-strain state and their changes during friction and wear was carried out based on the formulation and solution of the contact interaction problems of abrasive soil particles with the inhomogeneities of the composite coatings components based on ultra-high molecular weight polyethylene with fillers during strengthening of the working bodies of soil tillage and earthmoving machines.

Computer modeling was performed to study the nature of stress distribution in the reinforced surface layer of the working bodies of soil tillage and earthmoving machines in the area of the contact zone in stationary and dynamic conditions. The contact problem is formulated, the boundary conditions and the solution in the form of components of the stress field are given. The characteristics of the filler, their content in the composite material and coating are taken into account, the relationship between the stress-strain state and wear is established.

Key words: stress, contact, wear-resistant coatings, filler, composite material, ultra-high molecular weight polyethylene, working body of soil tillage and earthmoving machine

Introduction

Modern agrotechnological trends in soil cultivation by the working bodies of soil tillage and earthmoving machines (WBSTEM) set requirements for the producers of the agro-industrial sector to increase reliability and reduce energy and material costs of such machines for their cultivation.

One of the main properties of the soil, which determines the characteristic of the force interaction of the working surfaces of the WBSTEM with the technological environment, is the propensity of the contact area of the tillage layer to compaction [1]. In the process of tillage, the movement of cutting element (CE) of WBSTEM leads to partial compaction of soil particles in its layer, which are in contact with the working surface, as well as in the contact layer. The fractional redistribution of soil abrasive particles (AP) is accompanied by a decrease in the distance between them, pressing into the part of the layer above the cutting element and the formation of a reaction force.

Mechanics of contact interaction is one of the leading directions in agricultural mechanics. Despite the fact that solutions to a large number of contact problems have been obtained by both analytical and numerical methods, the creation and study of contact interaction models remains relevant even today in connection with the development of new composite materials and technologies, such as strengthening, due to the variety of processes

and phenomena occurring in the contact zone during friction and wear of the surfaces of the working bodies of WBSTEM, introducing new requirements for their operating conditions.

When setting classical contact problems, the model of a homogeneous isotropic body is mainly used and the interaction of smooth surfaces is considered [1, 2]. With the development of mathematical apparatus and rapid growth in computational power it became possible to take into account surface roughness and the viscoelastic properties of contacting bodies, the presence of films and coatings on the contact surface, the occurrence of adhesion, friction and wear phenomena when solving contact problems.

Research of contact interaction with bodies that have inhomogeneities of a mechanical, geometric and tribotechnical nature, creation of material models of triboelements (TE), working (technological) environments, formation of secondary structures (SS), movement of the boundary between phases under thermomechanical influences [3] is of increased interest both from the point of view of fundamental and applied science. Attention should be paid to research in the following directions: the introduction of additional parameters of the surface layers state of the WBSTEM and the contact zones with the particles of the soil environment, the determination of the ratios for these parameters, the experimental verification of the created physical and mathematical models, as well as the consideration of interphase boundaries during the strengthening of the surface layer of the WBSTEM and the kinetics of the new phase [4].

The improvement of any technological process of soil cultivation implies a decrease in its energy intensity.

The development of modern areas of materials science is associated with the development and application of promising materials based on various initial components, with the involvement of a wide range of resources and technologies, using different research methods, with the modification of components in order to obtain materials with improved properties or acquiring new functional properties that allow expand the scope of their application [1–8].

A promising material with a wide range of functional properties, which is used today in the field of production of WBSTEM to solve various tasks of increasing wear resistance and energy efficiency, is ultra-high molecular weight polyethylene (UHMWP). The advantages of UHMWP are a combination of high wear resistance, resistance to aggressive environments, low coefficient of friction, high impact strength, low brittleness temperature, which allows the use of products based on UHMWP, including extreme operating conditions (the brittleness temperature of the material is up to -200 °C) [2]. The limiting factors for the use of UHMWP are the low melting point (135–190 °C), due to which the upper limit of the material's operating temperature is 90 °C, as well as the high viscosity of the polymer melt, which complicates the process of its processing [3].

Inclusions, fillers, new phases are not only stress concentrators, but also their source, the local density changes, residual stresses arise. Technological residual stresses during the strengthening of WBSTEM can play both a positive and a negative role in the process of operation.

Literature review

A classic work, which presents a model for determining residual stresses caused by phase transformations in an unbounded body, is work [5]. This model, based on the solution of the planar problem of the theory of elasticity, determines the residual stresses inside local areas, inclusions, fillers, and phases and are resolved by means of a boundary transition. At the same time, it is assumed that the elastic characteristics do not change during the transformation process.

The solution of the planar periodic contact problem for the stamp system, taking into account the frictional forces, is given in works [1,4], where there is also an analysis of the stress-strain state of the surface layers. In [7], a periodic contact problem for a surface with sinusoidal undulations in two mutually perpendicular directions is considered. The general method of solving spatial and flat contact problems with wear at a constant contact area is described in [8]. The contact condition using the linear law of wear and integral representation of elastic movements due to contact pressure allows reducing the problem to the determination of eigenvalues and eigenfunctions of some integral operators. It has been proven that the pressure distribution at the point of contact assumes a stationary value during a steady mode of wear.

In works [9, 10], as well as in monographs [11, 13], mathematical formulations of a number of wear-contact problems for heterogeneous elastic bodies with variable surface wear resistance are considered. Such tasks arose in connection with the strengthening of WBSTEM with composite materials (CM) and composite coating (CC), local strengthening of their working surfaces. Some types of continuous surface strengthening are also taken into account, in particular with laser technologies, when it is impossible to achieve a uniform change in the surface structure of the WBSTEM. The latter issues play a decisive role in the problem of increasing the reliability and wear resistance of WBSTEM, and therefore require a solution.

Purpose

An analysis of the contact characteristics of the stress-strain state and their changes during friction and wear was carried out based on the formulation and solution of the problems of contact interaction of soil particles with

inhomogeneities of CM (CC) components based on ultra-high molecular weight polyethylene with fillers during strengthening of WBSTEM.

Methods

In the interaction process of WBSTEM with the soil, the latter undergoes a certain deformation, the load amount and bulk mass are constantly changing [4]. The movement of the working body causes compression deformations of the internal stress of the soil environment, the direction of action of which coincides with the direction of the absolute movement of soil particles of the compressed volume (contact layer), and the intensity decreases as it moves away from the executive surface into the depth of the interacting part of the formation.

Deformation of dense soil at a low stress level leads to an increase in volume, that is, its dilatation (volumetric expansion). Since the soil becomes less dense in places where the volume increases, which contributes to further deformation and increase in volume, the process is unstable. This indicates that deformations in the soil can concentrate, which leads to the appearance of fracture surfaces. Along the surfaces of the fracture, there are very thin expansion bands that differ in properties from the main mass of the soil. Deformation in dilation bands is greater in cases of shear failure than tensile failure, since friction processes are taken into account.

For a theoretical analysis of this influence, we will use the equation of mechanics of mixtures [13]. The condition of quasi-static deformation of heterogeneous materials can be presented in the form of an equilibrium equation:

$$\partial\overline{\sigma_{ij}^{(k)}} \cdot c_k/\partial x_i = 0, \tag{1}$$

where $\overline{\sigma_{ij}^{(k)}}$, c_k are the averaged component of the stress tensor and the content for the k-th component (phase) of the CM (CC). At the same time, the stress state in local areas has two components:

$$\sigma_{ij}^{(R)} = \sigma_{ij}^{(1)} + \sigma_{ij}^{(2)}. \tag{2}$$

where $\sigma_{ij}^{(1)}$ - stressed state of an infinite elastic plane with a filler (inclusion) of spherical shape;

$\sigma_{ij}^{(2)}$ - stressed state of the half-plane resulting from the action of a distributed load on its boundary (z = 0):

$p_f(x) = -\sigma_z^{(2)}|z = 0, q_f(x) = -\tau_{xz}^{(1)}|z = 0,$

which is introduced to implement boundary conditions. For this, it is necessary to fulfill the equality:

$$p_f(x) = \sigma_z^{(1)}|z = 0,\ q_f(x) = -\tau_{xz}^{(1)}|z = 0 \tag{3}$$

Solving the contact problem for a filler of size r makes it possible to estimate the stress $\sigma_{ij}^{(1)}$ in the cylindrical coordinate system:

$$\sigma_x^{(1)} = \begin{cases} -A, & x^2 + z^2 < r^2; \\ -Ar^2 \frac{x^2 - z^2}{(x^2+z^2)^2}, & x^2 + z^2 > r^2, \end{cases} \tag{4}$$

$$\sigma_z^{(1)} = \begin{cases} -A, & x^2 + z^2 < r^2; \\ -Ar^2 \frac{x^2 - z^2}{(x^2+z^2)^2}, & x^2 + z^2 > r^2, \end{cases} \tag{5}$$

$$\tau_{xz}^{(1)} = \begin{cases} 0, & x^2 + z^2 < r^2; \\ -2Ar^2 \frac{xz}{(x^2+z^2)^2}, & x^2 + z^2 > r^2, \end{cases} \tag{6}$$

Solving the contact problem to find the stress $\sigma_{ij}^{(2)}$ requires following boundary conditions:

$$p_f(x) = \begin{cases} -A, & |x| < r; \\ Ar^2 \frac{1}{x^2}, & |x| > r, \end{cases} \qquad q_f(x) = 0\ , z = 0. \tag{7}$$

If a normal load is applied to the boundary of the half-plane, then the stress components $\sigma_x^{(2)}, \sigma_z^{(2)}$ $\sigma_{ij}^{(2)}$ and $\tau_{xz}^{(2)}$ that are acting in the half-plane are as following:

$$\sigma_x^{(2)} = -\frac{2z}{\pi}\int_{-\infty}^{\infty} \frac{p_f(s)(x-s)^2 ds}{((x-s)^2+z^2)^2}, \sigma_z^{(2)} = -\frac{2z^3}{\pi}\int_{-\infty}^{\infty} \frac{p_f(s) ds}{((x-s)^2+z^2)^2}, \tau_{xz}^{(2)} = -\frac{2z^2}{\pi}\int_{-\infty}^{\infty} \frac{p_f(s)(x-s) ds}{((x-s)^2+z^2)^2}. \tag{8}$$

The study of the distribution of stresses in the area of local contacts of the surface reinforced layer of WBSTEM CM (CC) shows that the stress-strain state in these areas is a concentrator of residual stresses, and the most dangerous place, from the destruction point of view, is the area of the main material near the surface of the half-space. This result is in good agreement with experimental research and simulation data. A local maximum τ_{max} occurs on the axis of symmetry of the filler in the main material.

When studying the contact interaction of soil particles and an elastic half-space with fillers (inclusions) coming to the surface, it was assumed that the main material and the filler material (inclusions) are elastic and have the same Young's moduli E and Poisson's ratios μ. At the same time, the boundary conditions on the surface of the half-space at z = 0 are as follows:

$$\sigma_z|z=0=\begin{cases}p(x,y) & (x,y)\in\Omega\\ 0 & (x,y)\notin\Omega\end{cases},\quad \tau_{xz}|z=0=\tau_{yz}|z=0=0, \tag{9}$$

where $p\,(x, y)$ is a pressure inside the contact area.

It is assumed that the stress state that occurs during contact interaction does not lead to a change in the shape and size of the filler (inclusion) and the problem of determining the internal contact and residual stresses can be solved separately.

The stressed state of the half-space with a filler (inclusion) during contact interaction is determined by the superposition method:

$$\sigma_{ij}=\sigma_{ij}^{(C)}+\sigma_{ij}^{(R)}, \tag{10}$$

where $\sigma_{ij}^{(c)}$ - internal stresses arising as a result of contact interaction,

$\sigma_{ij}^{(R)}$ - residual stresses.

When solving the specified contact problem, the stress components are determined by ratios:

$$\sigma_x^C=-\frac{1}{2\pi}\iint_\Omega p\,(\xi,\eta)\left(\frac{z}{r^3}\left(\frac{3(x-\xi)^2}{r^2}-(1-2\mu)\right)+(1-2\nu)\left(\frac{(y-\eta)^2+z^2}{r^3(z+r)}-\frac{(x-\xi)^2}{r^2(z+r)^2}\right)\right)d\xi d\eta; \tag{11}$$

$$\sigma_y^{(C)}=-\frac{1}{2\pi}\iint_\Omega p\,(\xi,\eta)\left(\frac{z}{r^3}\left(\frac{3(y-\eta)^2}{r^2}-(1-2\mu)\right)+(1-2\nu)\left(\frac{(x-\xi)^2+z^2}{r^3(z+r)}-\frac{(y-\eta)^2}{r^2(z+r)^2}\right)\right)d\xi d\eta; \tag{12}$$

$$\sigma_z^{(C)}=-\frac{1}{2\pi}\iint_\Omega 3p\,(\xi,\eta)\frac{z^3}{r^5}d\xi d\eta; \tag{13}$$

$$\tau_{xy}^{(C)}=-\frac{1}{2\pi}\iint_\Omega p\,(\xi,\eta)\left(\frac{z}{r^3}\left(\frac{3(x-\xi)(y-\eta)z}{r^2}-(1-2\mu)\right)+(1-2\nu)\frac{(x-\xi)(y-n)(z-2r)}{r^3(r+z)^3}\right)d\xi d\eta; \tag{14}$$

$$\tau_{yz}^{(C)}=-\frac{1}{2\pi}\iint_\Omega 3p\,(\xi,\eta)\frac{(y-\eta)z^2}{r^5}d\xi d\eta,\ \tau_{xz}^{(C)}=-\frac{1}{2\pi}\iint_\Omega 3p\,(\xi,\eta)\frac{(x-\xi)z^2}{r^5}d\xi d\eta, \tag{15}$$

where $r^2=(x-\xi)^2+(y-\eta)^2+z^2$, and the distribution of residual stresses $\sigma_{ij}^{(R)}$ is calculated by the formula:

$$\sigma_{ij}^{(R)}=v\left(\sigma_x^{(R)}+\sigma_z^{(R)}\right) \tag{16}$$

At the same time, it is assumed that the indenter or a soil particle is spherical. Then the distribution of contact pressures is determined by the theory in works [1, 13], and the contact plane is a circle of radius a.

Let's consider the stress-strain state of the surface layer of the WBSTEM upon contact with the AP of the soil from an analytical point of view. The rate of change of the energy of the CM (CC) in the volume V_{sl} bounded by the surface of S_{fr} is equal to:

$$\int_V\frac{dU}{dt}dV_{sl}=\int_V\left(\frac{\partial\overline{v_i^{(k)}\sigma_{ij}^{(k)}}}{\partial x_i}\cdot c_k-\Delta U_{ic}\right)dV_{sl}, \tag{17}$$

where dU/dt, ΔU_{ic} – rate of change of internal energy and change of energy of interaction between AP and components (phases) of CM (CC);

$v_i^{(k)}$ – speed of the i-th AP interacting with the k-th component (phase).

On the other hand, there is a following equation for the plane of contact interaction:

$$\int_V dU/dt\,dV_{sl}=V\int_V\overline{v_i^{(k)}\sigma_{ij}^{(k)}}\cdot c_k\cdot n_j\,dV_{sl}, \tag{18}$$

where n_j – projection of the normal on the x-axis to the plane of contact interaction of the AP with the region of the k-th component (phase) of the CM (CC).

Taking into account the stress-deformed state of the surface layer of CM (CC) during friction and wear, the right-hand side of expression (17) takes the following form:

$$\int_V\overline{v_i^{(k)}\partial\sigma_{ij}^{(k)}}\cdot c_k dV_{sl}/\partial x_i+\int_V c_k\overline{\sigma_{ij}^{(k)}\varepsilon_{ij}^{(k)}}\,dV_{sl}=0{,}5\int_V c_k\overline{\sigma_{ij}^{(k)}\left(\partial v_i^{(k)}/\partial x_i+\partial v_j^{(k)}/\partial x_j\right)}\,dV_{sl}, \tag{19}$$

where $\varepsilon_{ij}^{(k)}$ – components of the strain tensor of k-th component;

v_i, v_j – velocity components on the corresponding axis x_i, x_j of the contact plane of the i-th AP with the k-th component (phase). The specific potential energy of deformation of CM (CC) is equal to:

$$U_{sen}=0{,}5\cdot c_k\overline{\sigma_{ij}^{(k)}}\cdot\overline{\varepsilon_{ij}^{(k)}}. \tag{20}$$

In the case of two-component CM (CP), we have the following equation:

$$U_{sen} = 0{,}5 \cdot \left(c_{v1} \left(\overline{\sigma_{ij}^{(1)}} \cdot \overline{\varepsilon_{ij}^{(1)}} + \Delta \left(\overline{\sigma_{ij}^{(1)}} \cdot \overline{\varepsilon_{ij}^{(1)}} \right) \right) + c_{v2} \overline{\sigma_{ij}^{(2)}} \cdot \overline{\varepsilon_{ij}^{(2)}} \right), \quad (21)$$

where c_{v1}, c_{v2} – corresponding matrix and filler content in CM (CC): $c_{v1} + c_{v2} = 1$.

The change in the specific potential energy of deformation at the "filler-matrix" interface is equal to:

$$\Delta U_{sen} = 0{,}5 \cdot c_{v1} \cdot \Delta \left(\overline{\sigma_{ij}^{(1)}} \cdot \overline{\varepsilon_{ij}^{(1)}} \right). \quad (22)$$

Deformation hardening of CM (CC) is determined by the expression:

$$\Delta\sigma_{c_2} = k_{зм} \bar{\lambda}^{-0{,}5} = K_{kr} \cdot \left(\varepsilon / \bar{\lambda} \right)^{0{,}5}, \quad (23)$$

where k_{str}, K_{rb} – respectively, parameters characterizing the physical essence of strengthening and robustness and structural factors of CM (CC) [14]; $\overline{\lambda}$ – the average distance between filler particles. Constant k_{str} is estimated by the formula:

$$k_{str} = C_f C_{op} E_{cm(cc)} \cdot b_B \left[\rho + \left(C_f C_{op} \rho_d + 1/b_B \right) \varepsilon \right]^{0{,}5}, \quad (24)$$

where C_f, C_{op} – respectively steel, characterizing the conditions of formation and operation of CM (CC); $E_{cm(cc)}$ – elastic modulus of CM (CC); b_B – Burgers vector; ρ_d – density of dislocations generated on the surface of separation of components (phases). According to Orovan's theory, supplemented [4], the k_{str} K_{rb} constant is equal to:

$$K_{kr} = \alpha_d E_{cm} {b_B}^{0{,}5} c_2^{0{,}25} \cdot K_f, \quad (25)$$

where α_d – constant value characterizing the deformation conditions; K_f – filler shape parameter:

$$K_f = \overline{\lambda} / \left(\left(\overline{\lambda} - \overline{d_c} \right)^2 + \overline{S}_{ac}^2 \right)^{0{,}5}, \quad (26)$$

where $\overline{d_c}$ – average size of components (phases); $\overline{S}_{ac}^2$ – the average distance between the axes of components (phases) of CM (CC). If correlation $\bar{d}_c / \overline{\lambda} \in [0;1]$, then $K_f \in [2;5]$.

To evaluate the influence of the phase transition (PT) during the formation of CM (CC) and deformation due to friction and wear, consider the strengthening of the matrix during the formation of the martensitic phase [12]. At the same time, according to [11], the stresses in the matrix are equal to:

$$\sigma_m = c_{0m} n_m (c_m)^{n_m}, \quad (27)$$

where c_{0m}, n_m – constant coefficients characterizing the flow of PT in the CM (CC) matrix; c_m – martensite content. Taking into account the autocatalytic nature of the martensitic transformation when coherent deformations occur in retained austenite, we have:

$$c_m = k_{1m} \varepsilon^{n_c} c_A. \quad (28)$$

where $k_{1м}$ – the proportionality coefficient characterizing the intensity of the flow of martensitic PT; n_c – exponent that takes into account the catalytic effect; c_A – the content of austenite in the CM (CC) matrix. Because $c_m + c_A = 1$, then from (28) we have the following equation:

$$c_m / (1 - c_m) = k_{1m} \varepsilon^{n_k}. \quad (29)$$

This dependence is confirmed by experimental data and is consistent with the data of the work [14]. According to the autocatalytic nature of the martensitic transformation, n_c=3. Considering formula (29), we have:

$$c_m = k_{1m} \varepsilon^3 / (1 + k_{1m} \varepsilon^3); \qquad c_A = (1 + k_{1m} \varepsilon^3)^{-1}. \quad (30)$$

In the process of friction and wear, the deformation strengthening of the surface layer of CM (CC) can be characterized by the ratio [13]:

$$\sigma = k_{str} [ln(1 + \varepsilon)]^{p_s}; \qquad \Delta\sigma = \sigma - \sigma_s = h_s \Delta \varepsilon^{a_s}, \quad (31)$$

where k_{str}, p_s, h_s, a_s – parameters of strain strengthening; $\Delta\varepsilon$ – the amount of deformation without an elastic component corresponding to the yield strength σ_y.

Based on relations (30) and (31), we have the following equation:

$$\sigma = k_{str} [ln(1 + \varepsilon)]^p [1 - (1 + 1/k_{1m} \varepsilon^3)^{-1}] + \sigma_m (1 + 1/k_{1m} \varepsilon^3)^{-n_{str}}, \quad (32)$$

where n_{str} – indicator of matrix strengthening by the formation of martensite.

According to the work [14], the parameter p_s=0,18, and σ_m is the stress of the matrix material, which consists entirely of martensite and depends on the strength of the martensite and the carbon content of the steel. This is explained by the proportionality of the formation rate of martensite nuclei to its volume fraction [5].

The change in stress at the PT during friction and wear of the CM (CC) is equal to:

$$\Delta\sigma_p = \frac{k_{str}^{cs}\Delta\varepsilon^a}{\sqrt{d}}\left(1-\left(1+\frac{1}{c_1\varepsilon^3}\right)^{-1}\right)+\sigma_m\left(1+\frac{1}{c_1\varepsilon^3}\right)^{-str}, \quad (33)$$

where $k_{str}^{cs} = C_f C_{op} r^{cs} \cdot E_m b^2$; r^{cs} – parameter of the cellular dislocation structure. With a uniform distribution of dislocations $r^{cs} = 1$.

Since friction and wear is a non-stationary process, the accumulated energy of elastic-plastic deformation is equal to:

$$U_{el}(t) = \int_0^{\varepsilon} \sigma(\varepsilon) d\varepsilon, \quad (34)$$

where $\sigma(\varepsilon)$ is determined by equation (33). Knowing the values U_{spec}, or U_{el}, q_{cr} – critical power of flow density, the amount of wear can be estimated:

$$u = C_f C_{op}/q_{kr} = C_f C_{op}/U_{spec}^{3/2}. \quad (35)$$

In the case of a two-phase CM (CC), we have:

$$U_{el} = \int_0^{\varepsilon_l} \Delta\sigma_{c_2} d\varepsilon = C_f C_{op} \cdot {\varepsilon_{ml}}^{3/2}/\sqrt{\bar{\lambda}^n}; \qquad u = C_f C_{op} \bar{\lambda}^{3/4} c_m^{-3/8} \varepsilon_{ml}^{-9/4}, \quad (36)$$

where ε_{ml} – the limit value of deformation of the matrix material.

The deformation of two-phase CM (CC) can be estimated using the formula:

$$\varepsilon_{cm(cc)} = \varepsilon_{dm} - \Delta\varepsilon = \varepsilon_{dm} - C_f C_{op} \cdot \varepsilon_m c_2 = \varepsilon_{dm} - a \cdot c_n/\bar{\lambda}^n, \quad (37)$$

where ε_{dm} – matrix deformation at c_n=0; $\Delta\varepsilon = f(c_n, \lambda)$ – reduction of plasticity due to the presence of a brittle phase (filler); ε_m – matrix deformation: $\varepsilon_m = C_f C_{op}/\bar{\lambda}^n$; a, n – steels determined experimentally. If expression (37) is substituted into (36), we get the following:

$$u = C_f C_{op} \lambda^{3/4} {c_n}^{-3/8} \left(\varepsilon_{dm} - a \cdot c_n/\bar{\lambda}^n\right)^{-9/4}. \quad (38)$$

Results

During the interaction of WBSTEM with the soil, three types of soil deformations can be identified:

- microscale deformation within dilatation bands along the fracture surface;
- mutual rolling and sliding of the formed soil particles;
- deformation within soil particles, which is possible due to high soil moisture.

In the first two cases, the deformation is accompanied by an increase in volume, in the latter, compaction of soil particles may occur. Therefore, in the process of interaction of WBSTEM with the soil, the following deformations can also be distinguished: at a constant volume; during compaction; during expansion in the process of destruction. In field conditions, the general deformation of the soil consists of a collection of its various types, but one of them is the leading one.

When describing the interaction of WBSTEM with the soil layer, the theories of continuous deformable environments are quite acceptable. This approach allows to describe the process of deformation, movement and mixing of soil particles on the working surface of the WBSTEM. Without researching these processes, it is impossible to establish the regularities of the interaction of WBSTEM with the soil and to describe the stress-strain state of the soil.

Research shows that by comparing the natural volumetric mass of the soil with the optimal one, it is possible to determine the rational method of cultivation and the degree of action on the soil. The results of the study of the amount and nature of the wear of standard WBSTEM during operation indicate their dependence on the type of soil, the ratio of phase components and the stress-strain state. The dependence of the wear of cutting elements (CE) on the amount of stress in the soil layer adjacent to the WBSTEM is shown in Fig. 1.

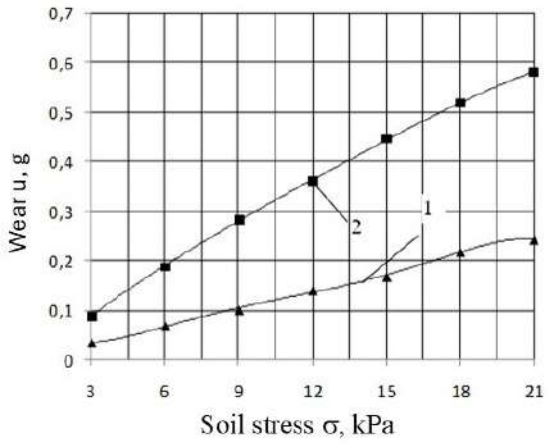

Fig. 1. Dependence of the wear of the toe of the one-sided paw (1) and the horizontal CE slot cutter (2) on the amount of soil stress in ordinary black soil (L=8,52 km, v= 1,4 m/s, W=10%)

It is shown that the wear of CE of WBSTEM increases with an increase in soil stress.

At that time, during the interaction of abrasive particles (AP) of the soil with the surface of WBSTEM, strengthened by CM (CC), the values of the components of the stress tensor σ_{ij} change in the local areas of the surfaces. The results of computer modeling of the stress fields during the action of high frequency on the working surface of the WBSTEM, carried out according to the developed methodology [14], in cases with unreinforced and strengthened CM (CC) TE in the mode of static and dynamic loading are shown in Fig. 2.

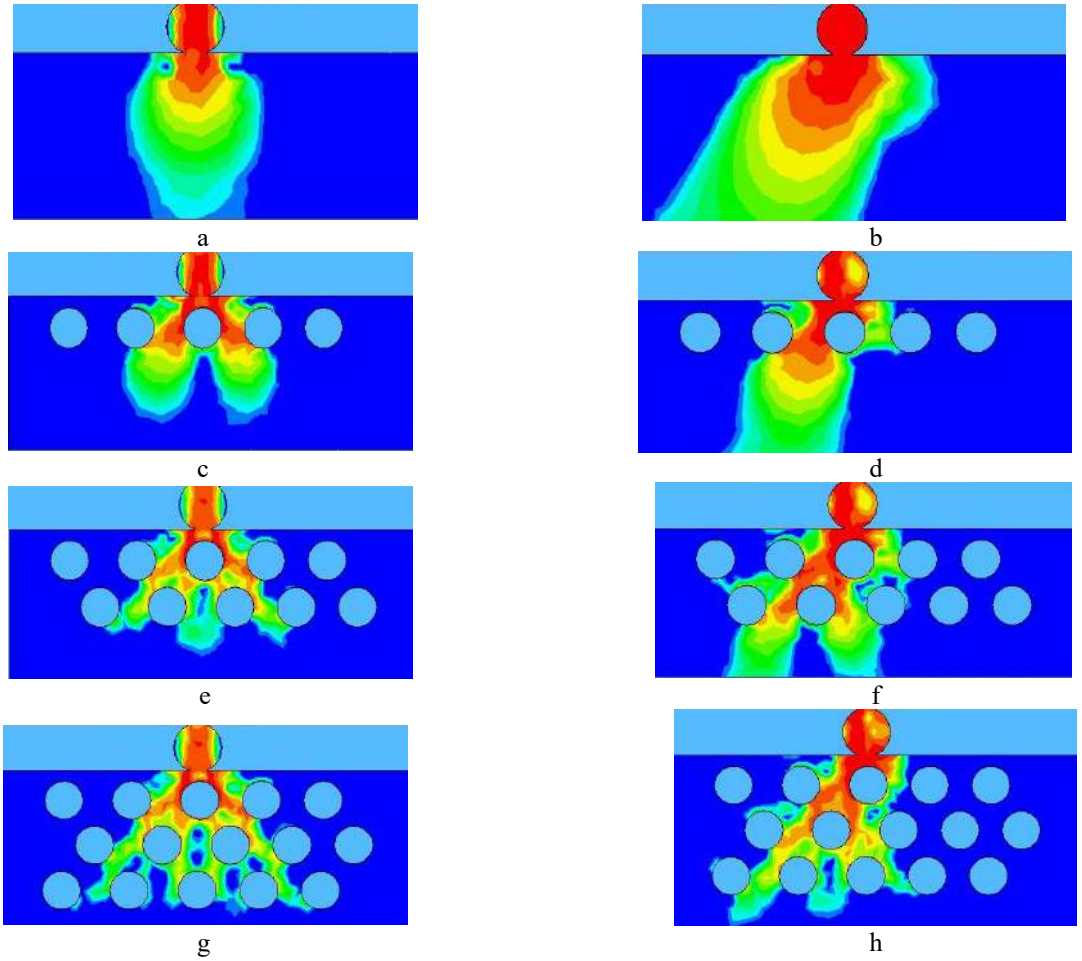

Fig. 2. Characteristic graphs of stresses in the contact areas of WBSTEM when acting on the surface of the WBSTEM: a – without coating $\overline{v} = 0$; b – without coating $\overline{v} \neq 0$; c – with a single-layer CC on TE-2, $\overline{v} = 0$; d – with a single-layer CC, $\overline{v} \neq 0$; e – with two-layer CC on TE-2, $\overline{v} = 0$; f – with two-layer CC, $\overline{v} \neq 0$; g – with a three-layer CC, $\overline{v} = 0$; h – with a three-layer CC, $\overline{v} \neq 0$

It can be seen that the region of the stress-strain state of the zone of contact with the AP is concentrated in the reinforced layer of the CM (CC), and in the dynamic load mode, the stress profile is transformed in the direction of the relative movement of the TE (Fig. 2, b, d, e, h).

Experimental studies have determined that the wear resistance of CM (CC) is primarily due to the presence of the strengthening component molybdenum disulfide MoS_2 in 5 and 10 wt.% with preliminary dispersion (filler, inclusion, phase) and phase transformation in the matrix.

The development of a mechanism for increasing the wear resistance of composites based on UHMWP during the interaction in the WBSTEM-soil tribosystem involves taking into account a number of factors:

- lack of interphase interaction between the polymer matrix and filler particles pressed deep, which determines effective absorption of energy without destruction of the composite during triboloading;
- the effect of filler particles on a change in size and shape, which in the vast majority of cases is accompanied by a noticeable decrease in mechanical properties, but may not lead to a decrease in wear resistance;
- interaction of the surface of the steel counterbody with the polymer matrix and filler particles protruding above its surface.

The microstructure of the surface reinforced layers of CE of WBSTEM was studied using a PEM 106 microscope. The PEM method allows studying the topography and chemical composition of the surface without prior mechanical processing or etching.

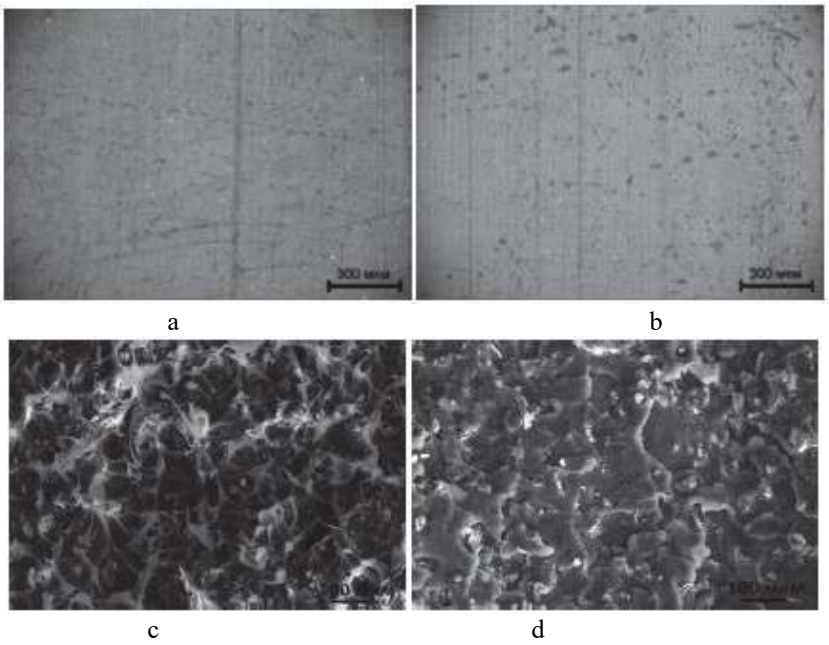

Fig. 3. The microstructure of the friction zones of the surface strengthened layers of CE of WBSTEM UHMWP: a, c - MoS_2 5 wt.%, b, d - MoS_2 5 wt.%,

In the compositions of UHMWP MoS_2 *n* wt.% the smoothest wear surface is observed in the composition at the content of MoS_2 10 wt.%. A different pattern of changes in the supramolecular structure is observed with increasing filler content MoS_2, which determines the nature of samples destruction of experimental compositions.

Conclusions

1. The stress-strain state of the soil as a continuous solid medium under the action of the WBSTEM was considered, and the dependence of wear on the stress in the soil for different types of WBSTEM was experimentally revealed.

2. The solution of the contact problem of an abrasive soil particle action on the strengthened CM (CC) and the unreinforced surface layers of WBSTEM was considered using the method of computer modeling of stress fields. It was found that particles of fillers (inclusions) redistribute stress fields in both static and dynamic cases, and for a given CM (CC) there is a certain thickness of the strengthened layer when the stress field is completely concentrated in it.

3. From a theoretical point of view, based on the boundary conditions, the field of residual and contact stresses of the surface layers strengthened by CM (CC) under loading by the action of an abrasive particle as an indenter is considered.

4. Taking into account the stress-strain state, strain hardening and evaluation of the effect of phase transformation during the formation and deformation of CM (CC) during friction and wear are considered. These are primarily martensitic-austenitic transformations. The relationship between stress in the surface layer of CM (CC) and wear characteristics was established, which makes it possible to design an effective reinforced layer on WBSTEM.

5. Experimental studies have shown that the wear resistance of CM (CC) is primarily due to the presence of the strengthening component molybdenum disulfide MoS2 in 5 wt.% and 10 wt.% with preliminary dispersion (filler, inclusions, phases) and phase transformation in the matrix.

References

1. Aulin V.V., Lysenko S.V., Hrynkiv A.V., Pashynskyi M.V. 2022. Improvement of tribological characteristics of coupling parts "shaft-sleeve" with polymer and polymer-composite materials Problems of Tribology , V. 27, No. 3/105-2022, 96-107. https://doi.org/10.31891/2079-1372-2022-105-3-96-107 [English]

2. Aulin V., Lyashuk O., Tykhyi A., Karpushyn S., Denysiuk N. 2018. Influence of rheological properties of a soil layer adjacent to the working body cutting element on the mechanism of soil cultivation Acta Technologica Agriculture, vol 4 Nitra, Slovaca Universitas Agriculturae Nitriae.. pp. 153-159. https://doi.org/10.2478/ata-2018-0028 [English]

3. Aulin V., Chernovol M., Pankov A., Zamota T., Panayotov K. 2017. Sowing machines and systems based on the elements of fluidics INMATEH - Agricultural Engineering vol 53, no. 3, pp. 21–28. https://doi.org/10.35633/inmateh-67-20 [Ukr]

4. Bahadur, S.; Schwartz, C. 2013. Chapter 2—The effect of nanoparticle fillers on transfer film formation and the tribological behavior of polymers. In Tribology of Polymeric Nanocomposites. Friction and Wear of Bulk Materials and Coatings, 2nd ed.; Friedrich, K., Schlarb, A., Eds.; Butterworth-Heinemann: Oxford, UK,; pp. 23–48. [English]

5. Panin S., Alexenko V., Buslovich D. 2022. High Performance Polymer Composites: A Role of Transfer Films in Ensuring Tribological Properties Polymers, 14, 975. https://doi.org/10.3390/polym14050975 [English]

6. Aulin V.V, Tykhyi A.A., Karpushyn S.O. 2012. Self-sharpening of cutting elements of soil tillage and excavation machines in conditions of strengthening of their working surfaces. Collection of scientific works of Khark. national car –road university transport. - Vestnyk Kharkovskoho nats. avtomobylno-dorozhnoho unyversyteta". Kharkov: KhNADU. *Vol.* 57. S. 188-194. [Ukr]

7. Briscoe, B.J.; Sinha, S.K. 2013. Chapter 1—Tribological applications of polymers and their composites–past, present and future prospects. In Tribology of Polymeric Nanocomposites. Friction and Wear of Bulk Materials and Coatings, 2nd ed.; Friedrich, K., Schlarb, A., Eds.; Butterworth-Heinemann: Oxford, UK, pp. 1–22. [English]

8. Huang, W. – Liu, D.Y. – Zhao, B.Y. – FENG, Y.B. – XIA, Y.C. 2014. Study on the rheological properties and constitutive model of shenzhen mucky soft soil. In Journal of Engineering Science and Technology Review, 2014vol. 7, no. 3 pp. 55–61. [English]

9. Puhan, D.; Jiang, S.; Wong, J.S.S. 2022. Effect of carbon fiber inclusions on polymeric transfer film formation on steel. Compos. Sci. Technol. 217, 109084. [English]

10. Teamrat, A.G., Dani, O.R. 2001. Rheological properties of wet soils and clays under steady and oscillatory stresses. In Soil Science Society of America Journal, vol. 65, no.3, pp. 624–637. [English]

11. Ťavodová, M. – Kalincová, D. – Kotus, M. – Pavlík, Ľ. 2018. The Possibility of Increasing the Wearing Resistance of Mulcher Tools. In Acta Technologica Agriculturae, vol. 21, no. 2. pp. 94–100. [English]

12. Tolnai, R. – Čičo , P. – Kováč, I. 2006Impact strength of steels as a criterion of material resistance. In Acta Technologica Agriculturae.vol. 9, no. 1, pp. 17–19. [English]

13. S. E. Artemenko, Y.. A. Kadykova 2008 Polymer composite materials based on carbon, basalt, and glass fibres; Fibre Che-mistry, Vol. 40, No. 1, pp. 37-39. https://doi.org/10.1007/s10692-008-9010-0 [English]

14. Demian, C.; Liao, H.; Lachat, R.; Costil, S. 2013 Investigation of surface properties and mechanical and tribological behaviors of polyimide based composite coatings. Surf. Coat. Technol. 235, 603–610. [English]

Тихий А.А., Аулін В.В., Пашинський М.В., Боровік А.Є. Триботехнічні процеси взаємодії середовища ґрунту з робочими органами ґрунтообробних та землерийних машин, зміцненими композиційними матеріалами

В роботі наведено результати дослідження напружено-деформованого стану середовища ґрунту, як безперервної моделі наповненої абразивними частинками, під дією робочих органів ґрунтообробних і землерийних машин. Враховано одну з основних властивостей ґрунту, що визначає характеристику силової взаємодії робочих поверхонь робочих органів ґрунтообробних і землерийних машин з технологічним середовищем, а саме схильність контактного шару оброблюваного пласту до ущільнення.

Експериментальним шляхом встановлено зв'язок напруження в середовищі ґрунту з величиною зносу робочих органів ґрунтообробних і землерийних машин. Представлено теоретичний аналіз напружено-деформованого стану контактуючої області зміцненого поверхневого шару робочих органів ґрунтообробних і землерийних машин, з наповнювачем, включеннями або зміцнювальною фазою.

Проведено аналіз контактних характеристик напружено-деформованого стану та їх зміни при терті та зношуванні на основі постановки і розв'язання задач контактної взаємодії абразивних частинок ґрунту з неоднорідностями компонентів композиційних покриттів на основі надвисокомолекулярного поліетилену з наповнювачами при зміцненні робочих органів ґрунтообробних і землерийних машин.

Виконано комп'ютерне моделювання для дослідження характеру розподілу напружень в зміцненому поверхневому шарі різальних елементів робочих органів ґрунтообробних і землерийних машин в області контактної зони в стаціонарних та динамічних умовах. Сформульована контактна задача, наведено граничні умови та розв'язок у вигляді складових поля напруження.

Враховано характеристики наповнювача, їх вміст в композиційному матеріалі і покритті, встановлено зв'язок між напружено-деформованим станом і величиною зносу.

Keywords: напруження, контакт, зносостійкі покриття, композиційний матеріал, наповнювач, надвисокомолекулярний поліетилен, покриття, знос, робочий орган ґрунтообробної та землерийної машини.

Problems of Tribology, *V. 29, No32/113-2024*

Problems of Tribology
Website: http://tribology.khnu.km.ua/index.php/ProbTrib
E-mail: tribology@khmnu.edu.ua

INFORMATION ABOUT JOURNAL"PROBLEMS OF TRIBOLOGY"

POLICY (GOAL AND TASKS)

"Problems of Tribology (Problems of Tribology)" - an international scientific journal.

Along with the main task of collecting information from tribology, the journal also performs organizational and coordinating functions:

- coordination of scientific and technical work in the field of tribology;
- organization of conferences, sympsiums;
- organization of work on the creation of databases and expert systems in the field of tribology;
- the organization of communications and information exchange between specialists in the field of tribology internationally.

2. The journal contains articles directly or indirectly related to tribology, including:

- theoretical problems (physics, chemistry, mechanics, mathematics)
- experimental methods and research results;
- contact mechanics, friction, wear, lubrication, durability and reliability of friction units of machines and units;
- scientific, technical and production problems of manufacturing, repair, improving the quality, reliability and durability of friction;
- technological and structural methods of improving wear resistance, frictional and anti-friction properties of friction units;
- problems of tribo materials science;
- methodological and methodological issues of training specialists in tribology.

3. The main requirements of the article is the novelty and completeness of information.

Articles of theoretical content should include theoretical explanation (possibly in the form of an annex to the article) to assess the scientific novelty of the publication.

Experimental articles should contain complete information about the methodology, conditions and results of the experiment.

Technological profile articles should contain a description of the technology as much as possible. If it is impossible to disclose "know-how", the method of obtaining the necessary detailed information must be indicated.

4. All articles are reviewed by a closed double review for compliance with the topics and level requirements. At the same time, the authors are fully responsible for the content of the articles.

5. Due to the international nature of the journal it is preferably submit articles in English.

REQUIREMENTS TO THE ARTICLES

In order to publish an article in the journal authors should submit it by e-mail.

Text of an article should be laid out on A4 format (210 x 297 mm) page with the following margins set: left and right – 2.0 cm, top and bottom – 2.5 cm. Use the font Times New Roman throughout, single-spacing, 10-point type and 1.0 cm indention for body text. Use lower-case bold 14-point type for headings. Put subheadings in bold.

Article structure:

– Universal Decimal classification index (in the upper left corner).

– Initials and surnames of all authors (no more than 4 people) and the article title (up to 10 words) in Ukrainian, Russian and English (one-column format).

– Abstract (200–300 words, only commonly accepted terminology) in Englishshould be structured and contain the following elements: purpose, methodology, findings, originality, practical value, keywords (6–8 words), one-column format. The abstract should not repeat the heading of the article.

– Body text.

– Reference list.

– Abstracts and keywords (up to 6–8words) in the Ukrainian and Russian languages;

Each article should include the following sections:

– An introduction, indicating article’s scientific problem.

– An analysis of the recent research and publications.

– Unsolved aspects of the problem.
– Objectives of the article.
– Presentation of the main research and explanation of scientific results.
– Research conclusions and recommendations for further research in this area.
– The title and number of the project in terms of whichthe presented results were obtained and Acknowledgements to the organizations and/or people contributing to or sponsoring the project (at the discretion of the author)

The recommended length of articles (including text, tables, and figures) is 6–9 pages. Figures should not exceed 25 % of length of an article. The text should be laconic, and should not contain duplicated information. No running titles and section brakes should be applied in the file.

Figures must be provided both in color and grayscale. They must be included in the text after corresponding references and given as separate files TIFF, JPG. EPS (300 dpi). The preferable width for the figures is 8.15 cm; not more than 17 cm for maps, charts, etc. All figures should be placed within the text, not in tables. Lettering, lines and symbols must be readable. Captions under the figures should contain order number and description of the figure and should be put in Italics. Placing the figure numbers and captions inside figures is not allowed.

Equationsshould be entered using Microsoft Word for Windows Editor plug-in or Microsoft Equation, 10-point type. The equations sited in the text are to be numbered in order of their appearance in the text (number in brackets with right justify). Equations should be column width (<8 cm). Long formulas should be divided into parts of 8 cm width. Before and after each formula there should be one empty line. Physical quantities should be measured in SI units. An integer part should be separated from a decimal by a dot.

Tablesmust be in portrait orientation, have titles and be numbered. Preferably tables should not exceed 1 page in length; width should make 8.15 cm or 17 cm. It is recommended to use 8–9-point type (not smaller than 6-point type for big data).

References(no more than 15 items, published not earlier than 5 years before, no more than 20%of self-citations) should be listed in the order of appearance in the text of the article. The in-text references should be given in square brackets.

Also the author should submit the following data about all authors of the article: surname, name and patronymic, academic degree, academic rank, place of employment (complete name of organization), position, city, country, phone number, e-mail and authors' ORCID identifier, in a separate file in English, Ukrainian and Russian (one-column format, comma-separated).

REVIEW PROCEDURE

All manuscripts are initially treated by editors to assess their compliance with the requirements of the journal and the subject.

After the editor decision the manuscripts are sent to at least two external experts working in this area. **The manuscript goes double-blind peer review**, neither the authors nor the reviewers do not know each other.

Review comments transmitted to the author, together with a recommendation for a possible revision of the manuscript. Publishing editor reports to the authors about adopting manuscript without require revision or authors are given the opportunity to review the manuscript and submit it again, or manuscript rejected.

EDITORIAL ETHICS

Principles of professional ethics in the work of the editor and publisher

The editor of a peer-reviewed journal is responsible for deciding which of the articles submitted to the journal should be published. The validation of the work in question and its importance to researchers and readers must always drive such decisions.

- An editor should make decisions on which articles to publish based on representational faithfulness and scholarly importance of the proposed work.
- An editor should be alert to intellectual property issues and must not to publish information if there are reasons to think that it is plagiarism. ·
- An editor should evaluate manuscripts for their intellectual content without regard to race, gender, sexual orientation, religious belief, ethnic origin, citizenship, social set-up or political philosophy of the authors.
- Unpublished materials disclosed in a submitted manuscript must not be used in an editor's own research without the express written consent of the author. Privileged information or ideas obtained through peer review must be kept confidential and not used for personal advantage.
- An editor should take reasonably responsive measures when ethical complaints have been presented concerning a submitted manuscript or published paper, in conjunction with the publisher (or society). Every reported act of unethical publishing behavior must be looked into, even if it is discovered years after publication.

Publishers should provide reasonable practical support to editors and define the relationship between publishers, editor and other parties in a contract.

- Publishers should protect intellectual property and copyright.

- Publishers should foster editorial independence.
- Publishers should work with journal editors to set journal policies appropriately and aim to meet those policies, particularly with respect to editorial independence, research ethics, authorship, transparency and integrity (for example, conflicts of interest research funding, reporting standards), peer review and the role of the editorial team beyond that of the journal editor, appeals and complaints.
- Publishers should communicate and periodically review journal policies (for example, to authors, readers, peer reviewers).
- Publishers should assist the parties (for example, institutions, grant funders, governing bodies) responsible for the investigation of suspected research and publication misconduct and, where possible, facilitate in the resolution of these cases.
- Publishers are responsible for publishing corrections, clarifications and retractions.

Ethical principles in the reviewer work

Peer review assists the editor in making editorial decisions and through the editorial communications with the author may also assist the author in improving the paper. That is why actions of a reviewer should be unbiased.

- Any manuscripts received for review must be treated as confidential documents. They must not be shown to or discussed with others except as authorized by the editor.
- Reviews should be conducted objectively. Personal criticism of the author is inappropriate. Referees should express their views clearly with supporting arguments.
- Unpublished materials disclosed in a submitted manuscript must not be used in a reviewer's own research without the express written consent of the author. Privileged information or ideas obtained through peer review must be kept confidential and not used for personal advantage.
- Any selected referee who feels unqualified to review the research reported in a manuscript or knows that its prompt review will be impossible should notify the editor and excuse himself from the review process.

Principles that should guide the author of scientific publications

Authors realize that they are responsible for novelty and faithfulness of research results.

- Authors of reports of original research should present an accurate account of the work performed as well as an objective discussion of its significance. Underlying data should be represented accurately in the paper. A paper should contain sufficient detail and references to permit others to replicate the work. Fraudulent or knowingly inaccurate statements constitute unethical behavior and are unacceptable.
- An author should ensure that they have written entirely original works, and if the author has used the work and/or words of others, then this has been appropriately cited or quoted. Plagiarism in all its forms constitutes unethical publishing behavior and is unacceptable.
- Proper acknowledgment of the work of others must always be given. Author should cite publications that have been influential in determining the nature of the reported work. Information obtained privately, as in conversation, correspondence, or discussion with third parties, must not be used or reported without explicit, written permission from the source. Information obtained in the course of confidential services, such as refereeing manuscripts or grant applications, must not be used without the explicit written permission of the author of the work involved in these services.
- An author should not in general publish manuscripts describing essentially the same research in more than one journal or primary publication. Submitting the same manuscript to more than one journal concurrently constitutes unethical publishing behavior and is unacceptable. In general, an author should not submit for consideration in another journal a previously published paper.
- All those who have made significant contributions should be listed as co-authors. Where there are others who have participated in certain substantive aspects of the research project, they should be acknowledged or listed as contributors. The corresponding author should ensure that all co-authors have seen and approved the final version of the paper and have agreed to its submission for publication.
- When an author discovers a significant error or inaccuracy in their own published work, it is the author's obligation to promptly notify the journal editor or publisher and cooperate with the editor to retract or correct the paper. If the editor or the publisher learns from a third party that a published work contains a significant error, it is the obligation of the author to promptly retract or correct the paper or provide evidence to the editor of the correctness of the original paper.

CONTACTS

International scientific journal “Problems of Tribology”,
Khmelnitsky National University,
Institutskaia str. 11, Khmelnitsky, 29016, Ukraine
phone +380975546925
E-mail: tribosenator@gmail.com
Internet: http://tribology.khnu.km.ua